Investigating the Effects of Isolation Activities Following a Pipe Burst in a Water Distribution Network and Potential Mitigation Strategies

by

Yuan Tan

A thesis submitted to for the degree of Master of Philosophy

The University of Adelaide

School of Architecture and Civil Engineering

August 2023

Table of Contents

List of Figures

List of Tables

ABSTRACT

The maintenance of water distribution networks' integrity is crucial for ensuring high-quality potable water supply. Structural defects or failure within pipelines, such as leakage and bursts, can lead to physical water losses and contaminant intrusion. Despite the abundance of studies on water losses caused by pipe leakage and bursts, research on contaminant intrusion due to operational shutdown behaviours following pipe bursts is limited. There is also a dearth of investigation into the subsequent effects on water quality and the development of potential mitigation plans.

In order to evaluate the effects of isolation activities following a pipe burst in a water distribution network and potential mitigation, computer programs EPANET and PODDS EPANET were used to develop simplified water distribution networks which in turn were utilised to analyse potential contamination risks. The findings in this study suggest that the implementation of valve shutdown operations to isolate pipe bursts in water distribution networks may lead to contaminant intrusion. This intrusion can occur due to the suction effect induced by negative pressure during the isolation activities. The prevention of contaminant intrusion during isolation activities is a crucial consideration for maintaining high potable water quality. To mitigate the intrusion of exterior contaminants into pipes during isolation activities, valve shutdown sequences were evaluated using hydraulic modelling in EPANET to determine the most effective operational shutdown sequence. Both fixed demand and pressure dependent demand modelling approaches were adopted to perform the hydraulic modelling study. The findings suggest that contaminant intrusion can be eliminated by applying the most effective valve shutdown sequence(s). The results also reveal that intrusion volume can be minimised by adopting optimal valve shutdown sequences. Nonetheless, it is inevitable for limitations to arise when utilising hydraulic modeling software to analyse common water distribution networks. The complexity and size of a water distribution network can simply increase by having more valves, pumps, pipes, etc. The validation of hydraulic models can be challenging when the real water distribution network is very complex. Therefore, the results presented in this study provide reasonable simulations of potential contaminant intrusion during the operational shutdown process following a pipe burst. The results assist utility operators to further understand contaminant intrusion caused by operational shutdown behaviours. They also provide an insight to utility operators to mitigate the risk.

This investigation further examined the impact of the shutdown duration time of isolation valves, node elevations, and isolation block sizes on intrusion volumes. The results reveal that shortening the shutdown duration time of isolation valves reduces intrusion volumes. For example, in a pressure-dependent demand single pipe model which consists of two isolation valves, there is a potential to reduce the intrusion volume by $1m^3$ if the valve shutdown time can be reduced by 12 mins. The findings also suggest that changes in node elevations can increase intrusion volume in a hydraulic model where pressure dependent demand modelling approach is adopted. Water distribution network models characterized by a steeper topology between the reservoir and a burst pipe increase intrusion volumes. For instance, an 11 m increase of the elevation between the reservoir and a burst pipe can lead to additional 0.37 m^3 of intrusion volume. The results further indicate a smaller isolation block will reduce demand within the block, thus lowering intrusion volumes. The impacts of the shutdown duration time of isolation valves and isolation block sizes on intrusion volumes were observed irrespective of the type of demand modelling approach employed. However, the results imply that adopting the pressure dependent demand modelling approach leads to 69% lower intrusion volumes due to the network demand's sensitivity to changes in nodal pressure.

The research on simulated pipe bursts and operational shutdown activities also examined their subsequent effects on turbidity in water distribution network models. The results reveal that both pipe bursts and isolation activities significantly impact turbidity in water distribution pipes, particularly in pipes distributing substantial amounts of water in the network. The results also show that alterations in valve shutdown sequences closely relate to sensitive turbidity responses in water distribution pipes. For example, some turbidity spikes can reach approximately 100 NTU in conditioned water distribution models where the initial turbidity readings in pipelines are maintained below 0.4 NTU. However, the magnitude of the impact depends on the initial yield of the biofilm and the location of pipes within the water distribution network.

In accordance with the above findings, the most effective valve shutdown sequence(s) should be implemented to minimise intrusion volumes during isolation activities and reduce the impacts on turbidity. To reduce intrusion volumes, water utility operators may shorten the shutdown duration time of isolation valves and decrease the isolation block sizes to exclude

more demand nodes and reduce the demand within the block. To reduce the impacts of isolation activities on turbidity, they may avoid disturbing the primary water distribution pipes in a WDN.

HDR Thesis Declaration

I certify that this work contains no material which has been accepted for the award of any other degree or diploma in my name, in any university or other tertiary institution and, to the best of my knowledge and belief, contains no material previously published or written by another person, except where due reference has been made in the text. In addition, I certify that no part of this work will, in the future, be used in a submission in my name, for any other degree or diploma in any university or other tertiary institution without the prior approval of the University of Adelaide and where applicable, any partner institution responsible for the joint award of this degree.

I give permission for the digital version of my thesis to be made available on the web, via the University's digital research repository, the Library Search and also through web search engines, unless permission has been granted by the University to restrict access for a period of time.

Signature:

Name: Yuan Tan

Date: 13 August 2023

Acknowledgements

First and foremost, I want to extend my gratitude to Professor Martin Lambert for his generous and kind support since my arrival in Adelaide. His support, especially during the tough times of the pandemic, has been a real boost, helping me navigate through the challenges of studying and living abroad. Without Martin's support, my journey in Australia wouldn't be what it is today.

A big thank you is owed to Dr. Nhu Cuong Do for his invaluable contributions to my academic study. Nhu's expertise in hydraulic modelling and computer programming has strengthened my studies. His overseas experiences have become a source of inspiration. I am sincerely thankful for his kindness.

I am also deeply appreciative of Dr. Mark Stephens's supervision and swift response to the unexpected changes in my project. His constructive feedback has been invaluable, providing me with valuable insights into the real world of water supply industry.

I extend my thanks to Dr. Wei Zeng and Dr. Jessica Bohorquez for their assistance in my studies of hydraulics. I also want to thank Brenton Howie, Simon Golding, and Mark Peacock for their generous support in my experimental study. I owe Dr. Susan Mowbray a big thank you for her support in enhancing the quality of my thesis.

Lastly, I want to express my gratitude to my family and friends. I want you to know how much you mean to me. Your love and firm support are worth more than I can express on paper.

Chapter 1 Introduction

Water distribution networks (WDNs) are indispensable elements of urban infrastructure. This means regular upkeep is essential to optimize the potential of WDNs to supply high-quality potable water to consumers. However, most WDNs are buried underground, making it difficult to monitor, maintain and manage the condition of pipeline assets. Events such as pipe leakage or bursts can occur due to corrosion, poor connections, excessive pressure, construction work, etc can result in physical water losses. They can also significantly affect water quality, posing a potential risk to public health.

The majority of existing research on WDNs focuses on quantifying the physical and economic losses of water due to pipe leakage and bursts (e.g., Kingdom et al., 2006; WSAA, 2019). There are limited studies that investigate the intrusion of environmental contaminants such as organic matter, nutrients, and pathogens due to pipe leakage or bursts and the subsequent water quality issues. Researchers have substantiated the potential intrusion of exterior environmental contaminants into water distribution pipes through pipe leakage using experimental analysis (Fontanazza et al., 2015). They have displayed a new analytical expression to address the intrusion of contaminants into underground water distribution pipes under steady-state conditions (Collins and Boxall, 2013). Researchers have also detected and determined bacterial indicators of fecal contamination as a potential source of contamination to WDNs from flooded air release valve vaults (Besner et al., 2010).

Pipe leakage or burst can lead to a pipe rupture. The intrusion of contaminants into a pipe network through a pipe rupture can occur for various reasons. It may occur when the external pressure is greater than the internal pressure of the pipe near the rupture. The external pressure may be as high as the water head of the flooded sinkhole caused by the pipe burst or a flooded valve chamber (Besner et al., 2010). Despite the fact that internal pressure within WDNs is typically higher than the external pressure, the impacts of external pressure on water distribution pipelines can be significant. A high water table above an underground pipe can create external pressure on the pipe, leading to pipe leakage or burst (Gullick et al., 2004). For example, Perth, a coastal city in Western Australia, is prone to high water tables which can damage underground pipelines (Thompson et al., 2021). Contaminants may

intrude into the pipelines through the rupture. During network repair and maintenance, when a segment of the network is depressurized or isolated, the internal pressure of the pipes within this network segment may become lower than the external pressure. Low pressure can also be experienced in a pipe during transient events (Gullick et al., 2004; Boulos et al., 2005; Collins et al., 2012) or when excessive water is withdrawn from the WDN. Additionally, a WDN can experience intermittent water supply (IWS) when the network is unable to maintain positive pressures, with IWS potentially causing contaminant intrusion into underground pipes through leakage or backflow of untreated water through household taps under low or negative pressure (Fontanazza et al., 2015; Erickson et al., 2017).

This thesis first investigates contaminant intrusion in basic WDN models due to pipe leakages and/or bursts and explores how isolation activities, implemented to minimize the impact on customers (from a supply interruption rather than water quality viewpoint), may be optimized to reduce the intrusion of contaminants.

This is important because contaminant intrusion caused by isolation activities can affect water quality in WDNs. Turbidity, which measures the quantity of light scattered and absorbed by particles in water, is one of the commonly used physical indicators of water quality (U.S. EPA, 2004) as turbidity may increase dramatically due to flow changes in a water pipe. Turbidity is a better indicator of water quality in water prediction models because it is more stable than free residual chlorine in the same network or from one network to another (Francisque et al., 2014).

An isolation activity involves shutting off isolation valves in a sequence. Valve shutdown sequences can be altered by modifying the order in which the isolation valves are closed. This may affect the flow in different pipes at different times. Alternatively, valve shutdown sequences can be changed by selecting different sets of valves, as long as the operational shutdown sequence can isolate the burst from the WDN. Since different isolation valves are employed, different sets of pipes may be included in the isolation block which results in more or less flow being affected.

Considering these factors, the following objectives guide this research:

- To understand the basic hydraulic models, such as single water distribution pipe and single loop WDN models, it is essential to simulate isolation activities and demonstrate their potential for triggering contaminant intrusion.
- To explore and determine the effects of shutdown duration time of isolation valves, node elevation, and demand modelling approaches (i.e., fixed demand or pressure-dependent demand modelling approaches) on contaminant intrusion during the valve shutdown process.
- To eliminate or minimize contaminant intrusion in WDNs by determining the most effective valve shutdown sequence(s) in basic WDN models.
- To explore how isolation block sizes, the duration of shutdown time of isolation valves, and node elevations can increase the risk of contaminant intrusion in more complex WDNs.
- To analyze turbidity changes before and after pipe bursts in WDNs and both within and outside of an isolation block.
- To study the potential impacts of valve shutdown sequences on turbidity due to switching the order of shutting down a set of isolation valves.
- To study the potential impacts of valve shutdown sequences on turbidity due to changing the set of isolation valves.

How this research achieves these objectives is detailed in the following chapters.

- Chapter 2 critically reviews the relevant literature on contaminant intrusion, pipe failures and sinkholes, isolation valves, hydraulic modelling of water distribution networks, as well as turbidity and numerical modelling of turbidity. It also outlines the essential role of isolation block size, isolation valves and the duration of shutdown time in reducing the risk of contaminant intrusion in WDNs.
- Chapter 3 outlines the basic hydraulic models and shows the potential for isolation activities to cause contaminant intrusion in the WDN models. It also demonstrates the effects of adopting different duration of shutdown time of isolation valves, demand modelling approaches, and node elevation on intrusion volume during the isolation activities.

- Chapter 4 examines the feasibility of preventing contaminant intrusion in simple loop WDN models. It also illustrates how intrusion volume can be minimized in loop WDN models where contaminant intrusion cannot be eliminated.
- Chapter 5 details three factors that can increase the risk of contaminant intrusion in more complex WDN models which consist of multiple loops, including the isolation block sizes, shutdown duration time of isolation valves, and node elevations.
- Chapter 6 explores the changes of turbidity in water distribution pipes due to the occurrence of a pipe burst and the implementation of isolation operations in WDN models. The turbidity measurements both within and outside of an isolation block are analyzed to determine the effects of a burst and of isolation activities at different locations in a WDN model.
- Chapter 7 outlines the complex factors that inform the selection of isolation valves and decisions of shutdown operations that use different valve shutdown sequences. The corresponding effects of different valve shutdown sequences on turbidity are determined.
- Chapter 8 concludes the thesis.

Chapter 2 Literature Review

2.1 Contaminant Intrusion

Source water needs to undergo regulated treatment in a water treatment facility prior to distribution to consumers, as it contains various pathogens that could potentially harm public health and human well-being. Despite this, treated water can still be exposed to contamination during the supply process through distribution pipes, which could pose risks to consumers. Water contamination is recognized as a major cause of significant public health concerns, according to the Sector Monitoring Report released by the World Health Organization (WHO, 1990).

Contaminants can enter WDNs through different mechanisms, such as internal pipe corrosion, biofilm detachment from the internal pipe wall, and external intrusion. The Flint water crisis in Michigan, USA, between 2014 and 2019, was primarily caused by lead leaching from corroded pipes into the potable water supply network (USA CDC, 2016). Researchers have investigated the correlation between shear stress and biofilm detachment and found that changes in shear stress can trigger biofilm to detach from the internal pipe wall, thus, posing risks to the water quality in WDNs (Douterelo et al., 2016; Ginige et al., 2011; Volk et al., 2000).

Studies have also examined the potential for contaminant intrusion in WDNs, which refers to the entry of harmful chemicals and pathogens into the network (Mansour-Rezaei et al., 2014). The presence of contaminants near the network, pathways for external contaminants to enter water distribution pipes, and driving forces are the three prerequisites for contaminant intrusion (Islam et al., 2015; Mansour-Rezaei et al., 2014).

This research introduces sinkholes (contaminant tanks) formed by pipe bursts, where external contaminants mix with potable water. Consequently, contaminated water accumulates in the sinkhole. The study also assumes that an orifice formed by a pipe burst can serve as a pathway for contaminated water to enter a ruptured pipeline, thus posing a risk of contamination. The driving forces behind this process are the suction effects at the orifice resulting from specific isolation valve shutdown sequences.

Prior research has identified various routes through which pollutants can enter a pipe from the external environment. For example, untreated water can infiltrate a water distribution pipeline through defective joint seals that may leak under negative pressure circumstances (LeChevallier et al., 2003). Another route involves external contaminated water infiltrating a WDN through the pipeline itself. For instance, during an isolation activity where two valves must be closed to isolate a pipeline, a large transient wave can generate if only one valve is not shut off. Transient waves occur when flow conditions in pipelines are disturbed (Collins et al., 2012). For instance, abrupt changes in transmission conditions (e.g., pipe break) and valve operations (e.g., valve opening and closing) can affect the flow conditions and create transient pressure waves. The transient wave propagates toward one end of the pipe and then reflects back to another end. Since water distribution pipes are closed by operating isolation valves, this transient wave will persist until friction can gradually dissipate kinetic energy. Negative pressures will occur, inducing a suction effect in the pipes. When the distribution network continues to meet water demand, contaminated water, a mixture of untreated water and the soil surrounding the burst pipe, may be sucked into the water distribution pipes through the rupture (LeChevallier et al., 2003). It is important to note that hydraulic transient waves are generated by disturbing the flow in a pipeline from one steady-state equilibrium condition to another. Transient waves are commonly simulated by conducting unsteady-state hydraulic modelling. In this research study, steady-state hydraulic analysis was conducted because the method is more practical for exploring the changes in flow and network pressure under short-term effects (e.g., pipe bursts and isolation activities) to the WDN models.

The concentration of chemical or microbial pollutants in water can significantly impact its quality, leading to potential public health risks when it exceeds regulated levels. For instance, a concentration of *E. coli* greater than 20,000 organisms per 100 mL in source water indicates contamination (NHMRC and NRMMC, 2011). The Melbourne guidelines for private drinking water supplies at commercial and community facilities stipulate that the safety standard for drinking water is to have no detectable *E. coli* in 100 mL (State of Victoria, 2009). Even if exterior microbial pollutants are diluted, a single organism of certain microbial species can still cause infection (LeChevallier et al., 2003). Table 2-1 presents the drinking water guideline for major chemicals. Heavy metals like arsenic, copper, lead, and mercury have been confirmed to pose significant public health risks and must be maintained at extremely low levels in drinking water. Besides microbes and chemicals, aesthetic parameters should also be considered. Table 2-2 lists aesthetic parameters such as sulfate, pH, total

dissolved solids, total hardness, and turbidity, which can affect the taste, odour, and appearance of drinking water. Turbidity, for example, measures the clarity of drinking water. When turbidity exceeds 5 NTU (nephelometric turbidity units, the unit of measurement for turbidity), drinking water can appear cloudy because of the increased amount of suspended solids and microorganisms, reflecting more light during turbidity measurements. The method for measuring turbidity in water will be discussed in detail in Section 2.5.

Table 2-1. Regulated level for selected chemicals in drinking water.

Chemicals	Regulated Level (mg/L)
Arsenic	0.007
Cadmium	0.002
Chromium	0.05
Copper	2
Fluoride	1.5
Lead	0.01
Manganese	0.5

Table 2-2. Regulatory requirements of Australian drinking water aesthetic parameters.

Aesthetic Parameter	Australian Drinking Water Regulatory Requirement
Sulfate	250 mg/L
pH	6.5–8.5
Total dissolved solids	500 mg/L
Total hardness	200 mg/L
Turbidity	5 NTU (< 1 NTU is desirable)

Previous studies have been limited in scope, focusing mainly on leakage-related contaminant intrusion. Several authors have provided evidence of contaminant intrusion from loose valves and pipe leaks in water supply networks. Jones et al. (2019) argued that pipe leaks are potential openings for contaminants to enter a WDN from surrounding soil and untreated water. Fontanazza et al. (2015) also noted that water distribution networks are vulnerable to external pollutant intrusion if there is a loss of physical integrity, such as a pipe crack. According to a study conducted by engineers at the University of Sheffield, significant pressure drops were responsible for drawing contaminants and water from outside the

pipeline into a damaged section of the pipe. These pressure drops may result from not only abnormal water demand in the network but valve or pump failures (Fox et al., 2015). In addition to pipe leaks or cracks, incorrect valve shutdown operations during isolation activities may also be a significant cause of contaminant intrusion. Prior studies have discussed that valve operations, such as opening and closure, can result in low or negative pressure events within WDNs (Kirmeyer et al., 2001; Mansour-Rezaei et al., 2014; Fox et al., 2015; Berglund et al., 2020). These events have been identified as a cause of contaminant intrusion, leading to deterioration of the water quality. However, there has been limited research conducted on the potential link between incorrect operational shutdown sequence and the potential for contaminant intrusion.

Pollutants can enter WDNs when pipes are not supplied and are partially empty, in addition to low or negative pressure events (Fontanazza et al., 2015). Erickson et al. (2017) demonstrated that negative pressures can pose a potential risk of triggering contaminant intrusion in intermittent WDNs. Intermittent distribution is a type of water supply service in some countries like Italy, India and Vietnam but not in Australia. This distribution service operates daily by leaving pipes empty at atmospheric pressure and providing drinking water to consumers for less than 24 h. Intermittent distribution has been found to allow a large volume of external pollutants to enter WDNs. When operational valves in an intermittent distribution network are turned on or off cyclically, pollutants can enter the empty pipelines (i.e., unpressurised pipelines) and compromise water quality (Fontanazza et al., 2015).

2.2 Pipe Failures and Sinkholes

Pipes are crucial components of WDNs that can rupture or collapse due to aging and corrosion or when maximum pressure is reached. A pipe rupture is defined as a break in a pipe that may or may not lead to ultimate pipe collapse. It usually results in immediate pipe leaks or bursts. A break in a pipe indicates a fracture or separation of the asset; however, it may not lead to a complete pipe rupture or collapse. A pipe collapse refers to the ultimate structural failure of a pipeline. High stresses in pipes induced by vacuum conditions can cause the failures of thin-walled pipes. Additionally, pipe failure may occur when a pipe suffers cavitation. For example, abrupt interruption to pipe flow may cause pressure drops to the vapor pressure of water in the pipe and ultimately lead to vacuum collapse. Pipe failures can also occur due to gradual corrosion of the pipe wall resulting from pipe leaks and

repeated transients within the pipe (Boulos et al., 2005). Most pipe failures are caused by aging and corrosion. Pipe failures due to leaks or bursts can lead to undesirable interruptions in the supply of potable water in WDNs and eventually impacting consumers.

Pipe failures caused by leaks have the potential to cause ground subsidence and sinkholes (Ali and Choi, 2019). Sinkholes, a type of cavity formation in the ground, can occur naturally and anthropogenically. Natural sinkholes are formed when surface rocks (e.g., limestone and carbonate rocks) are dissolved by water. In contrast, man-made sinkholes can be caused by groundwater pumping and large-scale construction activities **(**Tihansky, 1999). Additionally, leaky pipes or pipe failures are often associated with the creation of man-made sinkholes. Potable water or sewage that leaks from underground pipes gradually erodes the surrounding soil, creating cavities that can reduce the bearing capacity of the soil layer and ultimately cause sinkholes (Ali and Choi, 2019; Van et al., 2019; Tihanskv, 1999). Meanwhile, potable water that leaks or bursts from a WDN pipeline can mix with chemicals and microbes from the surrounding soil, resulting in contaminated water in the sinkhole. Contaminated water may intrude into the water supply mains through the pipe rupture, leading to potential health risks to customers.

Pipe failures cause not only potential harm to public health and safety but also incur economic losses. One of the significant economic losses caused by pipe failures is the loss of a considerable amount of water. For example, according to the report of the Water Corporation in Western Australia, around 10 billion liters of water were lost in 2014 due to pipe leaks and bursts (Office of the Auditor General Western Australia, 2014). In Melbourne, approximately 48 billion liters of non-revenue water loss were recorded in 2016, including seven to eight billion liters of water loss due to undetected pipe leakages (Melbourne Water, 2016). Such water losses can interrupt the sustainable supply of water and reduce revenue. For instance, the replacement of over 34,000 km of water distribution pipes to supply potable water to 992,170 properties in Western Australia can cost a total of $11.72 billion. Thus, the failure of one or more pipelines can lead to a high cost of asset replacement.

The aforementioned evidence highlights the importance of addressing pipe leakage or bursts by repairing or replacing damaged pipes. The process of replacing a damaged pipe involves locating the damaged section, excavating the damaged pipes, selecting appropriate repair

materials, isolating the damaged pipes (if valves are accessible and operable), draining the pipe contents, replacing the damaged pipes with new ones, testing the pipeline connections for any leakage, purging and decontaminating, and backfilling the site with appropriate soil (JCM Industries, 2019). During the repair process, the damaged pipe must be isolated, which requires a specific sequence of isolation valves to be operated to create an isolation block.

2.3 Isolation Valves

As discussed in Section 2.2, the proper shutdown of broken pipelines through isolation valves is a crucial step during the process of repairing damaged pipes. Isolation valves play a critical role in ensuring the reliability of WDNs and are key components used to isolate pipe leaks or breaks (Liu et al., 2017; Do et al., 2018). A water distribution network lacking an adequate number of operable isolation valves or a well-designed geographical allocation of isolation valves is likely to fail, especially during isolation activities (Walski, 1993), due to inefficient isolation of a specific part of a WDN, extended service interruption time for maintenance, etc When a pipe fails, part of the WDN must be isolated from the rest of the network, and these isolated blocks were defined as ‘segments’ by Walski in 1993. Since incorrect or slow operational responses can deteriorate the pipe leakage or bursts and increase the number of consumers affected by the emergency incidents, researchers have been focused on the selection and implementation process of optimal isolation activities. These processes depend on the configuration of the affected network segments and the feasibility of isolating the damaged pipes through professional valve control options (Mahmoud et al., 2018). When analyzing the hydraulics of a WDN during a pipe burst, it is crucial to investigate the location of operable isolation valves, ensure the system can reflect the extent of operational shutdown behavior, and assess whether sufficient isolation valves are included in a WDN. Therefore, it is essential to identify network segments that can be isolated from the WDN by operating different numbers of valves (Walski, 1993).

2.4 Hydraulic Modelling of Water Supply Networks

Hydraulic modelling is an essential tool for simulating the distribution of water and improving the performance and reliability of WDNs. EPANET (Rossman, 2000) is a hydraulic software that uses links and nodes to represent pipes, junctions, and outlets in real-world WDNs. It was designed to analyze the quality of drinking water in WDNs. Nowadays, EPANET has been widely used to design WDNs and facilitate pipe sizing.

Additionally, hydraulic modelling can be used to optimize network design and operation (Mahmoud et al., 2018). Optimzer (Optimatics, 2023) is an optimization software which is capable of evaluating a large number of different WDNs design against their cost, hydraulic performance, energy, and water quality. Researchers and consultants have utilized Optimizer to reduce the cost of WDN design by 10-30% in comparison to manual pipe sizing.

When conducting hydraulic modelling, hydraulic models are often driven by either pressure or demand (Shirzad, 2020). In a demand-driven hydraulic analysis, the demand pattern can be either fixed or slowly fluctuate during the simulation period. This type of analysis will maintain the same supply of water even with pressure deficiencies in the model. Therefore, it may not accurately simulate water distribution when experiencing low or negative pressure (Muranho et al., 2020). On the other hand, a pressure-driven analysis takes into account nodal pressure and discharge throughout the entire WDN. Several studies have suggested that a pressure-driven analysis can provide a more accurate simulation of WDNs, especially when pressure deficits exist in the networks (Tanyimboh et al., 2003; Shirzad, 2020; Muranho et al., 2020; Khadr et al., 2022). Pressure deficit refers to a lack of minimum network pressure or negative pressure. This may result from the loss of pipeline integrity, such as pipe leaks or bursts. As a consequence, insufficient supply of potable water to satisfy nodal demands can be expected. A pressure-driven analysis reduce the nodal demands according to the available pressure at the nodes. Therefore, this approach can provide more realistic simulation outcomes.

Previous research has demonstrated the effectiveness of hydraulic modelling in optimizing water supply networks design and operations. For example, (Shamir, 1974) modified a program to allow for the optimization of system design and operation using a combination of generalized reduced gradient and penalty methods. Sterling and Bargiela (1984) developed an algorithm to determine optimal valve controls for minimizing pipe leaks due to overpressure. Alfonso et al. (2010) used hydraulic modelling to explore various flushing operations to minimize impacts on the population.

Meanwhile, many prior studies on valve operation have focused on relocating valves to improve network reliability (Bouchart and Goulter, 1991), analysing valve topology for

network reliability (Walski, 1993), determining optimal valve placement in networks (Cattafi et al., 2011), exploring the effects of valve failure in networks (Liu et al., 2017), and identifying partially closed valves (Do et al., 2018). However, hydraulic modelling of contaminant intrusion due to isolation activities following a pipe burst in WDNs is still limited.

2.5 Turbidity and Numerical Modelling of Turbidity

The provision of high-quality drinking water is essential for human well-being, and water supply utilities continuously monitor water quality to ensure its safety. For instance, the Environmental Policy and Planning Division at the Queensland Department of Environment and Science (2022) has adopted various indicators to assess water quality, such as physical and chemical, biological, toxicant, physical form, habitat, and hydrology indicators. Among the physical indicators, turbidity is a widely used parameter to indicate water quality by measuring the amount of light scattered and absorbed by particles in water (EPA-US, 2004; Burlingame et al., 1998). Turbidity readings have been effectively utilized in WDNs to detect and track potential transmission pipe breaks (EPA-US, 2018). For instance, Erickson et al. (2017) found that pipe failures can lead to contaminant intrusion from pipe breaks, resulting in significantly higher turbidity levels (greater than 100 NTU) in water distribution pipes.

Moreover, turbidity has been widely used by researchers to investigate water discoloration in WDNs, as well as to detect contaminant intrusion. In many published studies, turbidity has been used as a proxy for microbiological contamination in drinking water supply systems (de Roos et al., 2017). The turbidity in water supply pipes can also be impacted by particulates like slits, clay, and organic matter. Pollutants such as microorganisms, soils, and organic matter can enter water distribution pipes through contaminant intrusion, leading to a substantial increase in turbidity (EPA-US, 2018). Therefore, evaluating the turbidity profiles of potable water is a useful strategy to identify potential contaminant intrusion or discoloration in WDNs.

The investigation of turbidity has been conducted through laboratory and field tests (Starczewska et al., 2017; Husband and Boxall, 2010; Boxall and Saul, 2005), as well as numerical and analytical analysis (Mounce et al., 2015; Georgoulas et al., 2010; Chu et al., 1979). One widely used numerical model proposed in 2001 by Boxall et al. is the Prediction

and Control of Discolouration in Distribution Systems (PODDS), which assesses water discoloration using turbidity as a predictive index. This proactive approach to monitoring turbidity enables operators to analyze real-time water quality and ensure high-quality WDNs.

The PODDS model identifies empirical parameters, including hydraulic shear stress and turbidity potential, that are associated with the mobilization of biofilms on internal pipe walls. When the hydraulic shear stress exceeds the conditioned cohesive strength, biofilms detach from the internal pipe walls, resulting in an increase in turbidity.

Previous studies have found a correlation between the current layer strength and the potential for water discoloration (i.e., increased turbidity), as shown in Eq. 1.

$$\tau_s' = \frac{C^b - C_{max}}{k} \tag{1}$$

where τ_s' is the current layer strength, C is the turbidity potential, b is the power term for nonlinear forms of the relationship, C_{max} is the maximum turbidity potential and k is the gradient term of the correlation.

The model also suggests that disequilibria hydraulic conditions such as pipe bursts, operational activities, and increased peak daily flow lead to excess shear stress and ultimately result in water discoloration due to the mobilization of biofilm layers. The relationship between layer mobilization and excess shear stress is shown in Eq. 2.

$$R = P(\tau_a - \tau_s')^n \tag{2}$$

where R is the rate of supply, τ_a is the applied shear stress, P is the gradient term, and n is the power term. The excess shear stress, described by the term $(\tau_a - \tau_s')$, must remain positive so that the erosion of layers may be triggered and result in water discolouration.

While the primary objective of this model is to evaluate the turbidity response to variations in hydraulic conditions within WDNs, it also presents Eq. 3 for simulating the accumulation or regeneration of materials.

$$\Delta C_r = P' \Delta t P T^l {\tau_s'}^m \tag{3}$$

where ΔC_r is the incremental changes in layer turbidity potential, P' is an empirical time-based constant, T is temperature, l is a power term to enable temperature dependence of

material accumulation, and m is a power term to allow accumulation to associate with current layer strength.

Chapter 3 Modelling of Potential Contaminant Intrusion During the Process of Isolating a Pipe Burst in Simple WDN Models

3.1 Introduction of the Background and Approach

Pipe bursts in WDNs are inevitable because of the deterioration of water distribution pipes due to corrosion, external pressures, etc. Ongoing monitoring and maintenance is therefore necessary to reduce pipe burst in WDNs due to the deterioration of pipes from corrosion. The potential risk of contaminant intrusion can result from pipe bursts. This chapter examines potential contaminant intrusion during isolation activities in simple hydraulic models – a single water distribution pipe and a single loop WDN.

To investigate the occurrence of contaminant intrusion following a pipe burst, steady state extended-period simulation models were built using the EPANET hydraulic model (Rossman, 2000). The following assumptions and steps were implemented to establish the hydraulic models, including the single water pipe and loop WDN models, and set up of the sinkhole and burst water pipe:

- Establish water distribution pipes:
  (1) To ensure compliance with the WSAA Water Supply Code of Australia, the water mains in both the single pipe and loop WDN models were made of PE100 PN16 DN160 pipes; a minimum diameter of DN100 is required for all water supply networks with firefighting capability and to satisfy the preferred pipe material applications within SA Water's WSNs (SA Water, 2011). Therefore, the internal diameter (ID) and outside diameter (OD) of the pipes in the hydraulic models were 130 mm and 160 mm, respectively.
  (2) The cover depth, which is the distance between the water supply main and the ground surface level, was 1100 mm. This value falls between the required minimum (750 mm) and maximum (1200 mm) cover depths for water mains (SA Water, 2023), thus, satisfying the technical requirements for water assets. It should be noted that the minimum cover depth for water main installations varies depending on the nominal diameters of the pipes, whereas the maximum cover depth for water mains remains constant (1200 mm). For example, pipes with DN63-DN200 require a minimum of 750 mm cover depth, but pipes with DN375 require a minimum cover depth of 950 mm. Therefore, in real WDNs, pipelines may be installed at different depths.

(3) The pipes were connected to reservoirs, nodes, and isolation valves, with the specific connections varying depending on the model. The connections for each model are illustrated in the corresponding sections.

- Establish a sinkhole:

(4) A tank, named as the "contaminant tank", was added to the model to represent the total volume of contaminants held by the sinkhole caused by a pipe burst. The typical dimensions of a tank can vary depending on several conditions such as the depth of the pipe, soil conditions, and local topography. As depicted in Figure 3-9, the height of the sinkhole depends on the OD of the burst pipe and the cover depth. Therefore, a tank height of 1.26 m was assigned, which was calculated by summing the OD and cover depth. However, as mentioned in step (2), water mains can be installed at different depths. Thus, in reality, the size of the contaminant tank (sinkhole) can vary due to its height. In the event of a continuously pipe burst, a sinkhole may simply overflow, leading to the maximum volume of contaminated water exceeding that of the sinkhole's. This will be elaborated upon in Section 5.5.7.

(5) It was assumed that the shape of the sinkhole was conical. The size of a sinkhole can be affected by the type of surrounding soil and angle of repose values. Table 3-1 lists the angle of repose values for four types of soil (StructX, 2022), along with the sinkhole volumes which resulted from the assumed angle of repose values for each soil type. To reasonably simulate a sinkhole in the single pipe system and loop network, it was assumed that the surrounding soil of the burst pipe was wet natural sandy gravel, which has an angle of repose value of 25 degrees (Table 3-1). Hence, the side slope of the sinkhole was calculated as 65 degrees, as shown in Figure 3-9. The diameter of the sinkhole was calculated to be 5.40 m. The initial level of the contaminant tank is equivalent to the initial volume of contaminants held by a sinkhole. It was assumed as 0 because external contaminants cannot enter a water distribution pipeline unless a pathway and driving forces become available. As the contaminant filling process in a cone-shaped sinkhole is non-linear, a non-linear volume curve was prepared (Figure 3-10) and applied to the contaminant tank. The maximum volume of the contaminant tank was 9.63 m^3.

Figure 3-1 to 3-3 are screenshots taken from a real video of the suction effect at a pipe orifice. They demonstrate a sinkhole induced by a pipe burst and the potential

contaminant intrusion associated with the burst. Figure 3-1 shows an orifice created by a pipe burst. The surrounding soil mixes with potable water that escaped from the ruptured pipe, resulting in contaminated water. Before operators can isolate the burst, potable water from this pipe continues to escape from the orifice, creating a significant sinkhole, as shown in Figure 3-2. Based on the witness of the land depicted in Figure 3-2, the size of the sinkhole was considerably larger than the pipe rupture. Figure 3-3 illustrates a significant reduction in the level of contaminated water in the sinkhole. This may result from water evaporating into the atmosphere, water infiltrating into the ground soil, and so on. Nonetheless, potential contaminant intrusion events should not be neglected because it can also lead to contaminated water enter the ruptured pipe through the orifice.

Figure 3-1. The location of an orifice created by a burst pipe.

Figure 3-2. A sinkhole induced by the pipe burst introduced in Figure 3–1.

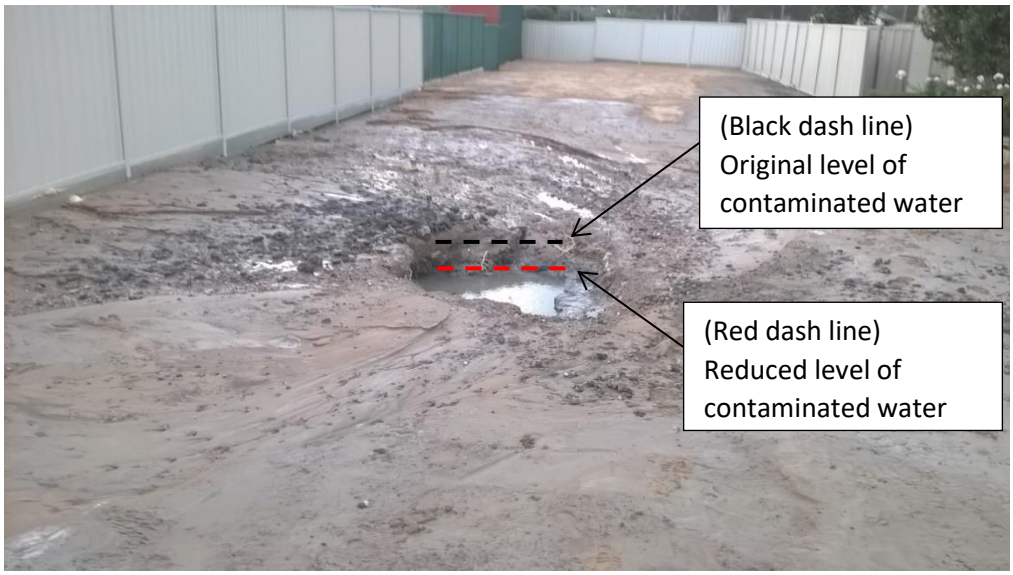

Figure 3-3. The level of contaminated water reduced due to potential intrusion of contaminated water into the pipe.

Contaminant intrusion can result from valve shutdown operations if customers are demanding water within and/or outside of an isolation block during the isolation activities. A series of figures were prepared to better illustrate the occurrence of contaminant intrusion in a burst water distribution pipe. Figure 3-4 shows a water distribution pipe buried underground and surrounded by soil. Under normal conditions, potable water flows through the pipe by gravitational force or pressure from one end to the other. If a pipe burst occurs, potable water will flow out of the pipe through the rupture and into the external environment, as shown in Figure 3-5. The flowing water can erode the surrounding soil, leading to the formation of a

sinkhole, as depicted in Figure 3-6. The mixture of potable water and soil in the sinkhole can contain various chemicals and microbes, making it a source of contaminants. During pipe repair, isolation valves (i.e., valves No. 1 and No. 2 in Figure 3-7) must be sequentially shut off to isolate the damaged pipeline. When there is water demand during isolation activities, negative pressure is created, resulting in a suction effect, as shown in Figure 3-7. Therefore, contaminated water from the sinkhole can travel from the rupture to household taps, leading to poor water quality. When isolation valve No. 2 is not fully closed (Figure 3-8), contaminated water can also infiltrate from the rupture to the damaged pipeline and flow to other network segments, deteriorating the water quality in the WDN.

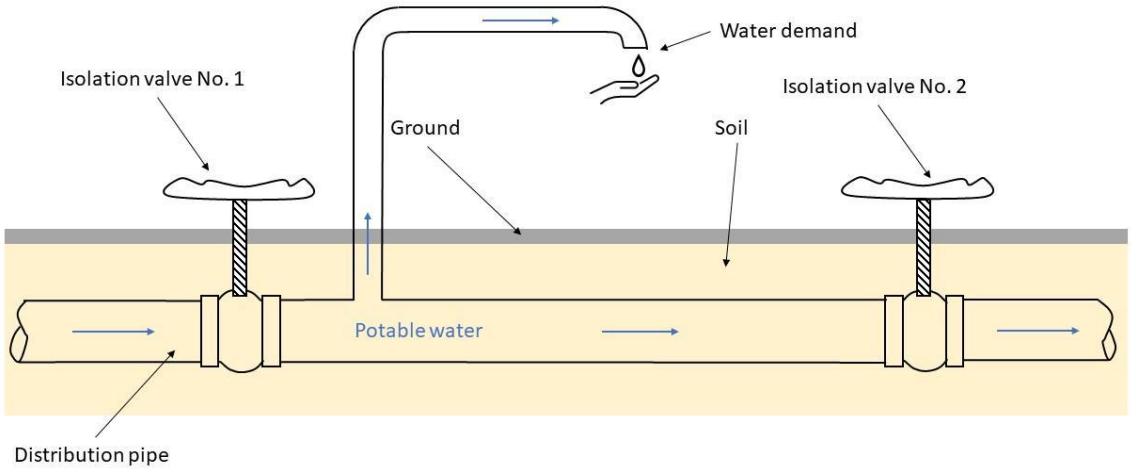

Figure 3-4. A normal water distribution pipe with two isolation valves situated on each side of the pipeline.

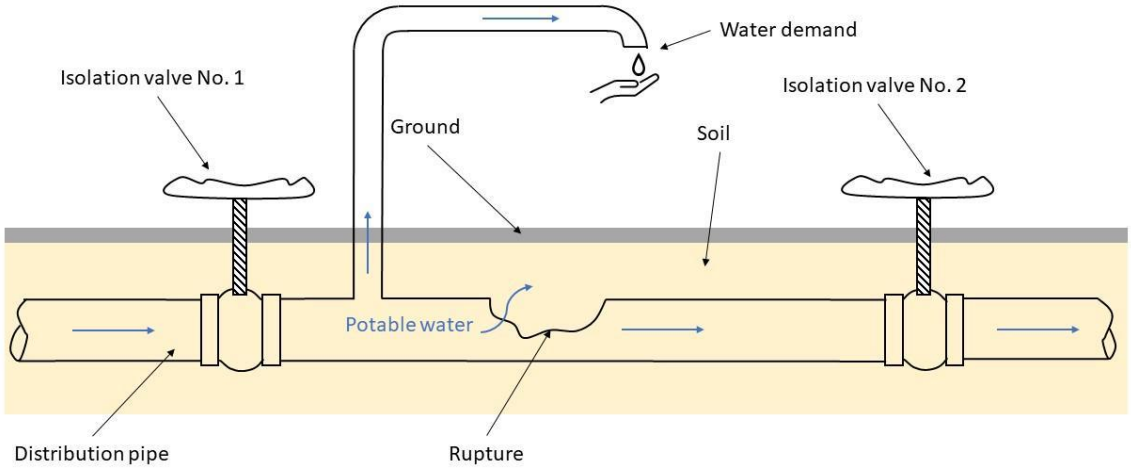

Figure 3-5. A burst occurs on the pipe, causing potable water to escape from this pipe through the rupture.

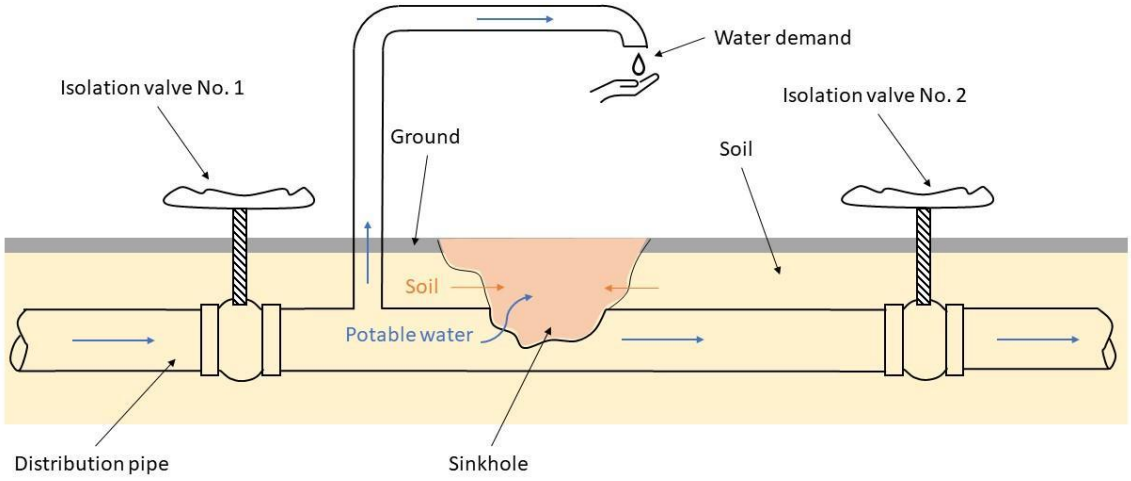

Figure 3-6. A sinkhole was induced by the rupture, leading to the surrounding soil mixing with potable water in the sinkhole.

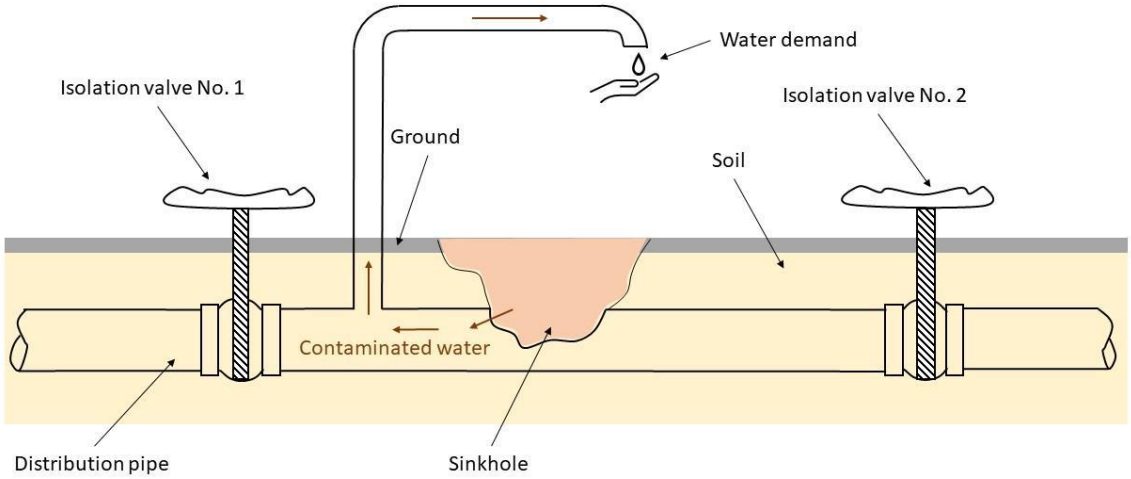

Figure 3-7. Due to the water demand during the isolation activities, negative pressure is created, which leads to a suction effect. Contaminated water can travel from the sinkhole to the distribution pipe and then reach household taps.

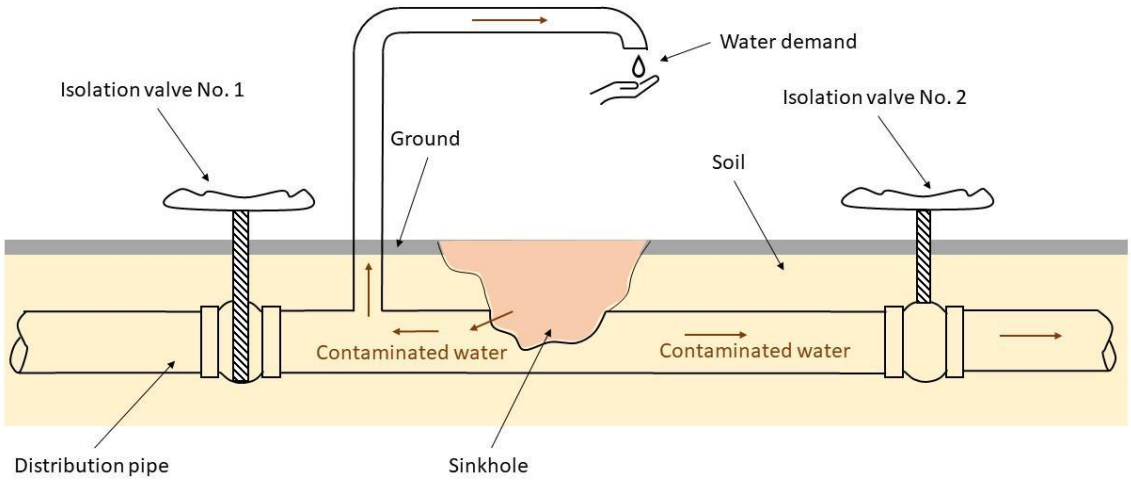

Figure 3-8. In addition to the infiltration from the sinkhole to household taps, contaminated water may also flow from the sinkhole to the distribution pipe and then travel to other network segments if isolation valve No.1 is shut off but isolation valve No.2 is still open.

The volume of a sinkhole can vary significantly, depending on factors such as the angle of repose value of the surrounding soil and other factors such as the cover depth of a particular pipe. A more detailed discussion about these factors is provided in Section 3.4.4.

Table 3-1. Sinkhole volumes calculated by assuming different types of soil and the angle of repose values (StructX, 2022).

Soil type	Angle of repose values (degree)	Assumed angle of repose values (degree)	Sinkhole volume (m^3)
Wet Clay or silt (loose)	20–25	20	16.19
Wet Sandy clay	15	15	29.88
Wet Sandy gravel (loose)	35–45	35	4.38
Wet Sandy gravel (natural)	25–30	25	9.63

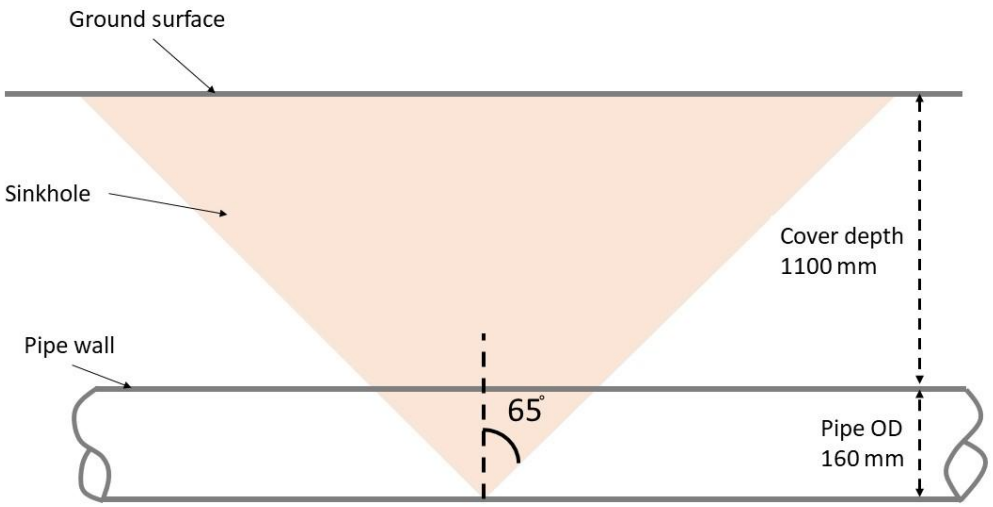

Figure 3-9. Schematic diagram (not-to-scale) of the assumed sinkhole induced by a pipe burst.

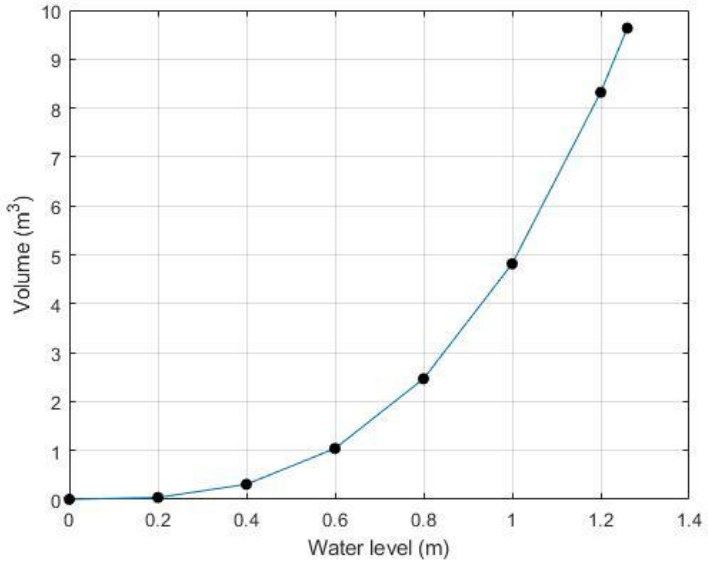

Figure 3-10. Contaminant tank volume with different water levels.

- Establish the burst water pipe:
  (6) A node was selected from the model to represent the location of the pipe burst.
  (7) The selected node was connected to the contaminant tank using a short (1 m long) and smooth (0.01 mm roughness) pipe named the "intrusion link". Flow from the burst pipe was directed to the contaminant tank through this link, and contaminants could flow back through the same link. The diameter of the intrusion link could be adjusted to simulate the required burst flow rate. For instance, a larger diameter intrusion link allowed more water to pass through, increasing the intrusion flow rate. The intrusion link was similar to a burst pipe, as the burst flow in this pipe could be adjusted by changing the internal diameter, similar to changing an orifice size. As an example, an intrusion link diameter of 37 mm was assumed to generate a 24.2 L/s burst flow rate. To model the isolation activities, valve control rules were implemented in the models using EPANET to shut off specific valves at desired times. Contaminant intrusion was determined by observing any changes in flow direction and flow volume in the intrusion link.

This set-up enabled the research to:

- Develop a mathematical formulation of pipe bursts in both single water distribution pipe and loop WDN configurations to help identify the potential occurrence of contaminant intrusion during the valve shutdown process.

- Assess the impact of two different demand modelling approaches (fixed demand and pressure-dependent demand) on the intrusion volumes. Both approaches were applied to the single water distribution pipe and loop WDN models to determine their respective intrusion volumes.
- Study the impact of shutdown duration time of isolation valves on intrusion volumes. The single pipe and loop WDN models were used to simulate different valve shutdown duration times and calculate the corresponding intrusion volumes.
- Evaluate the impact of node elevations on intrusion volumes. The default node elevations in the single pipe and loop WDN models were adjusted to determine how intrusion volumes were affected by strong outflows at lower levels in the network.

3.3 Study One: Contaminant Intrusion in a Single Water Distribution Pipe Model

3.3.1 Potential Contaminant Intrusion during Isolation Activities in a Single Pipe Model

3.3.1.1 Potential Contaminant Intrusion in a Fixed Demand Single Pipe Model

To demonstrate the consequences of a burst in a water distribution pipe, a model of a single pipe was used (Figure 3-11). This model consisted of a reservoir, two isolation valves (V1 and V2), a contaminant tank (introduced in Section 3.1), a demand node (shown in Figure 3-11), and four identical DN150 pipes with a total length of 300 m. The demand node was supplied only by gravity, introduced by different elevations at the reservoir and nodes. The demand node was assumed to supply 800 households, with a 5 L/s water demand, based on an average amount of water usage at 0.18 ML per household in Australia in the financial year of 2020-2021 (Australian Bureau of Statistics, 2022).

The assumed node elevations are depicted in Figure 3-12. The reservoir was assumed to be situated at the highest point (30 m), while the demand node was assumed to be located at the lowest point (10 m). Therefore, there was a pressure difference of 20 m in this single water distribution pipe model. These original node elevations were adjusted to analyze the impacts of node elevations on intrusion volumes in Section 3.3.4.

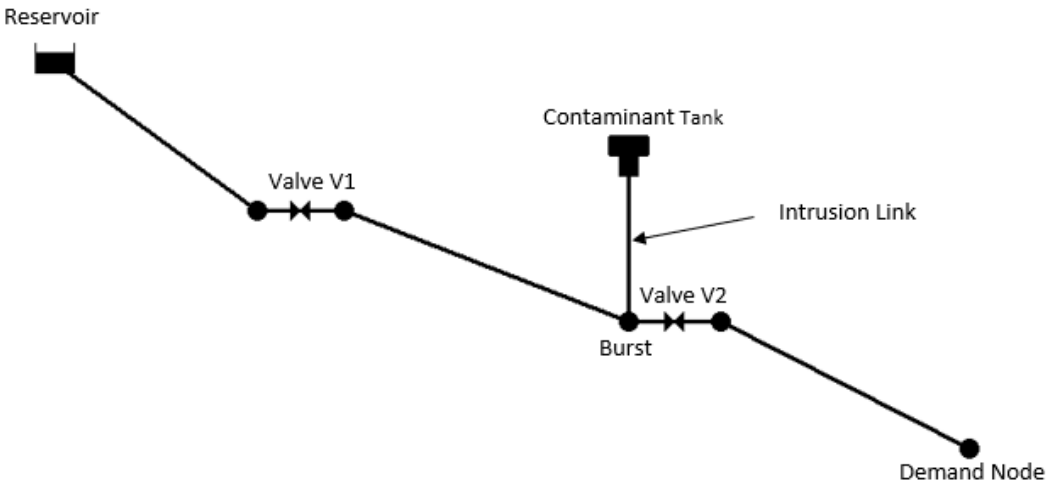

Figure 3-11. A single water distribution pipe model in EPANET.

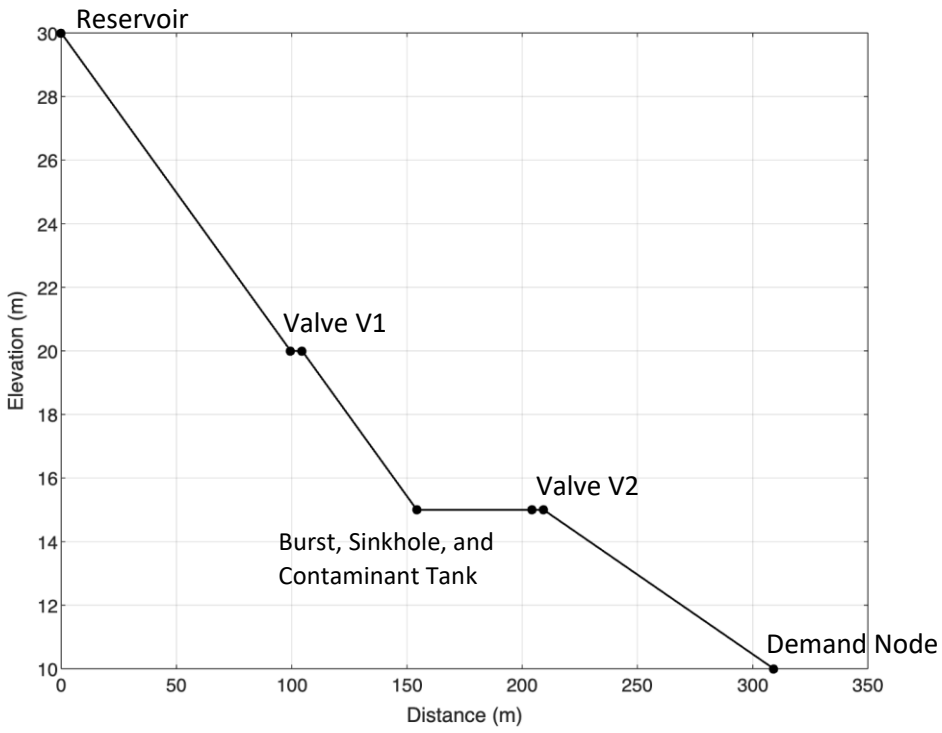

Figure 3-12. Longitudinal view of the single water distribution pipe.

In this single water distribution pipeline model, it was assumed that a burst occurred 200 m away from the reservoir at 02:00 (i.e., 2:00 am in a 24-hour time). A fixed demand modelling approach was applied to the simulation of the pipe burst and isolation activities in the single pipe model. The hydraulic time step was set to 1 min.

Figure 3-13 shows that the flow rate in the intrusion link dramatically increased to 25 L/s during the simulation, causing treated water to flow out of the pipeline through the intrusion link. Valve shutdown operations were not applied to isolate the burst, resulting in a burst flow

that slowly decreased for about 6 mins and then remained constant (indicated by the straight line) until the simulation ended at 03:00 (i.e., time is equal to 3 hours on x-axis in Figure 3-13).

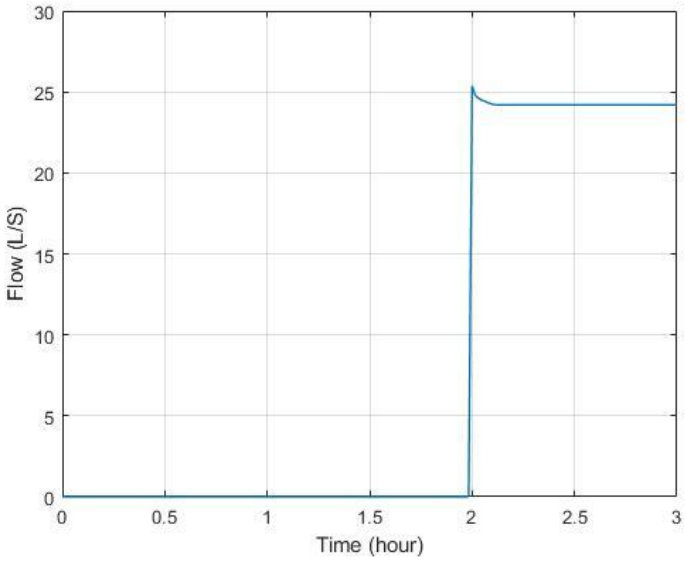

Figure 3-13. Flow in the intrusion link when having a pipe burst in the single water distribution pipe model using fixed demand modelling approach.

To isolate the burst, valve shutdown operations must be conducted before repairing the burst. Two valve shutdown sequences were employed for this purpose:

(1) shut off V1 prior to V2
(2) shut off V2 prior to V1

After simulating both valve shutdown sequences, it was determined that only sequence (1) resulted in contaminant intrusion during the isolation process. By shutting off V1 at 02:30 (30 mins after detecting the pipe burst) and V2 at 02:45, contaminant intrusion occurred at 02:30. Figure 3-14 shows that the flow in the intrusion link dramatically increase from 0 to 25 L/s at 02:00. This change is due to the pipe burst. The flow gradually decreased for several minutes until another dramatic drop from 24.5 L/s to 0. This means that the sinkhole was fully filled.

The flow started to drop from 0 to –5 L/s at 02:30, indicating the intrusion of untreated water into the pipeline from the external environment. It is noted that the flow profile in the intrusion link did not appear as an abrupt drop from 0 to -5 L/s at the exact shutdown time of V1 (i.e., 02:30). This was because EPANET computes the flow in a hydraulic simulation using discrete time steps. It cannot capture the exact time when the flow in the intrusion link

reaches -5 L/s. Thus, the flow profile showed a gradual decrease in flow approaching the shutdown time of V1. The flow eventually increased from -5 L/s to 0 at 02:45. Therefore, the contaminant intrusion lasted for 15 mins, resulting in a maximum intrusion volume of 4.20 m^3. The intrusion volume is a sum of the product from multiplying the inflow (demand) and time for every time step (1 min) during the period of contaminant intrusion. This mathematical operation was used to determine all intrusion volumes in this research.

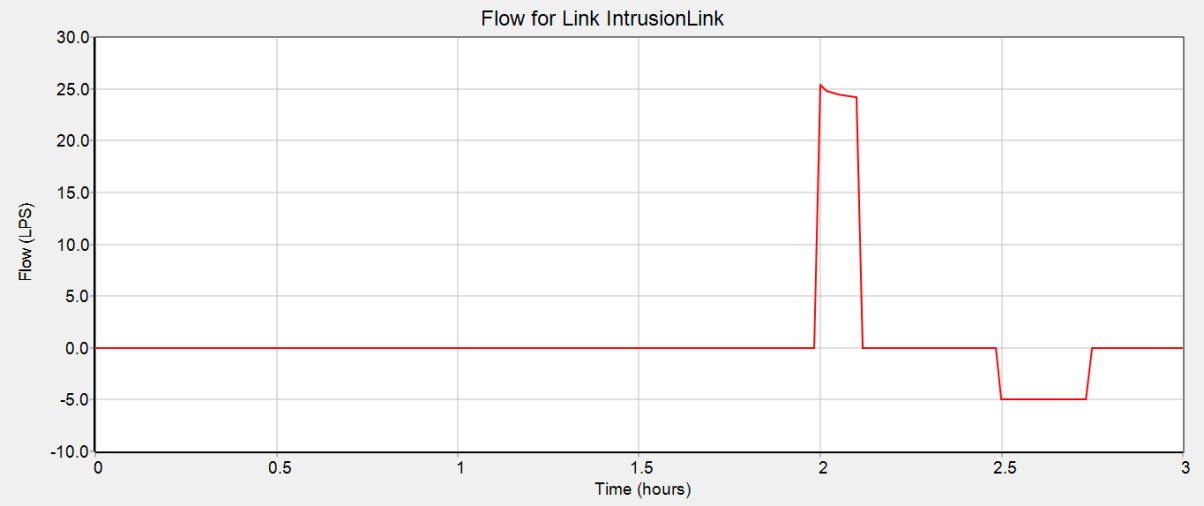

Figure 3-14. Flow in the intrusion link when adopting valve shutdown sequence 1 to isolate the burst in the single pipe model. The water demand in this model is fixed.

Figure 3-15 shows the hydraulic grade lines of the single pipe model's contaminant tank to demand node at three different time steps, including the initial condition of the simulation, burst condition after 2-hour simulation (simulation time 02:00), and burst condition after 3-hour simulation (simulation time 03:00). The initial condition is represented by the blue line. The burst conditions after 2-hour simulation and 3-hour simulation were represented by the red line and yellow line, respectively. The data point of the sinkhole shows an initial head of 44.9 m. The head increases above 46.0 m at 2-hour time step. Although the head of the sinkhole at the end of simulation (03:00) maintains above the initial value, it reveals an obvious drop compared to the value at 2-hour simulation time step. Therefore, it is confident that a pressure drop occurs between 02:00 and 03:00, which acts as the main driving force of contaminant intrusion. This result supports the findings in Figure 3-14.

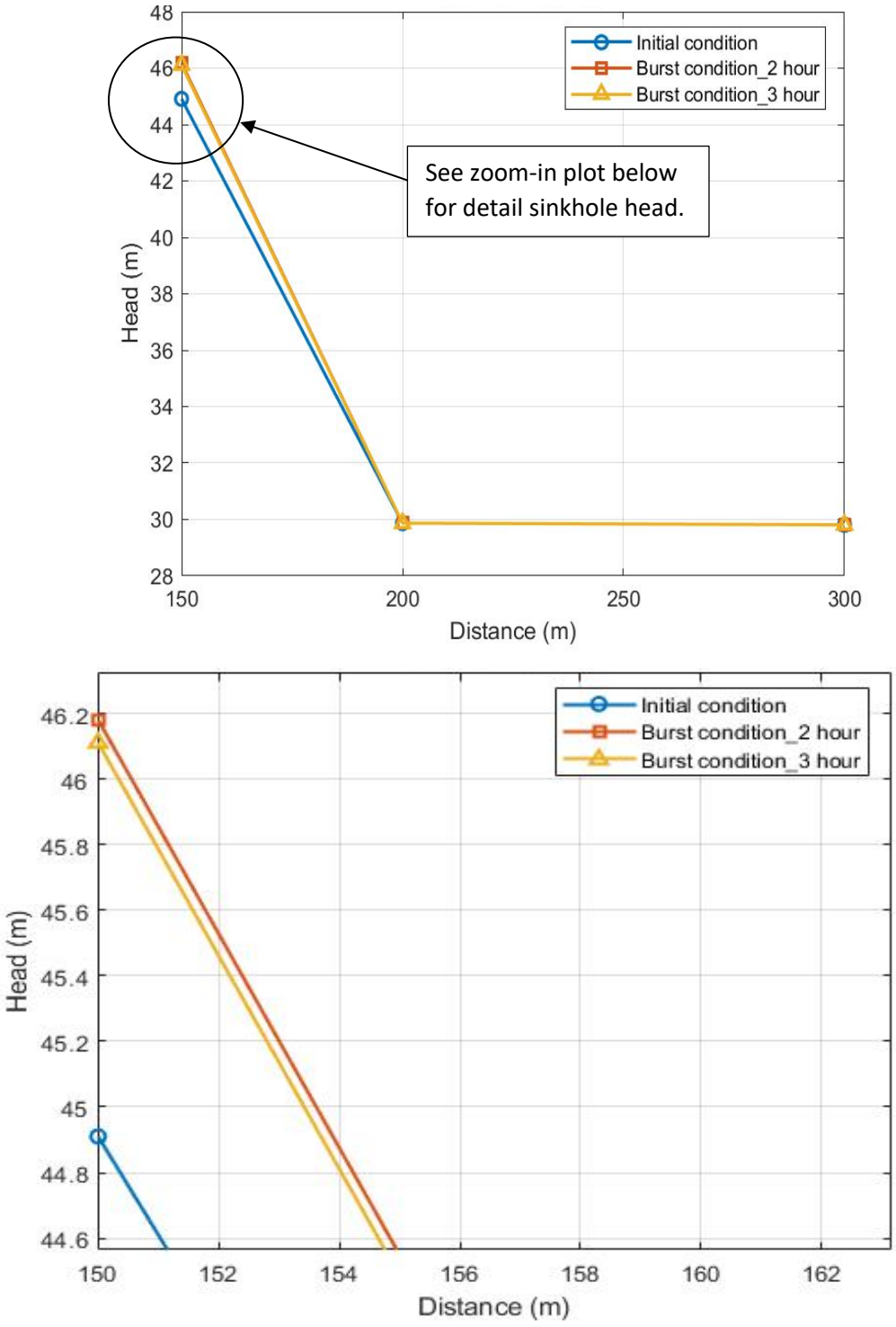

Figure 3-15. Hydraulic grade lines (top figure) of the single pipe model's sinkhole (contaminant tank) to demand node at three different simulation time steps, the initial condition, burst condition after 2-hour simulation, and burst condition after 3-hour simulation (end of the simulation). A zoom-in section of the hydraulic grade lines (bottom figure) to demonstrate the difference in sinkhole's head at three different time steps.

In contrast, valve shutdown sequence (2) did not result in contaminant intrusion. Figure 3-16 shows that the flow in the intrusion link reached 25 L/s when the pipe burst occurred in the model. It gradually decreased for about 6 mins before dropping to zero, indicating that the cone-shaped contaminant tank was fully filled within 10 mins. There was no significant drop

in flow in the intrusion link after the implementation of the valve shutdown sequence at 02:30, indicating no occurrence of contaminant intrusion in the simulation of applying valve shutdown sequence (2) to isolate the burst.

The different outcomes can be attributed to the location of the demand node and isolation valves. Isolation valve V1 was located upstream (i.e., closer to the reservoir), while isolation valve V2 was placed downstream. The demand node was located further downstream from valve V2. When V1 was closed first and the demand node was acquiring water, negative pressure was created and thus leading to a suction effect at the burst. Contaminated water could infiltrate into the pipeline through the ruptured pipe. In contrast, when V2 was closed first, contaminated water could not infiltrate into the pipeline because the demand node was isolated from the ruptured pipe. In this case, water would be drawn from the reservoir to the burst until V1 was closed and the water in the isolated pipe segment (i.e., pipe 2) was fully drawn.

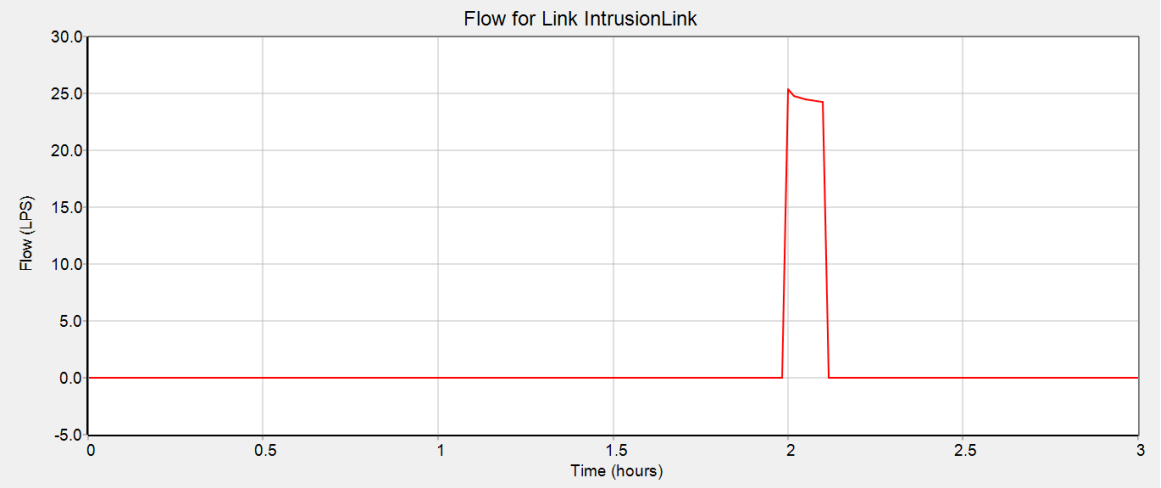

Figure 3-16. Flow in the intrusion link when applying valve shutdown sequence 2 to isolate the burst in the single pipe model. The water demand in this model is fixed.

The above results demonstrate that the valve shutdown sequence is a crucial factor in contaminant intrusion in WDNs. They also provide valuable insights into the challenges of determining the correct valve shutdown sequence(s) in a WDN consisting of numerous pipes, isolation valves, and demand nodes. In most cases, it would be necessary to shut off more than two isolation valves to isolate a ruptured pipe in a WDN. As a result, the isolation process following a pipe burst in a WDN can be complex.

Furthermore, the result implies the potential for valve shutdown operations to increase the intrusion volume - volume of a substantial quantity of contaminated water intruding into

water distribution pipelines. However, it should be noted that the network demand of a WDN may not remain constant in the event of a water pipe burst, primarily due to the pressure loss within the network. Therefore, the subsequent section employs the pressure-dependent demand modelling approach to simulate the same valve shutdown operations in the single pipe model to assess the potential changes in the intrusion volume.

3.3.1.2 Potential Contaminant Intrusion in a Pressure-dependent Demand Single Pipe Model

Adopting a pressure-dependent demand modelling approach to model the same isolation activities in the single pipe model resulted in a smaller intrusion volume. An emitter coefficient of 1.124 was applied to the demand node to simulate a demand equivalent to a fixed 5 L/s demand in the same model. The adoption of the pressure-dependent demand modelling method makes the water demand in this model sensitive to fluctuations in pressure. Valve shutdown sequence (1) as proposed in Section 3.3.1.1 was applied to the single pipe model to simulate isolation activities. Figure 3-17 shows that there was no intercept difference between the blue and brown lines between 02:00 to 02:10, thus, illustrating that the burst flow rate and the filling rate of the contaminant tank for the pressure-dependent demand modelling approach were the same as those for the fixed demand modeling approach. The figure also demonstrates that valve shutdown sequence (1) caused contaminant intrusion. Although both lines in this figure exhibit a significant drop in flow at 02:30, the flow rate (negative sign indicates an intrusion flow), obtained using a pressure-dependent demand modelling approach, increased from 5 L/s to 2.5 L/s during the same isolation process. Accordingly, the intrusion volume was determined to be 1.32 m^3, approximately 69% less than that obtained from the fixed demand modelling approach.

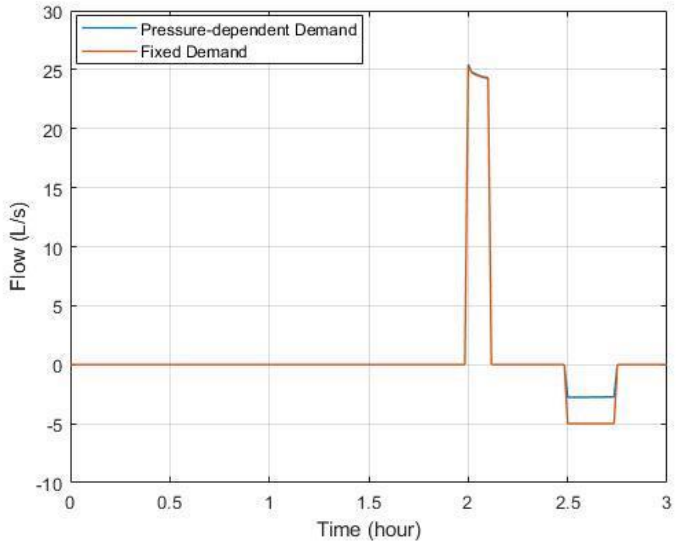

Figure 3-17. Comparison of flow in the intrusion link when implementing valve shutdown sequence 1 to isolate the burst in the single pipe model using pressure-dependent and fixed demand modelling approaches.

Similar to the results obtained using the fixed demand modelling approach, the implementation of valve shutdown sequence (2) did not cause contaminant intrusion even though the demand modelling was driven by pressure. Figure 3-18 shows that the flow in the intrusion link reached 25 L/s when the pipe burst occurred in the model. It gradually decreased over 6 mins before dropping to zero, indicating that the cone-shaped contaminant tank was fully filled. There was no significant drop in flow in the intrusion link at 02:30, indicating no occurrence of contaminant intrusion when applying valve shutdown sequence (2) to isolate the burst in the single pipe model.

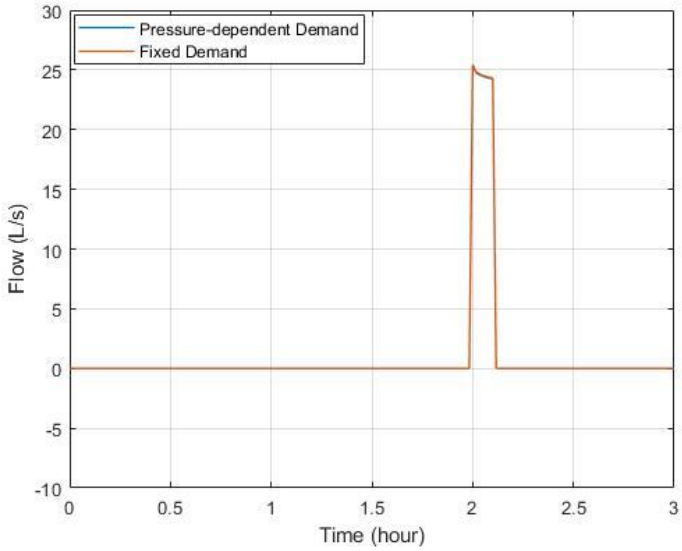

Figure 3-18. Comparison of flow in the intrusion link when implementing valve shutdown sequence 2 to isolate the burst in the single pipe model using pressure-dependent and fixed demand modelling approaches.

3.3.2 Impacts of the Shutdown Duration Time of Isolation Valves in a Single Pipe Model

3.3.2.1 Analysis of the Shutdown Time of Isolation Valves in a Fixed Demand Single Pipe Model

In addition to the factors analysed previously, the duration of shutdown time of isolation valves is another crucial consideration when examining the impact on contaminant intrusion. To enhance the efficiency of isolating pipe bursts, a shorter duration of shutdown time of isolation valves is crucial. A quicker response time will ensure successful isolation of the burst and lead to reduced intrusion volumes. It is thus imperative to assess the impact of various shutdown duration times of isolation valves and the corresponding intrusion volumes.

In Section 3.3.1, the maximum intrusion volume observed in a single pipe model utilizing a fixed demand modelling approach was 4.20 m^3. This volume was obtained when the entire isolation process was completed within 15 mins. To demonstrate the varying intrusion volumes that result from different shutdown duration times of isolation valves, four different shutdown duration times, namely 10, 15, 20, and 30 mins, were assumed and applied to isolate the same pipe burst in the single pipe model. There were only two isolation valves which needed to be closed to fully isolate the burst in the single pipe model. Thus, the shutdown duration time of isolation valves in this model simply represents the gap between two shutdown operations, which is also equivalent to the duration of the isolation process.

Table 3-2. The assumed shutdown times of isolation valves and corresponding intrusion volumes in a single pipe model where demand is fixed.

Shutdown Time of Isolation Valves (mins)	Intrusion Volume (m^3)
10	2.70
15	4.20
20	5.70
30	8.70

Table 3-2 presents the results that demonstrate the impact of valve shutdown duration times on intrusion volume. The data indicates that reducing the valve shutdown duration time from 15 mins to 10 mins can lead to a decrease in intrusion volume from 4.20 m^3 to 2.70 m^3. On the other hand, extending the valve shutdown duration time from 15 mins to 20 mins resulted in an increase in intrusion volume to 5.70 m^3, while further extending it to 30 mins caused the volume to increase to 8.70 m^3.

The results imply a potential correlation between the intrusion volume and shutdown duration time of isolation valves. The linear regression analysis shown in Figure 3-19 suggests a positive linear relationship (Eq. 4) between the shutdown duration time (t) in mins and intrusion volumes (V_{In}) in m^3 as follows:

$$V_{In} = 0.2862\ t \tag{4}$$

The finding indicates that by reducing shutdown duration time of isolation valves by 3.5 mins it is possible to reduce the intrusion volume by 1 m^3. Therefore, it is crucial to complete the isolation process as efficiently as possible to minimize the intrusion volume.

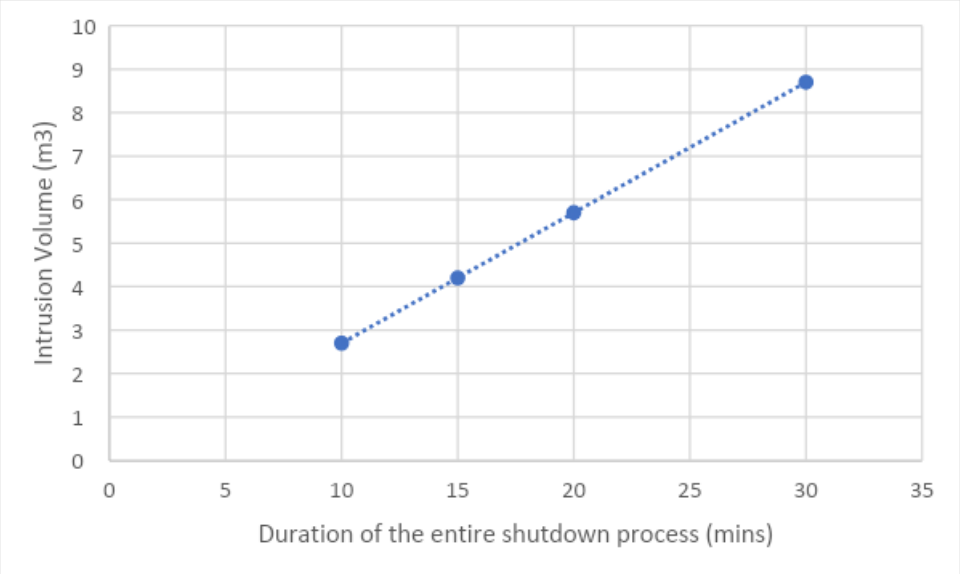

Figure 3-19. Correlation between total shutdown time and intrusion volumes in the single pipe model using fixed demand modelling approaches.

3.3.2.2 Analysis of the Shutdown Time of Isolation Valves in a Pressure-dependent Demand Single Pipe Model

Utilizing a pressure-dependent demand modelling approach to explore the impacts of the shutdown duration time of isolation valves on intrusion volumes support the findings in Section 3.3.2.1. The intrusion volume could be reduced by shortening the shutdown duration time of isolation valves. As shown in Table 3-3, reducing the shutdown time from 30 mins to 20 mins resulted in a reduction in intrusion volume from 2.46 m^3 to 1.65 m^3. Further reducing the shutdown duration time from 20 mins to 15 mins led to a decrease in intrusion volume

from 1.65 m^3 to 1.32 m^3. When the shutdown time was shortened by an additional 5 mins, the intrusion volume reduced to 0.83 m^3.

Table 3-3. Valve shutdown timing and corresponding intrusion volumes in a single water distribution pipeline model with a pressure-dependent demand modelling approach.

Shutdown Duration Time of Isolation Valves (mins)	**Intrusion volume (m^3)**
10	0.83
15	1.32
20	1.65
30	2.46

The outcomes achieved by using pressure-dependent demand in the single pipe model suggest that the intrusion volume correlates to the shutdown duration time of isolation valves. The linear regression analysis shown in Figure 3-20 illustrates a relationship (Eq. 5) between the total shutdown duration time (t) in mins and intrusion volumes (V_{In}) in m^3 as follows:

$$V_{In} = 0.0831\ t \tag{5}$$

The result shows that reducing shutdown duration time of isolation valves by 12 mins has the potential to reduce 1 m^3 of contaminant intrusion. Again, the findings obtained in this section imply that the isolation activities should be finished efficiently to minimize intrusion volumes.

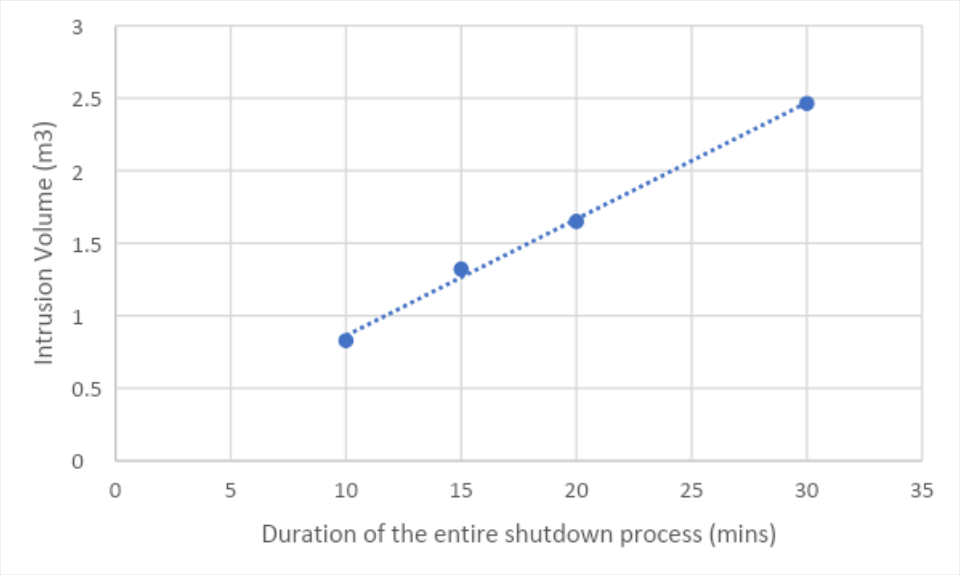

Figure 3-20. Correlation between total shutdown time and intrusion volumes in the single pipe model using pressure-dependent demand modelling approaches.

However, the shutdown duration time of isolation valves may depend on a range of other factors. For instance, isolation operations may require many valves to be turned, leading to difficulties in closing all isolation valves efficiently. In some circumstances, the maximum intrusion volume may be reached before operators can shut off all the required isolation valves. Therefore, the intrusion volume cannot be reduced even if operators have optimized the isolation activities.

3.3.3 Impacts of the Demand Modelling Approach Applied to a Single Pipe Model

The results obtained in Section 3.3.1 show that valve shutdown operations can cause contaminant intrusion in a single water distribution pipe model, regardless of which demand modelling method is used. Meanwhile, the outcomes discussed in Section 3.3.2 imply that the shutdown duration time of isolation valves can affect intrusion volumes in a single pipe model in which the demand is fixed or driven by pressure.

A fixed demand modelling approach is more suitable to use for modelling water demands that are independent of nodal pressure. For example, water demands from toilets and washing machines are based on volume. Thus, volume-based demands remain constant regardless of pressure in WDN models. Pressure-based demands, such as showers and pipe leaks, should be modelled via a pressure-dependent demand modelling approach. This can be achieved by applying an emitter coefficient instead of directly specifying a fixed demand flow at the demand node.

A pressure-dependent demand modelling approach makes the demand during the isolating process sensitive to the pressure variations in WDN models. For instance, when a pipe bursts, there is a loss of pressure in the neighboring pipes connected to the broken pipeline, causing a selected area within the WDN to experience low water pressure. Therefore, the water demand may be reduced due to the low-pressure conditions in the water distribution pipes. In this case, the adoption of a pressure-dependent demand modelling approach may provide a smaller but more realistic intrusion volume under pressure deficient conditions. In contrast, the fixed demand modelling method can provide a more straightforward indication of contaminant intrusion. It can lead to a higher estimated intrusion volume because the analysis assumes a worst-case scenario where demand remains constant under low-pressure conditions.

Similar outcomes have been discovered in the analysis of the impacts of valve shutdown sequences and the shutdown duration time of isolation valves, regardless of which demand modelling approach was used. However, there are factors which may only cause changes in intrusion volume when pressure-dependent demand modelling approach is used. These include node elevations (i.e., network topology) as detailed below.

3.3.4 Impacts of Node Elevations in a Single Pipe Model

3.3.4.1 Analysis of Node Elevations in a Fixed Demand Single Pipe Model

Node elevation, equivalent to the network topology, can significantly impact intrusion volumes for different demand modelling approaches. Figure 3-21 depicts the original and modified node elevations in a single water distribution pipe model. The green line represents the original elevations, while the blue line shows the adjusted elevations at nodes in the same model. Prior to modifying the node elevations, there was a 20 m elevation difference between the reservoir and the demand node (indicated by the green line). However, by increasing the elevations at V1, burst, sinkhole, contaminant tank, V2, and demand node, a flatter topology was simulated. As seen in Figure 3-21, the elevation difference between the reservoir and the

demand node is only 9 m after the topology of the model was changed (indicated by the blue line).

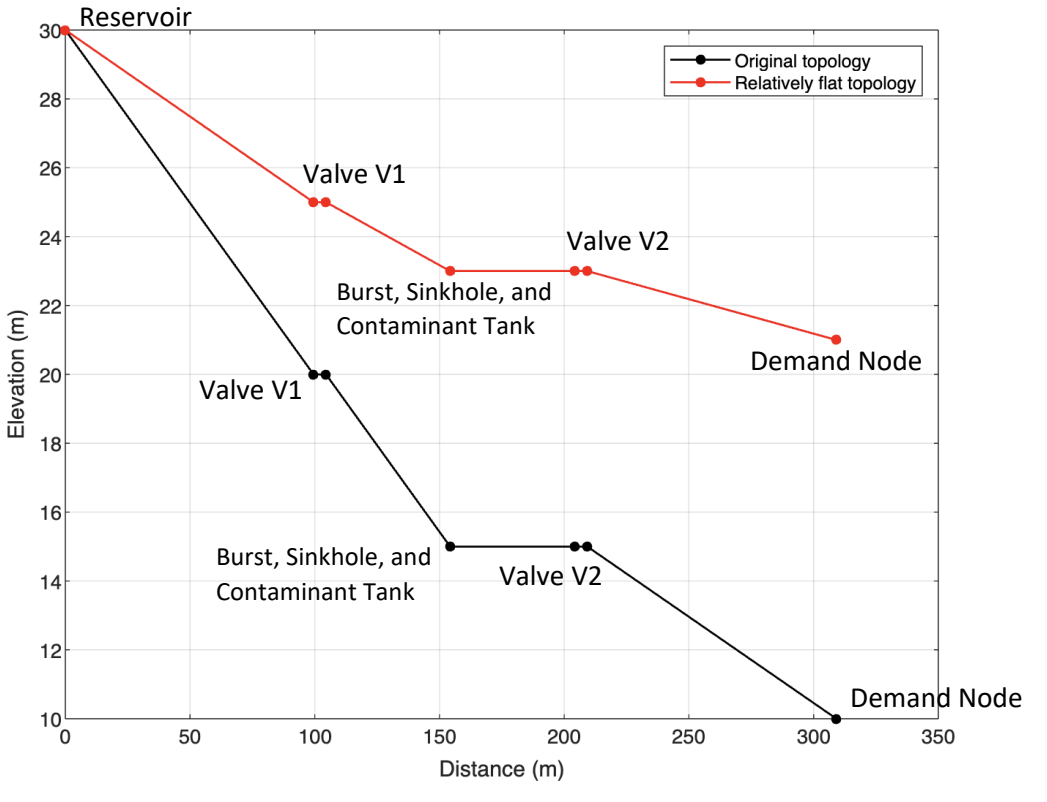

Figure 3-21. Original and adjusted longitudinal view for the single water distribution pipe model.

When a fixed demand modelling approach was employed to simulate valve shutdown operations and pipe bursts in a single water distribution pipe model, it was discovered that changes in topology had no effect on the intrusion flow and volume, as evidenced by the brown line that overlaid the blue lines between 02:30 and 02:45 in Figure 3-22. This is due to the fact that (1) the demand node remained at a lower elevation than the burst (i.e., equivalent to the sinkhole) after changing the topology, and (2) the network demand was not driven by pressure, thus, not affected by changes in node elevations.

The burst flow rate, however, declined as the topology became flatter, thereby leading to a longer duration of the pipe burst. The decrease in the elevation difference between the reservoir and the burst led to a reduction in pressure between the two points. As a result, the burst pipe experienced a decrease in available pressure, resulting in a lower flow rate. Figure 3-22 shows that the burst flow rate was 16 L/s at 02:00, which is 9 L/s lower than the value before modifying the node elevations. Since the burst flow rate was reduced due to a flatter

topology, the filling rate of the contaminant tank also decreased. Thus, the filling process of the contaminant tank was completed at approximately 02:15, which is 5 minutes longer than the outcome obtained before changing the node elevations.

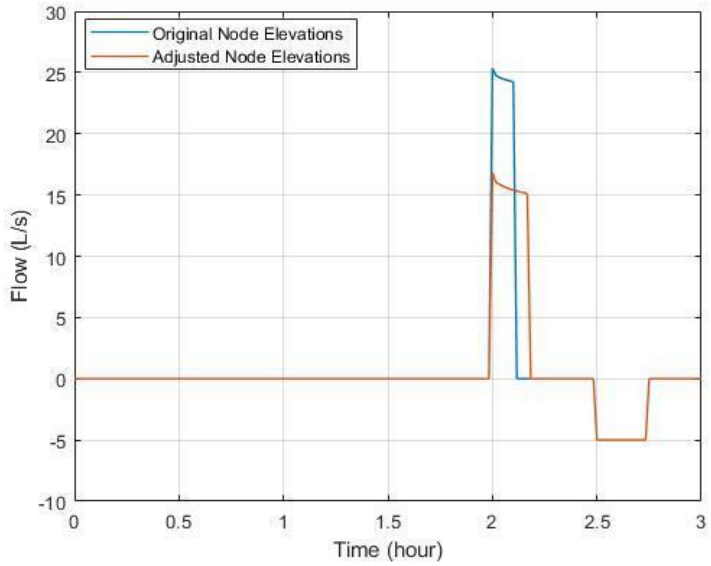

Figure 3-22. Comparison between flows in the intrusion link in the single pipe fixed demand model with original and adjusted topology.

3.3.4.2 Analysis of Node Elevations in a Pressure-dependent Demand Single Pipe Model

On the other hand, modifying the topology in the single water distribution pipe model with a pressure-dependent demand modelling approach resulted in changes to the contaminant intrusion flow rates. As depicted in Figure 3-23, similar to the values observed in Figure 3-22, the burst flow rate reduced significantly from 25 L/s to 16.5 L/s when the topology became flatter, thus, resulting in a longer filling process of the contaminant tank. Unlike the outcomes obtained in the single pipe model with fixed demand, there was a notable difference in the intrusion volume. The intrusion flow rate decreased, leading to a reduction in the intrusion volume from 1.32 m^3 to 0.95 m^3 after changing the node elevations in the single pipe model where demand was driven by pressure. These findings suggest that node elevation can affect intrusion volume when the demand in a single pipe model is driven by pressure. Node elevation can also affect the burst flow rate, regardless of the type of demand modelling approach applied to the single pipe model.

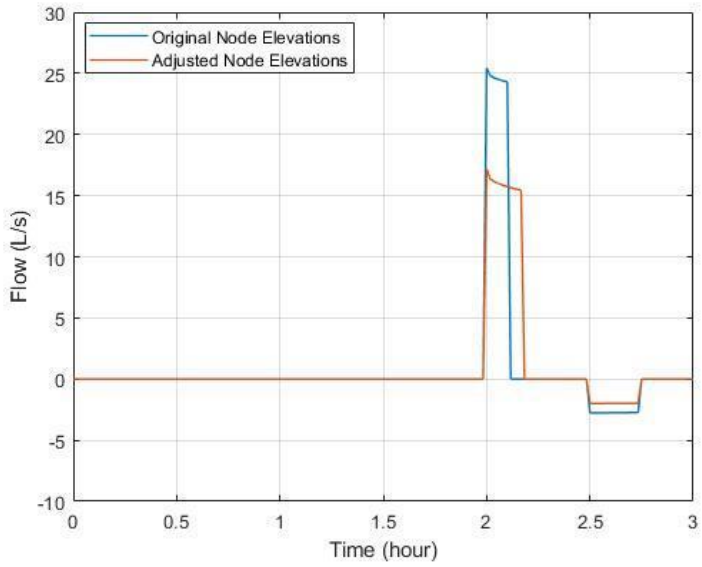

Figure 3-23. Comparison between flows in the intrusion link in the single pipe pressure-dependent demand model with original and adjusted topology.

3.4 Study Two: Contaminant Intrusion in a Loop Water Distribution Network Model

3.4.1 Potential Contaminant Intrusion during Isolation Activities in a Loop Model

3.4.1.1 Potential Contaminant Intrusion in a Fixed Demand Loop Model

When designing WDNs, energy and topologic redundancies are considered to enhance network reliability and reduce hydraulic failures. The concept of energy redundancy is to have nodal pressure greater than the design pressure and to enhance the efficiency of water distribution. Therefore, pipelines in WDNs will often be sized up so that the allowable nodal pressure is greater than the required minimum nodal pressure to satisfy network demand. The core concept of topologic redundancy is that water can be distributed to locations that are demanding water through multiple pathways to facilitate the flexibility and efficiency of water distribution. To achieve topologic redundancy, inter-connected closed loops are commonly designed for WDNs. Therefore, a loop network model is more representative of a real WDN than a single water distribution pipeline model, as it includes more nodes, valves, and pipelines to account for topological and energy redundancies. Accordingly, a single closed loop WDN model was employed to examine the difference in intrusion volumes between fixed or pressure-dependent demand modelling approaches, as well as the maximum intrusion volume resulting from the “worst-case” valve shutdown sequences, and to evaluate the impact of node elevation and valve shutdown timing on intrusion volumes, as shown in Figure 3-24.

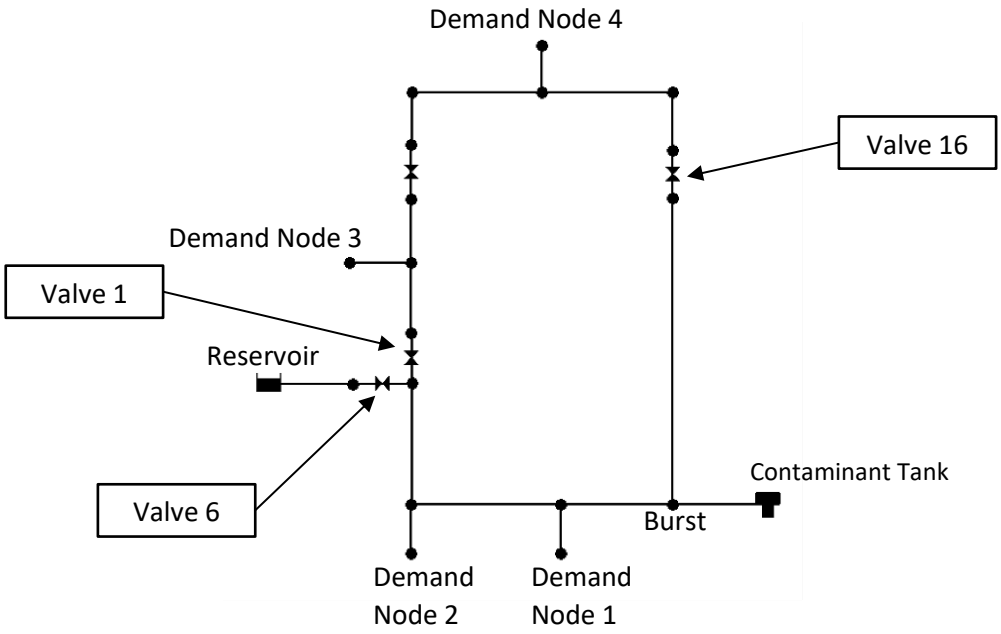

Figure 3-24. Schematic diagram for a single loop WDN model.

The single loop WDN consisted of a reservoir, a contaminant tank, 4 isolation valves, 4 nodes with a demand of 5 L each, a node presenting the burst, 11 pipes with an identical internal diameter of 154.08 mm and a length of 100 m each, an intrusion link connecting the burst and the contaminant tank, and 4 pipes with an identical internal diameter of 63 mm and a length of 5 m to link demand nodes to the network junction. In real-world WDNs, these 4 pipes are often known as meter connections. Different elevations were applied to the nodes, reservoir, and contaminant tank to complete the set up. They were adjusted in Section 3.4.3 to explore the effects of node elevations to intrusion volumes. During the isolation activities, negative demands were observed at nodes Demand2 and Demand3 (shown in Figure 3-24), indicating that potable water was flowing from household taps back to the water distribution network. This direction of supply did not meet the requirement of distributing water from network pipelines to household taps. To prevent negative demands, control valves were applied to the nodes with negative demands to ensure that no water flowed from household taps back to the pipes. To simulate a pipe burst and potential contaminant intrusion following isolation processes, a burst node, a contaminant tank, and an intrusion link, as formulated in Section 3.2, were added to the model.

A loop water distribution network model is typically more complex than a single pipe model due to the presence of numerous isolation valves. In such a looped model, the isolation process can be significantly more complicated as compared to the single pipe model. To fully

isolate a burst in a single loop model, it may be necessary to shut off three isolation valves, valves 1, 6, and 16. Therefore, examining the potential of different valve shutdown sequences to trigger contaminant intrusion in such a model becomes more important.

The following six valve shutdown sequences isolated the pipe burst as shown in Figure 3-24:

(1) 6–1–16
(2) 6–16–1
(3) 1–16–6
(4) 1–6–16
(5) 16–1–6
(6) 16–6–1

Although all the valve shutdown sequences tested in the model successfully isolated the burst, some sequences did not trigger contaminant intrusion in a closed loop WDN. Therefore, to investigate the effects of shutting off the isolation valves in different sequences, the valve shutdown duration time for the six shutdown sequences was fixed regardless of their order. The first isolation valve was always shut off at 02:30, while the second and third valves were always closed at 02:45 and 03:00, respectively. These valves were operated to isolate the pipe burst occurred at the same time slot (02:00) and location (bottom right corner of Figure 3-24). For the simulation of the isolation process in the loop WDN model using the fixed demand modelling approach, the demands at nodes Demand1, Demand2, Demand3, and Demand4 were kept constant at a rate of 5 L/s.

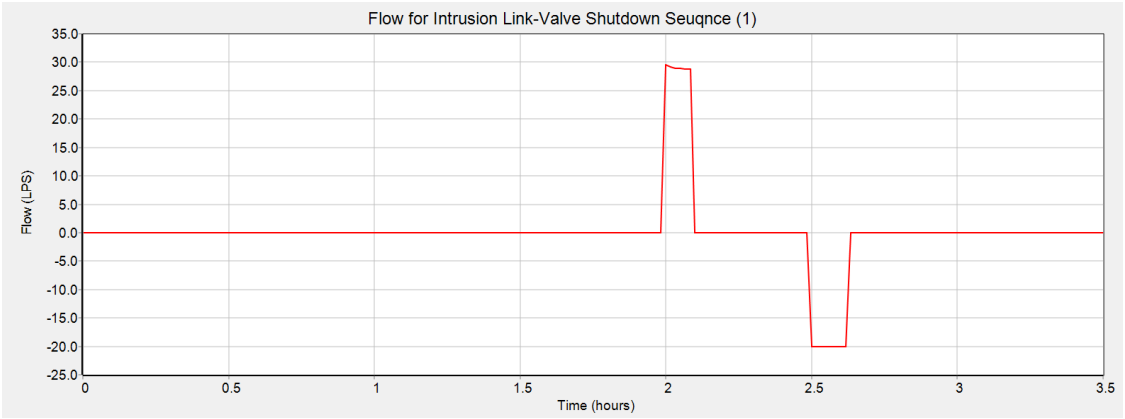
Flow for Intrusion Link-Valve Shutdown Seuqnce (1)
Flow (LPS)
35.0
30.0
25.0
20.0
15.0
10.0
5.0
0.0
-5.0
-10.0
-15.0
-20.0
-25.0
0
0.5
1
1.5
2
2.5
3
3.5
Time (hours)

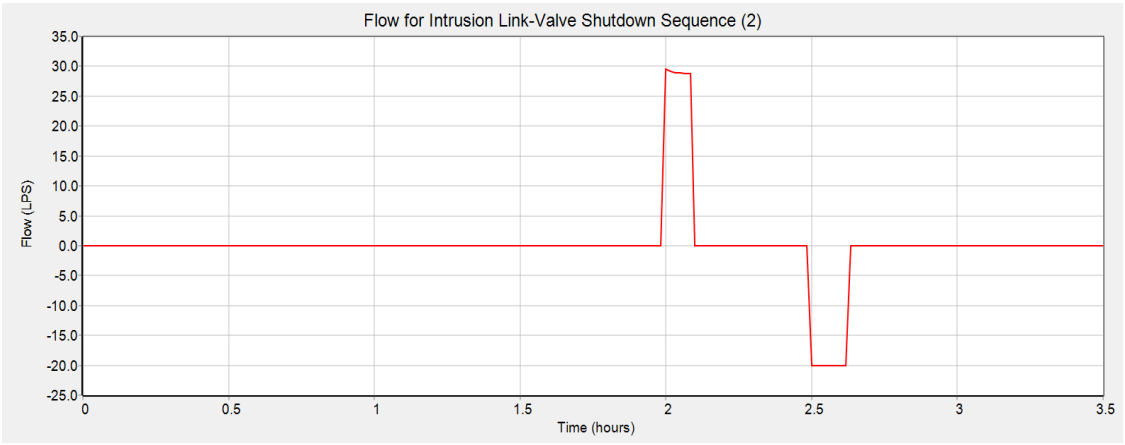
Flow for Intrusion Link-Valve Shutdown Sequence (2)
Flow (LPS)
35.0
30.0
25.0
20.0
15.0
10.0
5.0
0.0
-5.0
-10.0
-15.0
-20.0
-25.0
0
0.5
1
1.5
2
2.5
3
3.5
Time (hours)

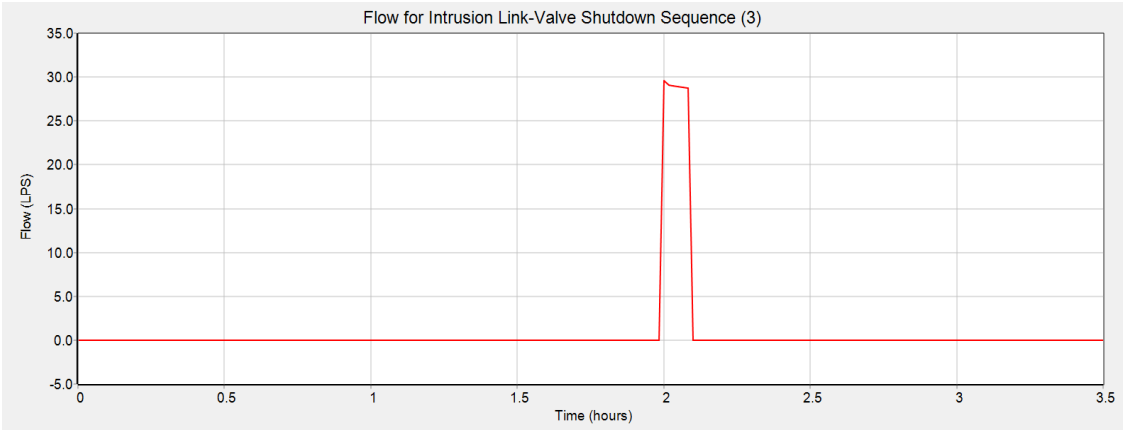
Flow for Intrusion Link-Valve Shutdown Sequence (3)
Flow (LPS)
35.0
30.0
25.0
20.0
15.0
10.0
5.0
0.0
-5.0
0
0.5
1
1.5
2
2.5
3
3.5
Time (hours)

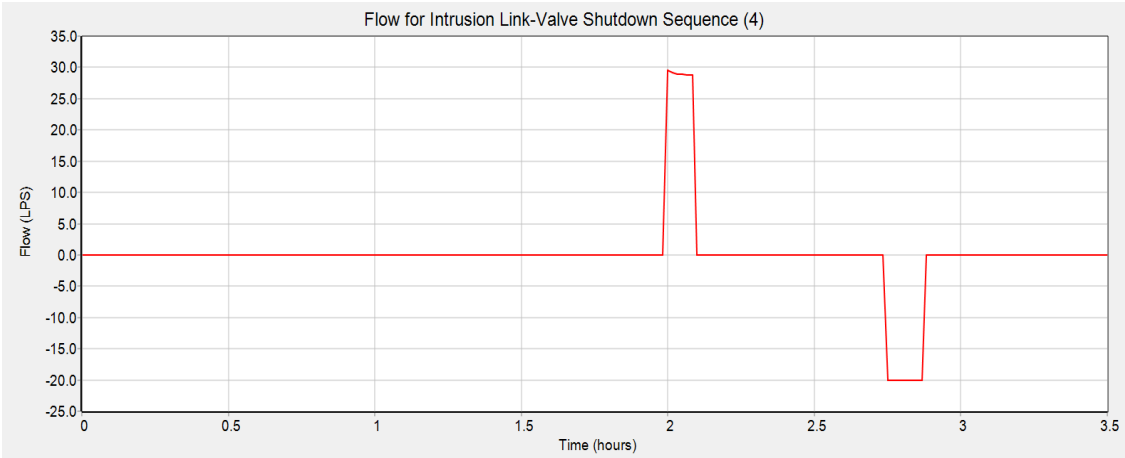
Flow for Intrusion Link-Valve Shutdown Sequence (4)
Flow (LPS)
35.0
30.0
25.0
20.0
15.0
10.0
5.0
0.0
-5.0
-10.0
-15.0
-20.0
-25.0
0
0.5
1
1.5
2
2.5
3
3.5
Time (hours)

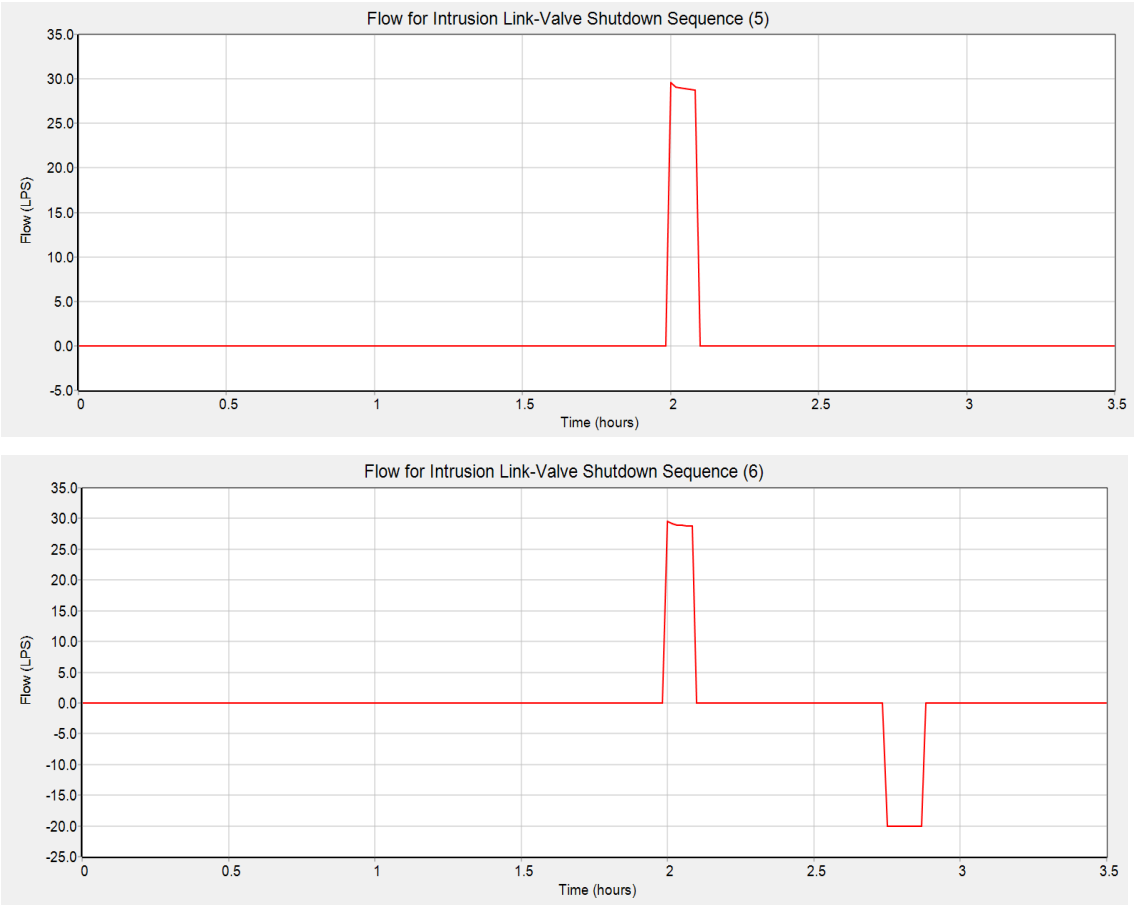

Figure 3-25. Six different valve shutdown sequences and their potential to trigger contaminant intrusion in the single loop WDN model using fixed demand modelling approach.

Figure 3-25 illustrates that valve shutdown sequences (3) and (5) were successful in isolating the burst without triggering contaminant intrusion in the model. To prevent contaminant intrusion, valve 6, which connects to the reservoir, should always be closed last, regardless of the shutdown sequence of valves 1 and 16. It was also observed that valve shutdown sequences (1) and (2) resulted in an earlier occurrence of contaminant intrusion (the U-shaped curve was seen between 02:30 and 02:37) than valve shutdown sequences (4) and (6), even though they resulted in the same intrusion flow rates (20 L/s) and intrusion volumes (8.4 m^3). These results indicate the operational shutdown sequence is a crucial factor that can become complicated when isolating a pipe burst and should be handled rigorously to prevent potential contaminant intrusion.

3.4.1.2 Potential Contaminant Intrusion in a Pressure-dependent Demand Loop Model

The impact of the demand modelling approach on intrusion volumes has been shown to be significant in a single water distribution pipe model. Therefore, it is important to investigate its effects in a single loop WDN model as well.

In order to fully isolate the burst in the single loop WDN model, valves 1, 6, and 16 must be shut off, with six different valve shutdown sequences being possible based on the principle of permutation. However, for the purpose of exploring the potential for valve shutdown sequences to cause contaminant intrusion in the loop model, only valve shutdown sequences (1) and (3) proposed in Section 3.4.1.1 were assessed because they showed distinct potential to cause contaminant intrusion. The shutdown duration times applied to valves 1, 6, and 16 were the same as in Section 3.4.1.1.

The use of a pressure-dependent demand modelling approach in simulating the valve shutdown sequence to isolate the burst in the loop network model resulted in a significant reduction in intrusion volume. The demand at four nodes was represented by applying emitter coefficients listed in Table 3-4, each reflecting a demand of 5 L/s for potable water.

Table 3-4. Emitter coefficients applied to four nodes with demand in the single loop WND model.

Node	Emitter Coefficient
Demand 1	1.050
Demand 2	1.780
Demand 3	1.045
Demand 4	0.915

The results depicted in Figure 3-26 show that despite the burst flow rate being minimally larger than the data obtained from a fixed demand modelling approach, the intrusion flow rate decreased significantly from 20 L/s to 4 L/s during the isolation process. The intrusion volume was calculated to be 3.71 m^3, which was approximately 56% less than that obtained from the fixed demand modelling approach. This outcome supports the findings in Sections 3.3.1.2, implying that a demand modelling approach can affect intrusion volumes in WDN models. The results further suggest that the pressure-dependent modelling approach is advantageous in simulating more realistic intrusion volumes in a WDN model under low pressure conditions because water demand will decline as pressure declines in the network.

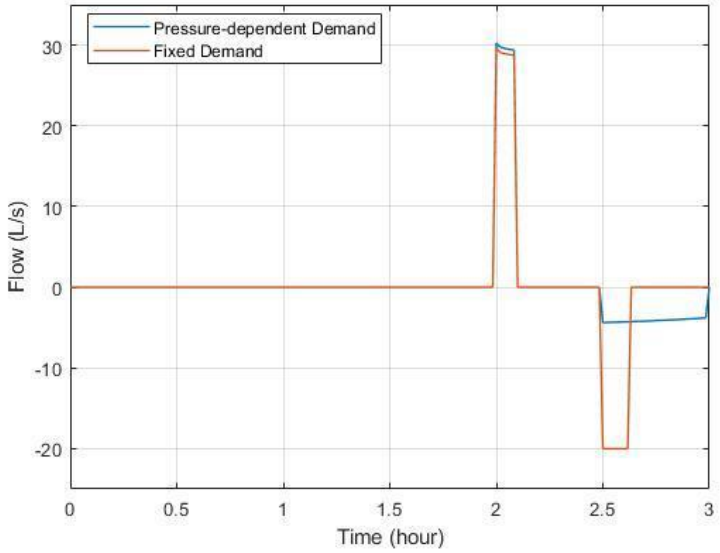

Figure 3-26. Comparison of flow in the intrusion link when implementing valve shutdown sequence 1 to isolate a pipe burst in the single loop WDN model using pressure-dependent and fixed demand modelling approaches.

Similar to the outcome obtained using fixed demand modelling approach, valve shutdown sequence (3) did not lead to contaminant intrusion when the demand in the single loop WDN model was driven by pressure. Figure 3-27 shows that the flow in the intrusion link reached approximately 30 L/s when the pipe burst occurred at 02:00 in the model. It gradually decreased for about 6 mins before dropping to zero, indicating that the cone-shaped contaminant tank was fully filled within 6 mins. There was no dramatic drop in flow in the intrusion link at 02:30, implying no contaminant intrusion occurred when applying valve shutdown sequence (3) to isolate the burst in the loop model.

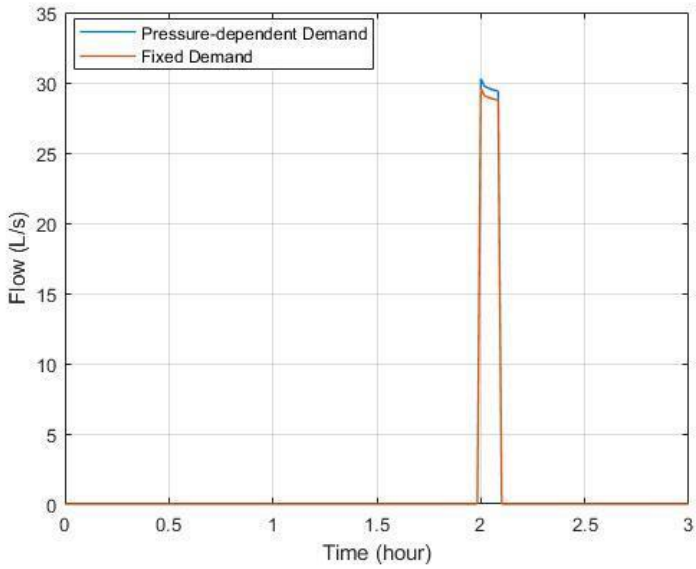

Figure 3-27. Comparison of flow in the intrusion link when implementing valve shutdown sequence 3 to isolate a pipe burst in the single loop WDN model using pressure-dependent and fixed demand modelling approaches.

3.4.2 Impacts of the Shutdown Duration Time of Isolation Valves in a Loop Model

3.4.2.1 Analysis of the Shutdown Time of Isolation Valves in a Fixed Demand Loop Model

As explained in Section 3.3.2, an effective valve shutdown process can reduce intrusion volume in a single water distribution pipe model. In a loop WDN model, where multiple pipes are connected in a loop and more isolation valves may need to be operated to isolate a damaged pipe, it is more critical to investigate the impact of shutdown duration time on intrusion volumes. To investigate this, the same analysis of the shutdown duration time of isolation valves was conducted in the loop WDN model using a fixed demand modelling approach.

Table 3-5. Valve shutdown timing and their corresponding intrusion volumes in a single loop WDN model (fixed demand).

Time Between the Operation of Every Two Valves (mins)	Shutdown Duration Time of Isolation Valves (mins)	Intrusion Volume (m^3)
10	20	9.60
15	30	9.60
20	40	9.60
30	60	9.60

The findings presented in Table 3-5 demonstrate that intrusion volumes did not reduce in the loop WDN model using a fixed demand modelling approach, regardless of the shutdown duration time of isolation valves. It was realized that the intrusion volume corresponding to 20-min shutdown duration time of isolation valves was extremely close to the maximum volume of the contaminant tank (9.63 m^3). The minor difference (0.03 m^3) was because the minimum report time step could not be less than 1 min in EPANET. However, if the simulation accounted for 1 more minute, the intrusion volume would exceed 9.63 m^3. Therefore, the simulation provided an intrusion volume that was reasonably close to the maximum volume of the contaminant tank.

The results imply that the shutdown duration time of isolation valves should be carefully considered when isolating a burst in a WDN; however, maximum intrusion volumes may be reached even if operators complete the isolation activities efficiently. This may be due to:

- The time required to complete many valve turns to fully close a single isolation valve.

- A minimum of two isolation valves must be fully closed to fully isolate a pipe burst. In most cases, more than two isolation valves must be fully shut off. Reasonable time is required to travel between each isolation valve. This time adds to the duration of the entire isolation process.
- The water demand within the isolation block is fixed and large. These two factors lead to the maximum intrusion volume being achieved in 20 minutes.
- The assumed volume of a contaminant tank is not considerably large. In this case, it was 9.63 m^3.

The results also suggest a potential to have greater intrusion volumes during isolation activities. The proposed volume of the contaminant tank (i.e., the total volume of contaminated water) was 9.63 m^3 in this study. This volume would increase when we set up a larger sinkhole in the hydraulic model. Therefore, the maximum intrusion volume could be greater than 9.63 m^3. The intrusion volume would also become more sensitive to the changes in shutdown duration time of isolation valves. The volume would increase significantly as the shutdown duration time of isolation valves became longer. A more detailed discussion is presented in Section 3.4.4.

The results discussed above prompted an analysis of the impacts of the shutdown duration time of isolation valves using a pressure-dependent demand modelling method because demand decreases under low-pressure conditions in a loop WDN model.

3.4.2.2 Analysis of the Shutdown Time of Isolation Valves in a Pressure-dependent Demand Loop Model

The results obtained using a pressure-dependent demand modelling approach differed from those gained from fixing the demand in the model. The findings presented in Table 3-6 demonstrate that the efficient operation of all isolation valves can minimize intrusion volumes in a pressure-dependent demand loop WDN model. Specifically, when the shutdown duration time of isolation valves reduced from 60 mins to 20 mins, the intrusion volume decreased from 6.41 m^3 to 2.53 m^3. By examining the data presented in columns 2 and 3 of the table, it was determined that an approximately additional 1 m^3 of contaminants may infiltrate into the pipe from the external environment if operators spend an additional 10 mins to complete the isolation process.

Table 3-6. Valve shutdown timing and their corresponding intrusion volumes in a single loop WDN model.

Time Between the Operation of Every Two Valves (mins)	Shutdown Duration Time of Isolation Valves (mins)	Intrusion Volume (m^3)
10	20	2.53
15	30	3.71
20	40	4.77
30	60	6.41

The relationship is supported by the polynomial regression analysis presented in Figure 3-28, which indicates a second order polynomial relationship between total shutdown duration time (t) and intrusion volume (V_{In}) as shown in Eq. 6 below. This correlation is only applicable to this single loop WDN model.

$$V_{In} = -0.0005\, t^2 + 0.14\, t \tag{6}$$

The results address the importance of rigorously considering shutdown duration time of isolation valves when performing isolation activities in a WDN. The results also indicate it is possible to minimize intrusion volumes during isolation activities by operating isolation valves with maximum efficiency.

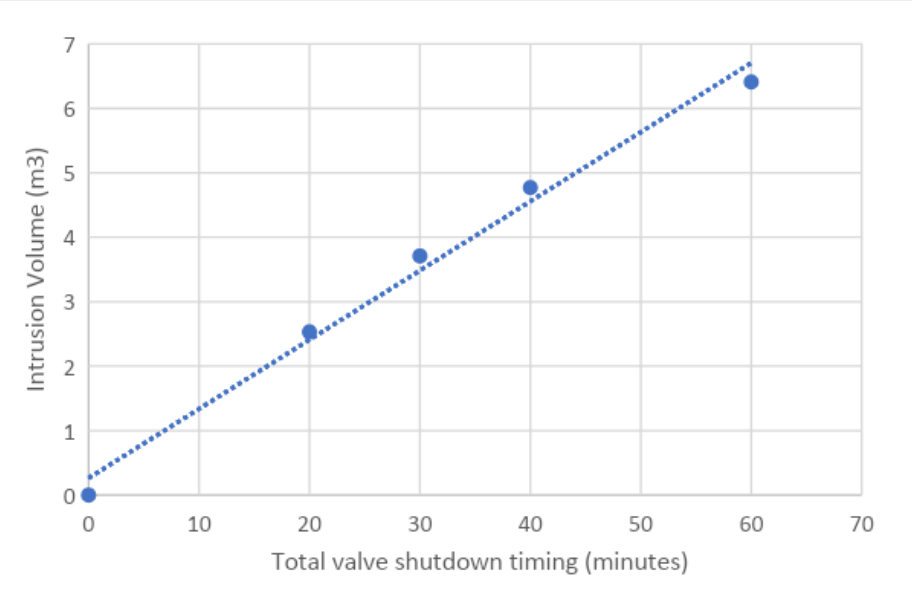

Figure 3-28. Correlation between total valve shutdown timing and intrusion volumes in the single loop WDN mode.

3.4.3 Impacts of Node Elevations in a Loop Model

3.4.3.1 Analysis of Node Elevations in a Fixed Demand Loop Model

Section 3.3.4.1 identified that node elevation alterations may not affect intrusion volumes in a single pipe model that uses a fixed demand modelling approach to simulate valve shutdown sequences for isolating pipe bursts. It was determined similar effects of node elevation should be observed in loop WDN models, as a WDN comprises multiple interconnected water distribution pipes.

To examine the effects of node elevation on intrusion volumes in a single loop WDN model with a fixed demand modelling approach, valve shutdown sequence (1) 6-1-16, as proposed in Section 3.4.1.1, was selected. The following variables were held as constant:

- Demands were fixed at 5 L/s for four nodes Demand1, Demand 2, Demand3, and Demand4.
- The size of the intrusion link remained constant. Thus, the burst flow rate before changing the network topology stayed the same at 30 L/s.
- The valve shutdown sequence and the shutdown duration time of isolation valves as shown below were held constant:

  (1) Close valve 6 at 02:30
  (2) Close valve 1 at 02:45
  (3) Close valve 16 at 03:00

The original node elevations are shown in Figure 3-29, and the altered node elevations are depicted in Figure 3-30. Table 3-7 compares the differences between the original and altered node elevations in the model.

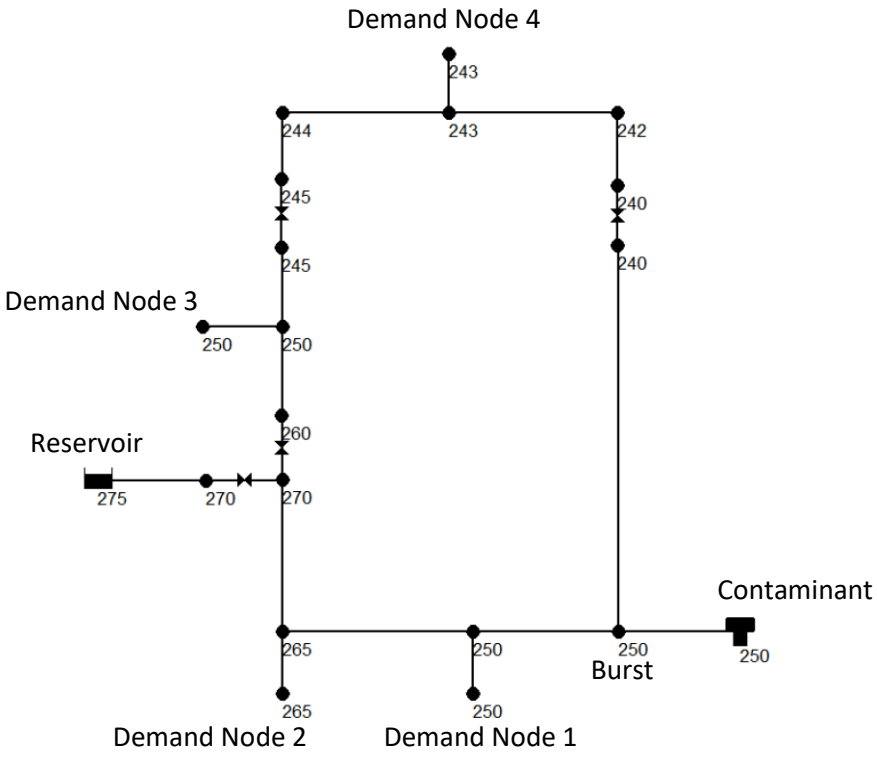

Figure 3-29. Original elevations at nodes in the single loop WDN model.

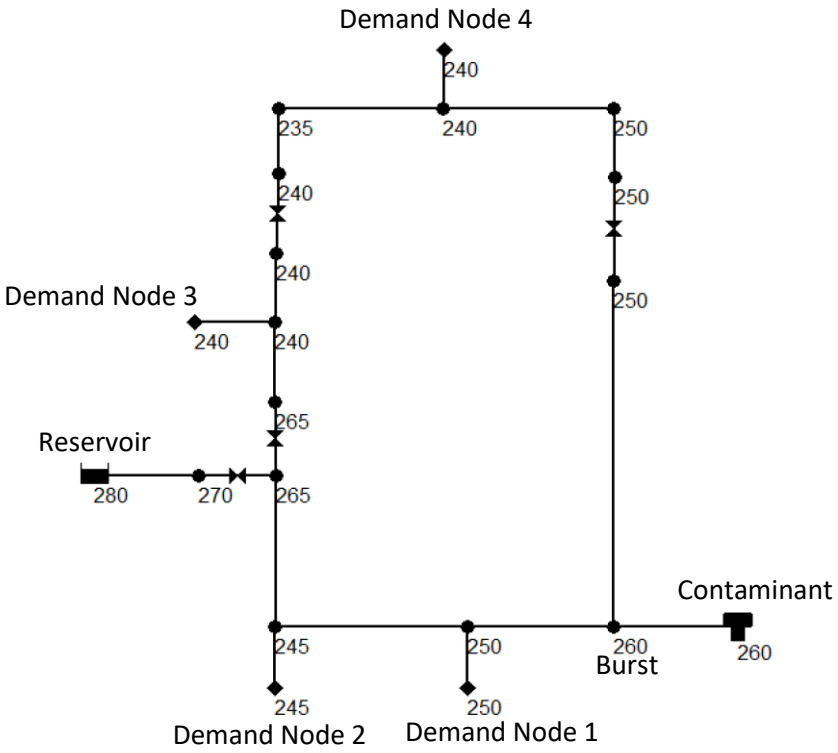

Figure 3-30. Altered elevations at nodes in the single loop WDN model.

Table 3-7. Comparison between the original and adjusted elevations at nodes in the single loop WDN model.

Node	Original Elevations (m)	Adjusted Elevations (m)
7	270	270
8	270	265
14	250	250
11	240	250
12	240	250
1	260	265
17	245	240
18	245	240
2	265	245
Burst	250	260
9	250	240
Demand3	250	240
4	244	235
5	242	250
6	243	240
Demand4	243	240
Demand2	265	245
Demand1	250	250
Reservoir	275	280
ContaminantTank	250	260

The results in Figure 3-31 show that the burst flow rate decreased from about 30 L/s to 25 L/s due to the changes of node elevation of the reservoir in the single loop WDN model. The intrusion flow rate remained constant but contaminant intrusion lasted longer after the node elevations were changed. Thus, the intrusion volume increased from 8.40 m^3 to 9.60 m^3. This indicates the contaminant tank became empty before the isolation activities were accomplished in the single loop WDN model where demand is fixed and when the node elevation was changed. It is noted that this result is different to that obtained in the single pipe model. This is due to the fact that the number of demand nodes situated below the burst and within the isolation block increased after the node elevations were adjusted. Thus, the water demands in the model increased, leading to a larger intrusion volume. The results suggest that node elevation can affect intrusion volume when the demand within an isolation

block in a WDN model is changed such that more demand is located below the burst elevation level.

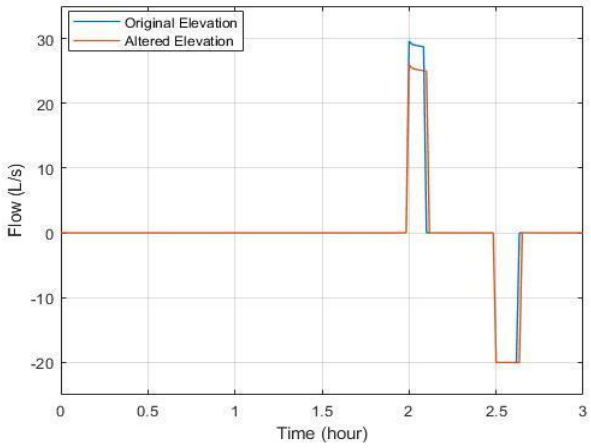

Figure 3-31. Comparison of flow in the intrusion link after completing isolation activities in the single loop WDN model with fixed demand modelling approach adopted.

3.4.3.2 Analysis of Node Elevations in a Pressure-dependent Demand Loop Model

This section illustrates how node elevation alternations could impact intrusion volumes in WDN models where demand is driven by pressure. Again, similar outcomes to the single water distribution pipe model were achieved in the loop WDN models because these systems are built with multiple interconnected water distribution pipes. In addition, the results suggest that node elevation alternations may have greater impacts on WDN models where demand is driven by pressure rather than where it remains constant.

To examine the effects of node elevation on intrusion volumes in a single loop WDN model with a pressure-dependent demand modelling approach employed, the emitter coefficients applied to the four demand nodes were adjusted (Table 3-8) to represent the same demand of 5 L/s. The burst flow rate, valve shutdown sequence and the shutdown duration time of isolation valves were kept the same as in Section 3.4.3.1.

Table 3-8. Updated emitter coefficients for the four nodes with demand in the single loop WDN model.

Node	Emitter Coefficient
Demand 1	0.948
Demand 2	0.872
Demand 3	0.812
Demand 4	0.813

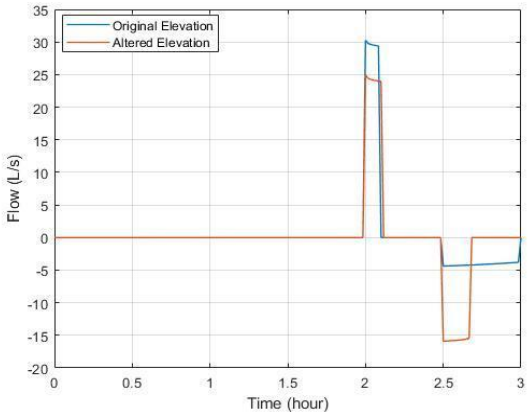

Figure 3-32. Comparison of flow in the intrusion link after completing isolation activities in the single loop WDN model with pressure-dependent demand modelling approach adopted.

Figure 3-32 shows that node elevation can have a significant impact on both burst flow rate and intrusion volumes in a single loop WDN model when using a pressure-dependent demand modelling approach. When the elevations were adjusted, the burst flow rate in the model decreased from 30 L/s to 26 L/s. The original elevations at the reservoir and the burst had a difference of 25 m, resulting in a pressure of 25 m between them, which led to a burst flow rate of 30 L/s. However, when the elevations were increased by 5 m and 10 m, respectively, the pressure between the reservoir and the burst decreased to 20 m, resulting in a lower burst flow rate of 26 L/s. Furthermore, because of the changes to the node elevations, the intrusion flow rate increased from approximately 4 L/s to 16 L/s, and the duration of contaminant intrusion became shorter.

In comparison to an intrusion volume of 3.71 m^3 resulting from the same isolation operations in the loop model with the original topology, a greater quantity of contaminants (5.66 m^3) infiltrated the pipes in this model due to the changes in node elevation. This was because all demand nodes in the altered model were at a lower elevation than the burst, causing them to contribute to negative pressure during the isolation activities. In contrast, in the original model, only one of the four demand nodes was situated below the burst, resulting in less negative pressure during isolation activities. Negative pressure facilitates contaminant intrusion as it creates a suction effect at the burst, allowing contaminants to be drawn from the external environment into the pipe. A weaker suction effect results in a lower intrusion volume due to the reduced negative pressure at the burst.

These results indicate that node elevation should be considered when analyzing pipe bursts and potential contaminant intrusion in WDN models, as nodal pressure can be affected by topology. Furthermore, the magnitude of negative pressure and water demand within an isolation block are the primary driving forces behind contaminant intrusion in WDNs. Lastly, more significant changes in intrusion volumes may be expected in WDN models in which demand is sensitive to pressure.

3.4.4 Factors Affecting the Volume of a Sinkhole and Intrusion Volumes

As discussed in Section 3.2, the maximum volume of the contaminants in the sinkhole was represented by the volume of the contaminant tank. In accordance with the results obtained in the single pipe and loop WDN models, the maximum intrusion volume was equivalent to the volume of the proposed contaminant tank. However, it should be noted that the volume of a contaminant tank (i.e., the sinkhole size) can vary depending on (1) the type of the soil surrounding a ruptured pipe (2) the angle of repose values of the soil, and (3) the depth of the sinkhole. Moreover, the analysis of contaminant intrusion in this study depends on assumptions about the factors mentioned above. As a result, intrusion volumes may vary significantly due to the size of the sinkhole. To illustrate the variation of intrusion volumes resulting from different sizes of sinkholes, several variables were assessed and the corresponding changes in the sinkhole volume were determined.

3.4.4.1 Impact of Sinkhole Depth on Sinkhole Volume

The depth of a sinkhole can significantly affect the sinkhole volume. The bottom of the sinkhole can be anywhere from the bottom of the pipeline upwards. We assumed that the bottom of the sinkhole was situated at the bottom of the ruptured pipe (Figure 3-9) and therefore obtained a sinkhole volume equal to 9.63 m^3. If the bottom of the sinkhole was located at the centreline of the ruptured pipe (Figure 3-33), the depth of the sinkhole would reduce to 1180 mm (1.18 m) and the diameter of the sinkhole would decrease to 5.06 m. Thus, the sinkhole volume was determined as 7.91 m^3.

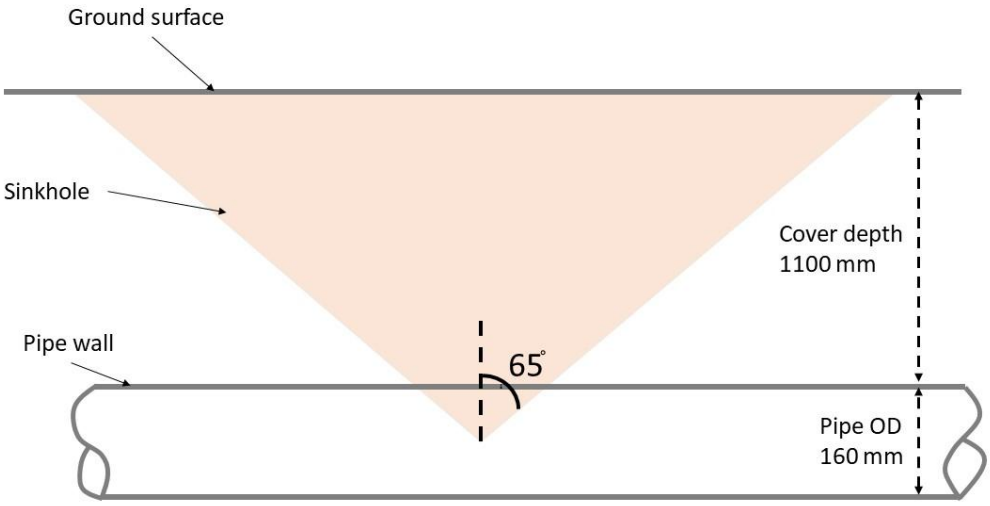

Figure 3-33. Schematic diagram (not-to-scale) of a sinkhole where the bottom was situated at half of the ruptured pipe.

However, if we assume that the bottom of the sinkhole was located at the top of the ruptured pipe (Figure 3-34), the depth of the sinkhole would be equal to the cover depth. The assumed cover depth was 1.1 m. Thus, the diameter of the sinkhole decreased to 4.72 m and the sinkhole volume further reduced to 6.41 m^3.

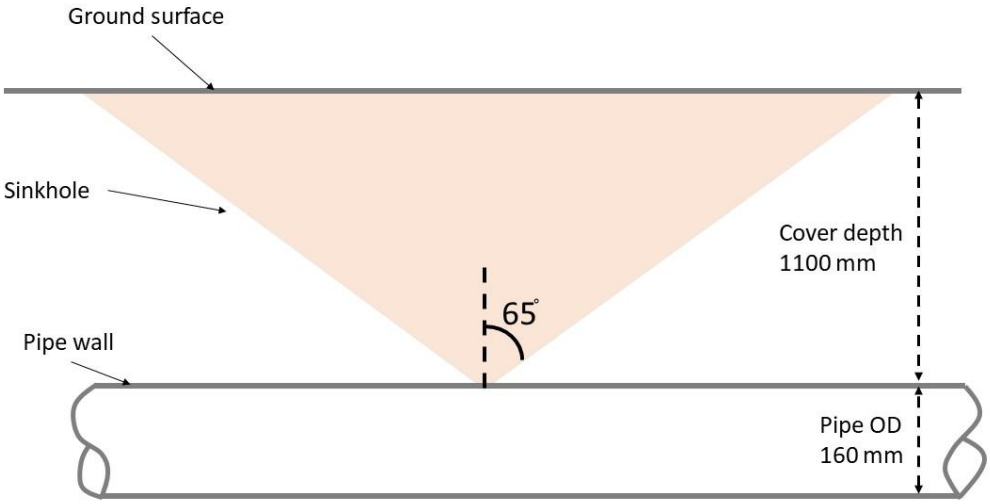

Figure 3-34. Schematic diagram (not-to-scale) of a sinkhole where the bottom was situated at the top of the ruptured pipe.

The minimum cover depth, based on standards, is 750 mm, whereas the maximum cover depth is 1200 mm (SA Water, 2023). If we adopt the minimum cover depth and assume that the bottom of the sinkhole was situated at the top of the ruptured pipeline (Figure 3-35), the sinkhole diameter decreases to 3.22 m and the sinkhole volume would further reduce to 2.03

m^3. Thus, the depth of a sinkhole, especially the location of the bottom of the sinkhole, will significantly affect the sinkhole volume. Accordingly, the intrusion volume can differ substantially.

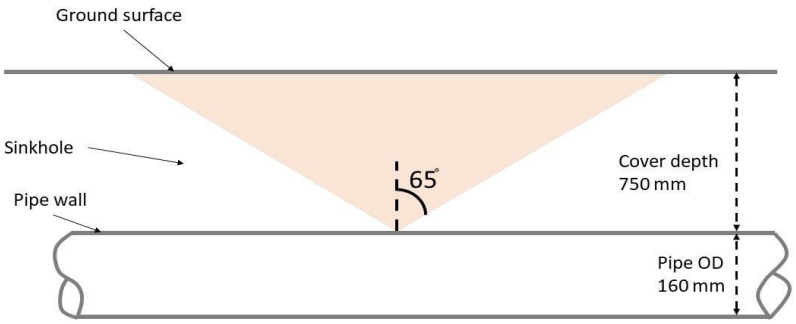

Figure 3-35. Schematic diagram (not-to-scale) of a sinkhole that has a depth equal to the minimum cover depth (750 mm).

3.4.4.2 Impact of Soil Surrounding the Ruptured Pipe on Sinkhole Volume

In Chapter 3, Table 3-1 shows four different soil types, the range of their angle of repose, and the intrusion volumes resulting from the different assumptions about the angle of repose. It was noted that the angle of repose is presented as a range and a singular value was assumed to determine the slide slope of the sinkhole. Moreover, soil friction angle can also affect the side slope of a sinkhole because of the stability of the soil. For instance, the soil friction angle falls within the range of 30-35 degrees for most compacted soils (Al-Hashemi et al., 2018). A good soil, which is possibly moist, may have a friction angle of 30 degrees, whereas a poor soil that may be wet will have a friction angle of 15 degrees (Watkins et al., 2010). As a result, the side slope of a sinkhole depends on the angle of the repose value and friction angle of the soil which forms the sinkhole. As shown in Table 3-9, for a sinkhole formed by wet sandy natural gravel, the soil friction angle was assumed between 15 to 30 degrees. Three different angle of repose values, namely 20, 25, and 30 degrees, were selected. Accordingly, the side slopes of the sinkhole and corresponding volumes were determined. In accordance with the angle of repose values, the sinkhole volume increased significantly from 6.28 m^3 to 15.81 m^3 because of a 10 degree increase in the side slope. Therefore, the type of soil surrounding a ruptured pipe can have a crucial impact on the volume of a sinkhole.

Table 3-9. Sinkhole volumes resulted from different angle of repose values of wet natural sandy gravel (Watkins et al, 2010).

Soil type	Assumed angle of repose values (degree)	Assumed friction angle (degree)	Side slope of the sinkhole	Sinkhole volume (m^3)
Wet Sandy gravel (natural)	20	Between 15 and 30	60	6.28
Wet Sandy gravel (natural)	25	Between 15 and 30	65	9.63
Wet Sandy gravel (natural)	30	Between 15 and 30	70	15.81

However, we may observe a potential to have a large intrusion volume in a small sinkhole. The intrusion volume can exceed the maximum volume of the sinkhole if a large amount of water is discharged from the ruptured pipe. Water can keep flowing from the burst pipe to the natural surface when the sinkhole is full. A more detailed discussion is provided in Section 5.5.7.

3.4.4.3 Impact of the Elevation of a Pipe Burst on Sinkhole Volume

If a burst occurs at a substantial low point in a WDN, the difference in pressure between the reservoir and the burst location can be significant, leading to a large sinkhole. When this pressure difference becomes extremely high (e.g., close to infinite), the burst location becomes a direct pathway from the reservoir (at high point or high pressure) to the burst (at low point or low pressure). Water will continuously fill the sinkhole to restore pressure balance. In a hydraulic model, it can be assumed that the contaminant tank has the potential to overflow. Thus, when a water pipe burst occurs, water will keep flowing from the rupture to the contaminant tank through the intrusion link. The sinkhole will be continuously filled with water from the ruptured pipe. Ultimately, water will overfill the sinkhole and flood the surrounding natural surface, resulting in a substantially larger sinkhole that may be viewed as a reservoir.

Chapter 4 Investigating the Best Valve Shutdown Sequence(s) to Eliminate or Minimize Contaminant Intrusion in Simple Loop WDN Models

4.1 Introduction

The preceding chapter examined the detrimental effects of operational shutdown procedures during isolation activities in WDNs. The results demonstrated that certain valve shutdown sequences can increase the likelihood of contaminant intrusion in WDNs. Even a small quantity of contaminants can cause acute health concerns if their concentrations are above the regulated levels. Thus, conducting a comprehensive assessment of all applicable valve shutdown sequences and determining the optimal operational shutdown sequence(s) that can prevent contaminant intrusion during isolation activities in WDNs is imperative. It is equally important to identify the most efficient valve shutdown sequence(s) that can minimize intrusion volumes in scenarios where it is not feasible to prevent contaminant intrusion.

The purpose of this chapter is to identify the most effective valve shutdown sequence(s) for eliminating contaminant intrusion or minimizing intrusion volumes during isolation procedures in simple loop WDNs using fixed demand and pressure-dependent demand modelling approach. The following two objectives underpinned the goal of identifying the most effective valve shutdown sequence(s) for preventing contaminant intrusion or reducing intrusion volumes during isolation activities in simple loop WDNs:

- To justify the feasibility of preventing contaminant intrusion by implementing the most effective valve shutdown sequence(s).
- To evaluate the best valve shutdown sequence(s) for minimizing intrusion volumes in situations where it is not feasible to prevent contaminant intrusion.

To facilitate understanding of the simulated outcomes, the same single loop WDN model and proposed valve shutdown sequences implemented in Chapter 3 were used again. The fixed and pressure-dependent demand approaches utilized in this model are introduced in Sections 4.2.1 and 4.2.2, respectively. As depicted in Figure 4-1, isolation valves 1, 6, and 16 needed

to be shut off to successfully isolate the burst in the single loop WDN model. The valve shutdown sequences proposed to isolate the burst pipe in the single loop WDN model were:

(1) 6–1–16
(2) 6–16–1
(3) 1–16–6
(4) 1–6–16
(5) 16–1–6
(6) 16–6–1

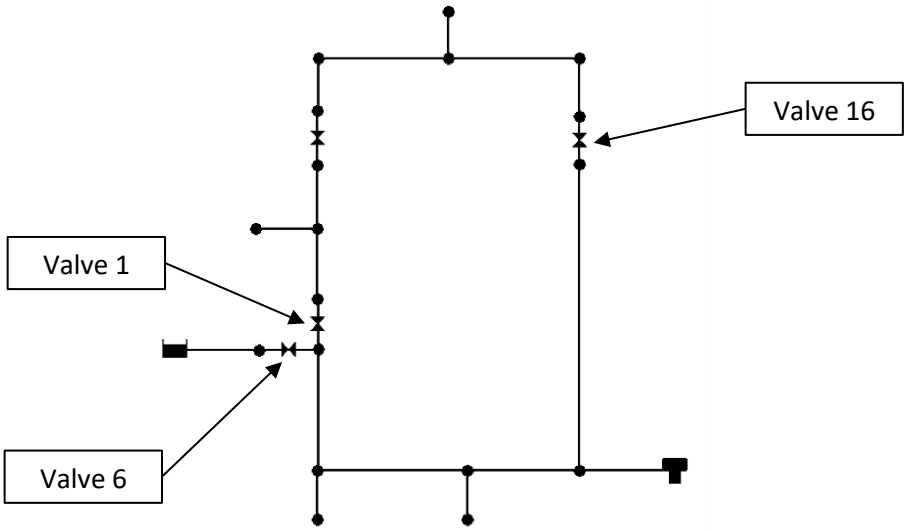

Figure 4-1. Locations for three isolation valves that were operated to isolate the burst in a single loop WDN model.

4.2 Elimination of Contaminant Intrusion Utilizing the Best Operational Shutdown Sequence(s)

4.2.1 Feasibility of Eliminating Contaminant Intrusion in a Fixed Demand Loop Model

To simulate the valve shutdown sequences in the single loop model using the fixed demand modelling approach, the demands at nodes Demand1, Demand2, Demand3, and Demand4 were fixed at 5 L/s. The result, shown in Figure 4-2, suggests that contaminant intrusion could be eliminated by adopting valve shutdown sequences (3) and (5) as the corresponding intrusion volumes were zero. In contrast, valve shutdown sequences (1), (2), (4), and (6) led to the same intrusion volume of 8.4 m^3. This finding implies that valve 6, which is situated

closest to the reservoir, should be closed at the end of a shutdown procedure to prevent contaminant intrusion during the isolation process in this model.

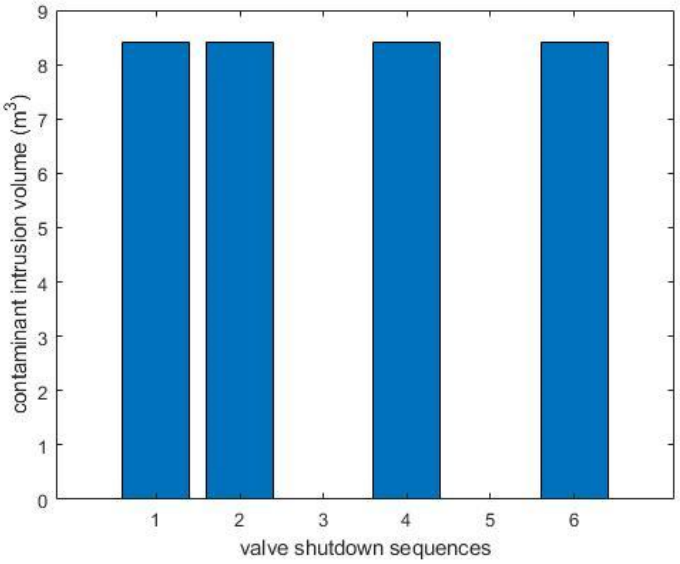

Figure 4-2. Intrusion volumes resulted from six different valve shutdown sequences in the single loop WDN model where demand is fixed.

4.2.2 Feasibility of Eliminating Contaminant Intrusion in a Pressure-dependent Demand Loop WDN Model

To switch from a fixed demand to a pressure-dependent demand modelling approach in this model, the fixed demand of each node was replaced by the emitter coefficients listed in Table 4-1.

Table 4-1. Emitter coefficients applied to four nodes with demand in the single loop WND model.

Node	Emitter Coefficient
Demand 1	1.050
Demand 2	1.780
Demand 3	1.045
Demand 4	0.915

Figure 4-3 demonstrates a similar outcome to the fixed demand modelling approach outcome in Section 4.2.1. It was feasible to prevent contaminant intrusion utilizing valve shutdown sequences (3) and (5). The adoption of other valve shutdown sequences caused contaminant intrusion in the model. The corresponding intrusion volumes were lower than the values (8.4 m^3) determined for the fixed demand model (see Figure 4-2). This is because the network

pressure reduced during a pipe burst incident and the demand was sensitive to the loss of pressure, as discussed in Section 3.3.3. Therefore, we observed lower intrusion volumes during the isolation activities in this analysis.

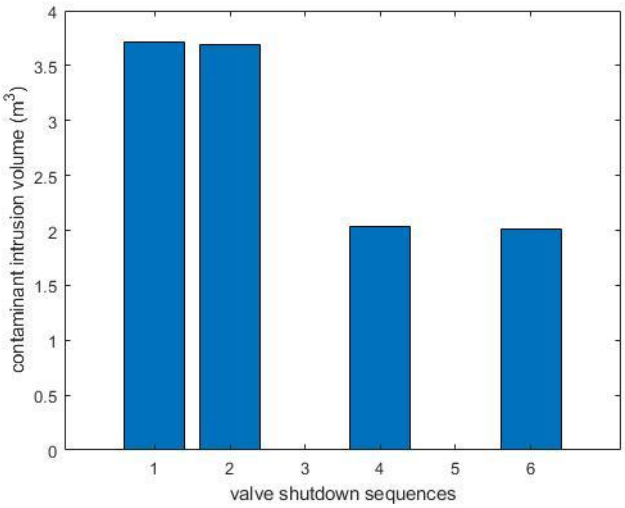

Figure 4-3. Intrusion volumes resulted from six different valve shutdown sequences in the single loop WDN model where demand is driven by pressure.

However, it is unlikely that contaminant intrusion can be avoided in WDNs of any size at all times. This indicates the potential for isolation activities to cause contaminant intrusion in WDNs. This also indicates it is necessary to identify the most effective valve shutdown sequence(s) for minimizing intrusion volumes.

4.3 Minimization of Contaminant Intrusion by Adopting the Most Effective Valve Shutdown Sequence(s)

In a moderately complex WDN model such as the triple-loop WDN model (Figure 4-4) in which the volume of the sinkhole is very large, contaminant intrusion may not be prevented by implementing the most effective valve shutdown sequence(s) to isolate a burst. The discussion in this section is based on the assumptions:

- The model consists of three loops that include six demand nodes.
- The burst is situated 400 m from the reservoir.
- The sinkhole is represented by the contaminant tank which is connected to the burst using the same intrusion link (1 m long and 0.01 mm roughness) formulated in Section 3.2.

- The cone-shaped contaminant tank (representing the total volume of contaminants held by the sinkhole caused by the burst) has a height of 1.26 m and diameter of 5.40 m, resulting in a volume of 9.63 m^3.

Simulations were conducted to isolate the burst using all applicable valve shutdown sequences and to determine the most effective valve shutdown sequence(s) to minimize the intrusion volume in fixed and pressure dependent demand triple-loop WDN models.

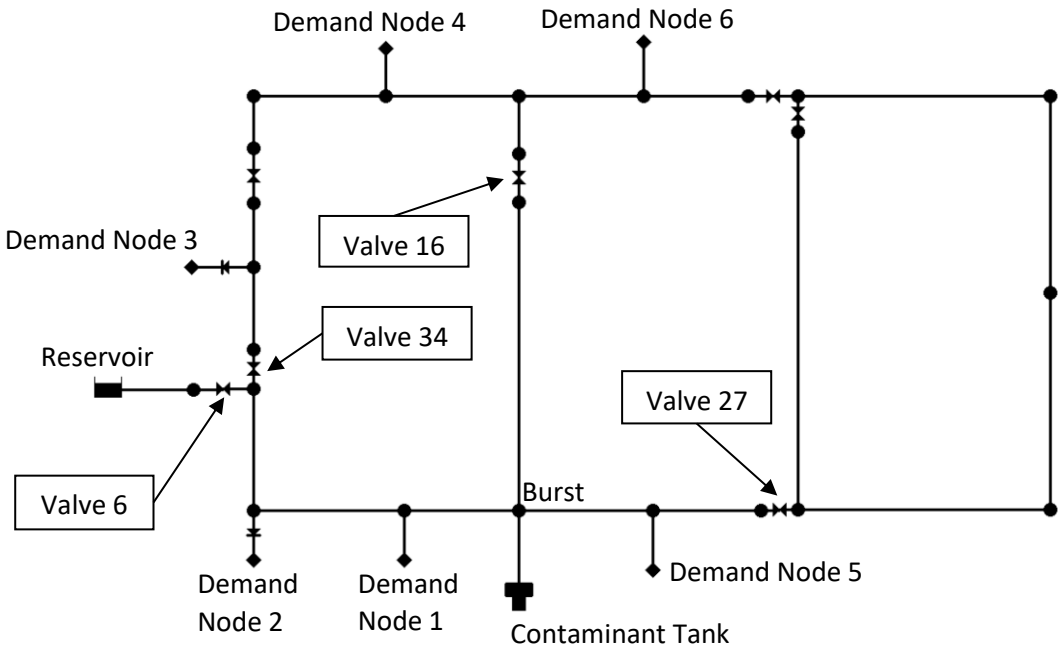

Figure 4-4. Schematic diagram of a triple loop WDN model.

4.3.1 Minimization of the Intrusion Volume in a Fixed Demand Loop Model

To simulate all applicable valve shutdown sequences in the triple-loop WDN model using the fixed demand modelling approach, the demands at 6 demand nodes (i.e, Demand1 to Demand 6 in Figure 4-4) were fixed at 5 L/s. To isolate the burst pipe, four isolation valves, namely valve 6, 16, 27, and 34, must be shut off. This led to 24 different valve shutdown sequences based on the principle of permutation. The results shown in Figure 4-5 demonstrate that all valve shutdown sequences adopted in the model would lead to contaminant intrusion.

However, the intrusion volume was minimized to approximately 5.4 m^3 using the following six valve shutdown sequences to isolate the burst:

(1)27-16-34-6

(2)27-34-16-6

(3)16-27-34-6

(4)16-34-27-6

(5)34-27-16-6

(6)34-16-27-6

The sequences listed above also indicate that valve 6, which is situated at the closest distance to the reservoir, should be closed at the end of a shutdown procedure to minimize the intrusion volume during the isolation activities in a fixed demand loop WDN model. Valve 6 is usually known as the inlet valve in a WDN. An inlet valve should be closed at the end of isolation activities to prevent additional water from entering the isolation block. Therefore, the repair work can be completed efficiently without the effects of additional flow from the reservoir while minimizing the volume of potential contaminant intrusion.

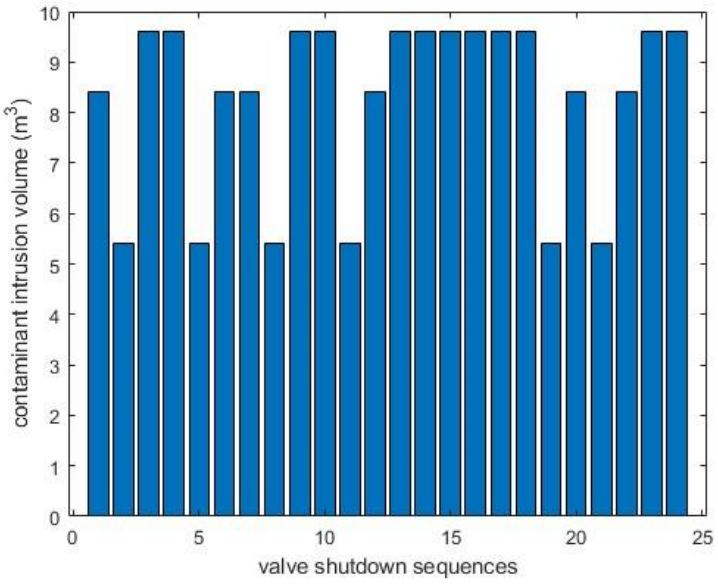

Figure 4-5. Intrusion volumes resulted from applying all applicable valve shutdown sequences to isolate a burst in the triple-loop WDN model where demand is fixed.

4.3.2 Minimization of the Intrusion Volume in a Pressure-dependent Demand Loop Model

To account for pressure deficiencies when a burst occurred in the model, a pressure dependent demand modelling approach was used in the same model. The following emitter coefficients (Table 4-2) were employed to simulate a demand of 5 L/s at each demand node.

Table 4-2. Emitter coefficients applied onto six nodes with demand in the triple loop WND model.

Node	Emitter Coefficients
Demand 1	1.083
Demand 2	1.95
Demand 3	1.075
Demand 4	0.942
Demand 5	0.977
Demand 6	0.912

Similar to the outcomes obtained in a fixed demand triple-loop WDN model, the results depicted in Figure 4-6 demonstrate contaminant intrusion could not be prevented in a pressure-dependent demand triple-loop WDN model. This indicates that contaminant intrusion may be a significant concern during isolation activities in moderately complex WDN models. However, the results also suggest that the intrusion volume may be minimized to 0.2 m^3 by applying the six best valve shutdown sequences which are identical to the sequences determined for the fixed demand triple-loop WDN model. These findings suggest it is worthwhile to explore more valve shutdown sequences to further minimize the volume of potential contaminant intrusion in WDNs.

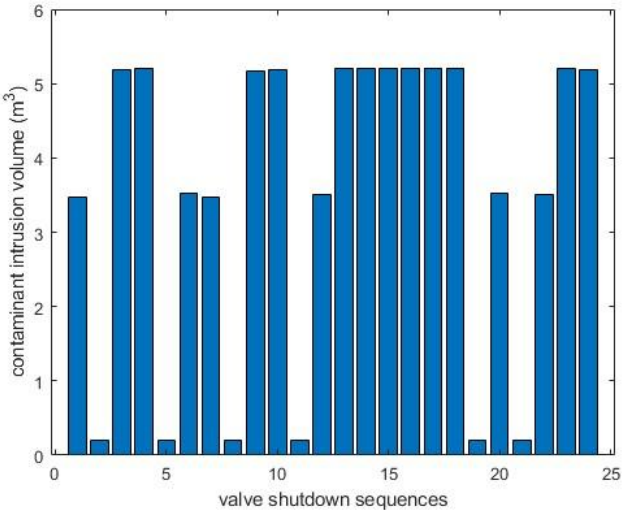

Figure 4-6. Intrusion volumes resulted from all applicable valve shutdown sequences implemented to isolate a burst in the triple loop WDN model where demand is driven by pressure.

Chapter 5 Factors That Can Increase the Risk of Contaminant Intrusion in More Complex Water Distribution Network Models

5.1 Introduction

The complex nature of real-world WDNs which are characterised by a large number of valves and nodes with different demands and elevations increases the potential for contaminant intrusion to occur. A detailed investigation to identify factors, such as the isolation block size, the shutdown duration time of isolation valves, and node elevations, may aid in effectively mitigating of the risk of contaminant intrusion in complex WDNs. This is the focus of this chapter.

This chapter studies several key factors that may increase the intrusion volume in complex WDN models. The following four objectives underpin the discussion:

- To assess the potential for valve shutdown operations to cause contaminant intrusion using the Paradise and Adelaide City WDN models.
- To study the impact of isolation block size on intrusion volumes in the Adelaide city WDN model. Different isolation blocks were proposed by selecting different isolating valves to operate.
- To evaluate the impacts of shutdown duration time of isolation valves on intrusion volumes in the Paradise WDN model.
- To analyze the effect of node elevations on intrusion volumes by assessing and comparing the intrusion volumes obtained in the Paradise and Adelaide city WDN models before and after the node elevation alterations.

5.2 Potential for Valve Shutdown Operations to Cause Contaminant Intrusion

5.2.1 Introduction to the Settings of the Hydraulic Models

As established in Chapter 3, valve shutdown operations can cause contaminant intrusion in both single water distribution pipe and single loop WDN models, regardless of whether the demand is fixed or pressure dependent. Real-world WDNs are significantly more complex than simple hydraulic models due to factors such as scale, topology, and water source availability. Therefore, it is important to further explore the potential for valve shutdown

operations to cause contaminant intrusion in more complex WDN models where demand is fixed or pressure dependent.

To achieve this goal, the two complex WDN models for Paradise and Adelaide city were utilized:

1. **The Paradise WDN model:**
    - Paradise is a suburban locality situated in north-eastern Adelaide. Figure 5-1 shows the distribution of node elevations in this model, with the highest node elevation recorded at approximately 150.0 m (yellow nodes) and the lowest node elevation at 63.4 m (dark-blue nodes). The reservoir has a total head of 170 m and 66 m water level (red node) and the burst is located at an elevation of about 70 m (green nodes). Therefore, the elevation difference of the reservoir and the burst in the Paradise model was approximately 100 m. The model comprises a single reservoir, 834 nodes, and 916 pipes of different lengths. In addition, 6 isolation valves were selected from the full data set in ArcGIS (Figure 5-2). They were applied to the model to enable the simulation of valve shutdown sequences.
    - Network demand is approximately 85 L/s, which is equivalent to 7 ML/d. This was the peak demand during the extended simulation period in the model.
    - The location marked as a red square in Figure 5-1 displays an intersection located at Reservoir Road and Belperio Court, where a pipe burst occurred in 2016 and a sinkhole formed. The precise node corresponding to the burst is presented in Figure 5-3. The isolation valves were also shown in the figure.
    - To simulate the burst in the model, a contaminant tank and an intrusion link identical in properties to those adopted in Chapter 3 were utilized.

2. **The Adelaide city WDN model:**
    - The Adelaide city WDN model (Figure 5-4) has a relatively flat topography with the elevation difference between most of the nodes within the city being 40-60 m. Each of the reservoirs (red node) has a total head of 102 - 103 m. The difference in elevation between the reservoir and the lowest node (light-blue node) is approximately 60 m which allows for the pressurization of the city WDN by remote tanks.

- The model comprises 10 source reservoirs, 1442 nodes, and 1776 pipes which differ in length and diameters. In addition, 7 isolation valves (Figure 5-6) were selected from the full data set in ArcGIS (Figure 5-5). They were added to the model to enable the simulation of operational shutdown sequences. Valve 39 was not necessary to be operated to isolate the burst. However, it replaced valve 32 to increase the size of the isolation block to enable the study of the effects of isolation block sizes on intrusion volumes.
- Network supply is approximately 225 L/s, which is equivalent to 20 ML/d. This was the peak demand during the extended simulation period in the model.
- The location marked as a red square in Figure 5-4 represents a pipe burst. The burst node is presented in Figure 5-6. The proposed isolation valves are also shown in that figure. The contaminant tank and intrusion link utilized in the Paradise WDN model were adopted again to simulate the burst in the Adelaide city WDN model.

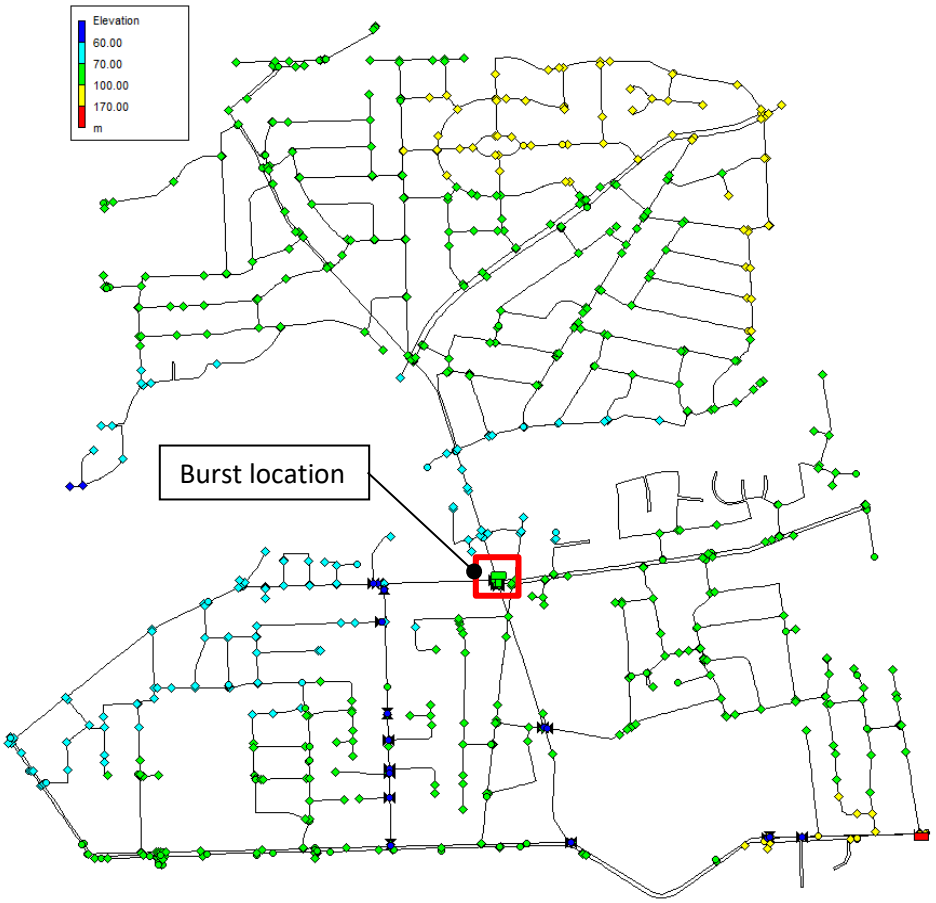

Figure 5-1. Distribution of node elevation and the location of a pipe burst in the Paradise WDN model (more details are shown in Figure 5-2).

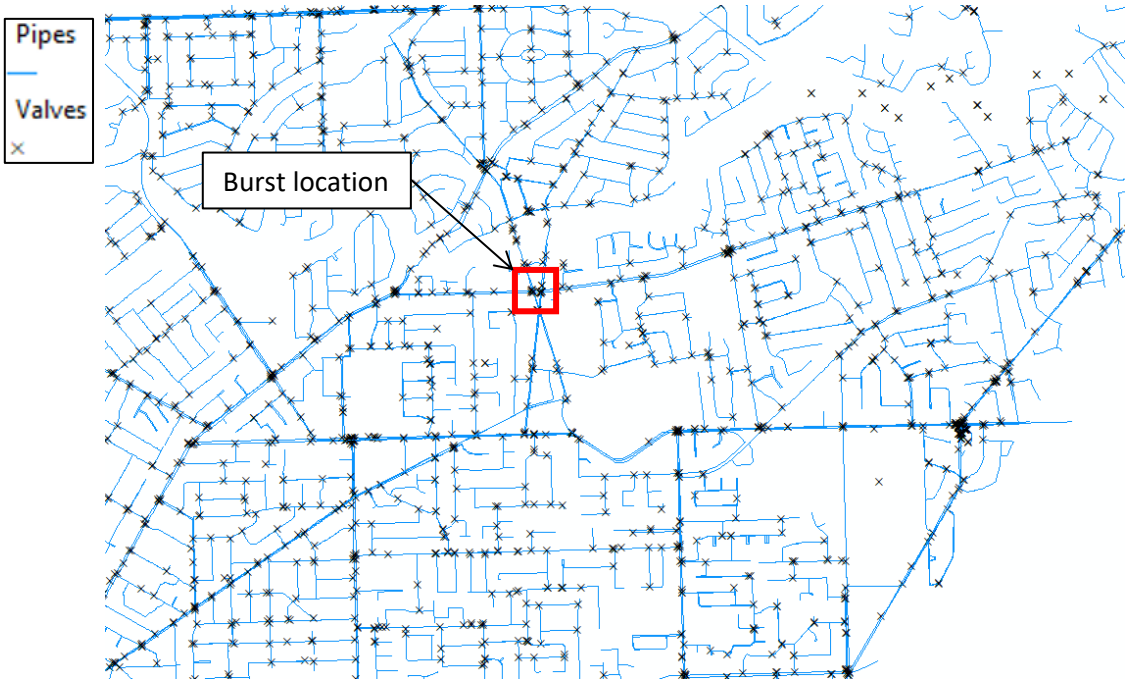

Figure 5-2. Full set of isolation valves in the Paradise WDN model in ArcGIS.

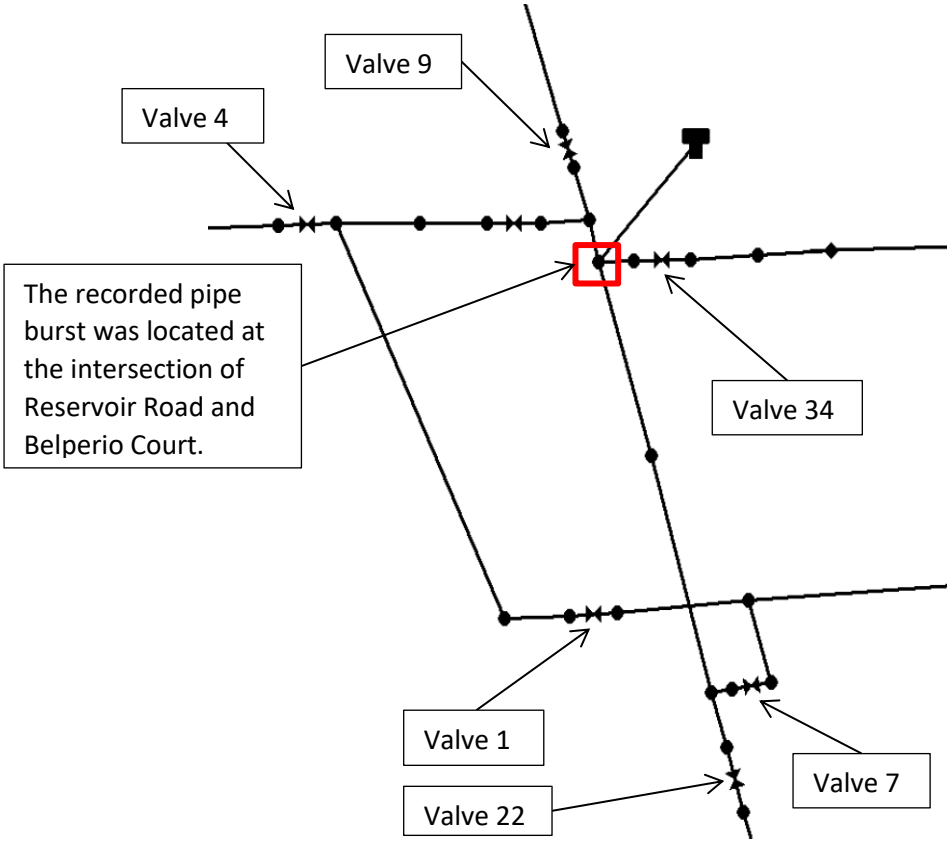

Figure 5-3. Locations of the pipe burst and isolating valves in the Paradise WDN model.

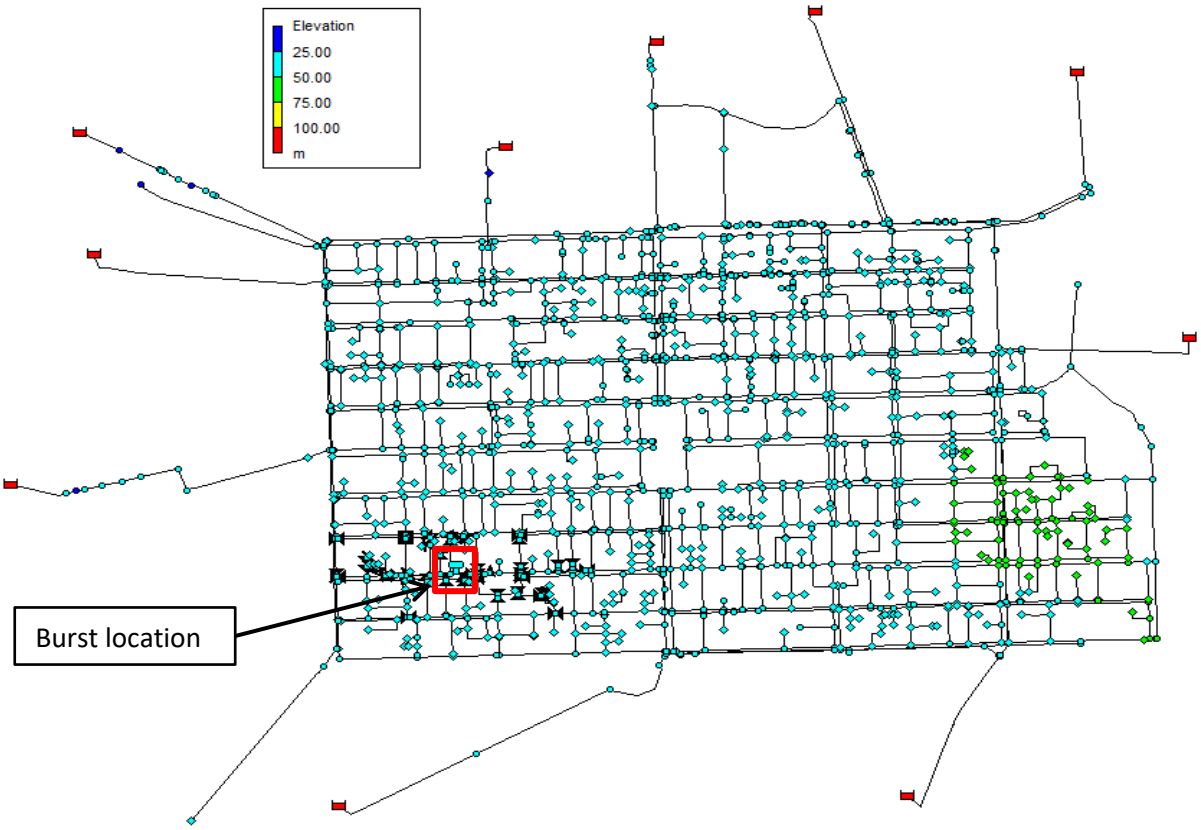

Figure 5-4. Distribution of node elevations and the location of the pipe burst in the Adelaide city WDN model.

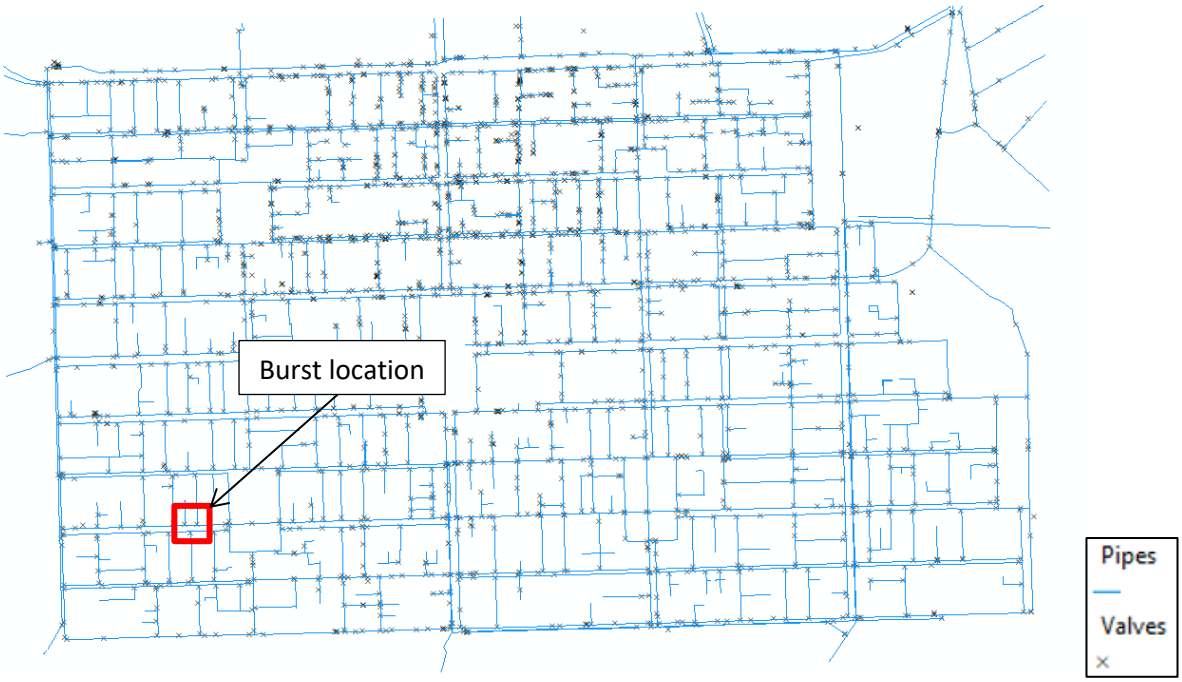

Figure 5-5. Full set of isolation valves in the Adelaide city WDN model in ArcGIS.

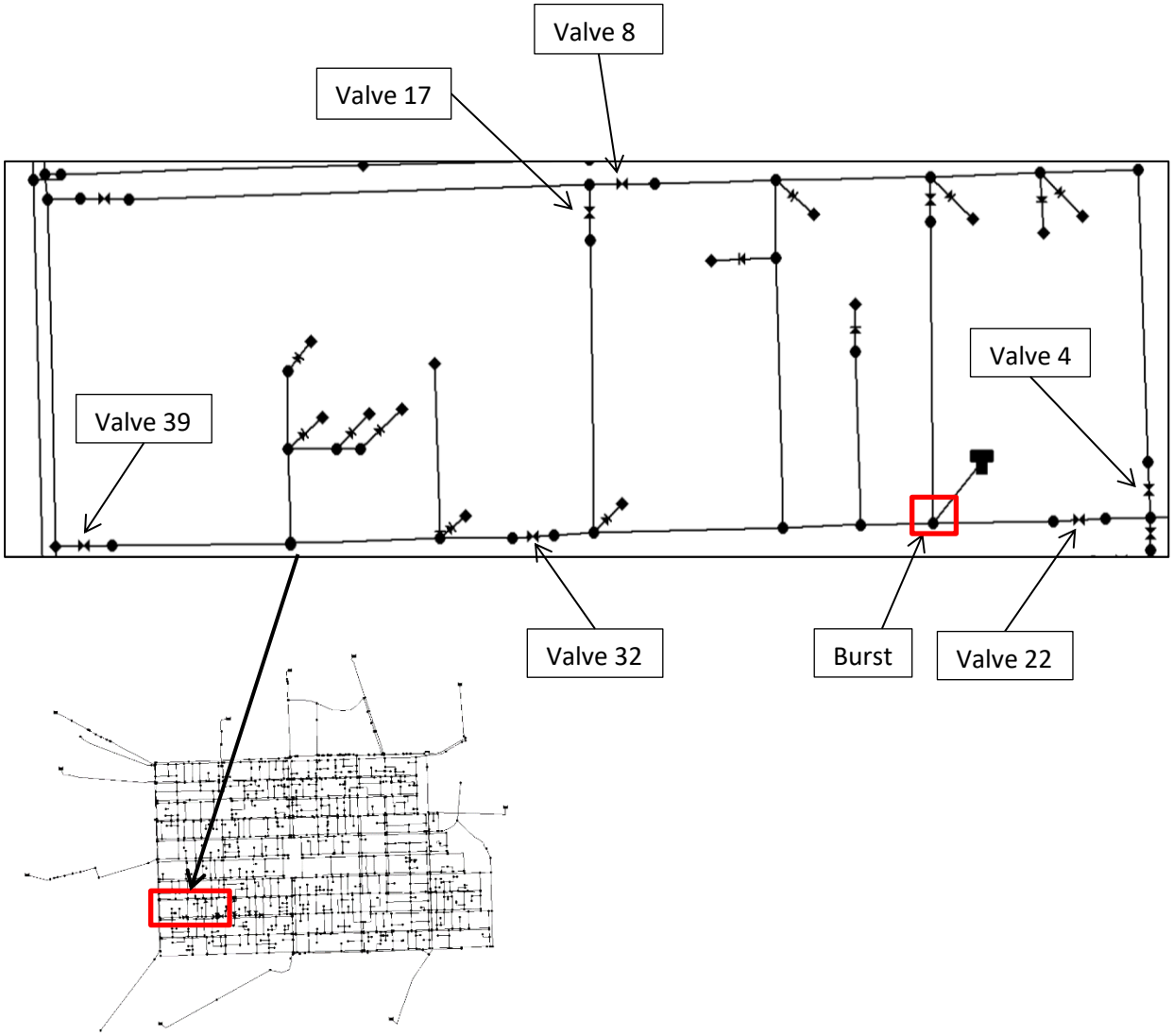

Figure 5-6. The selected isolation valves that were operated in the Adelaide city WDN model.

5.2.2 Potential Contaminant Intrusion in the Paradise WDN Model

In the Paradise WDN model it was assumed that the pipe burst occurred at 00:30 and the isolation activity was completed by 02:15. It was also assumed that the water supply service was interrupted until 04:00. The burst was isolated by shutting off isolation valves (Figure 5-3) in the following sequence and times:

1) Close valve 7 at 01:00
2) Close valve 4 at 01:15
3) Close valve 34 at 01:30
4) Close valve 22 at 01:45
5) Close valve 9 at 02:00

6) Close valve 1 at 02:15

Simulating the valve shutdown operations in the fixed and pressure dependent demand models identified that the burst flow dramatically reached 35 L/s at 00:30 (Figure 5-7) in a fixed demand model. This value was approximately 30.5 L/s at the same time step in a pressure dependent demand model. Both flow patterns gradually decreased for several minutes and then continued at a stable rate until 02:00. This was because the shape of the simulated sinkhole (contaminant tank in the model) is a cone. This sinkhole could also overflow after it was fully filled with contaminated water. The intrusion flow dramatically dropped below zero at 02:00, indicating that the shutdown operation of valve 9 led to contaminant intrusion in the Paradise WDN model. This result was observed for the models with fixed and pressure dependent demands. We observed intrusion flows after 02:15 for both models because demand nodes within the isolated blocks were demanding water between 02:15 to 04:00.

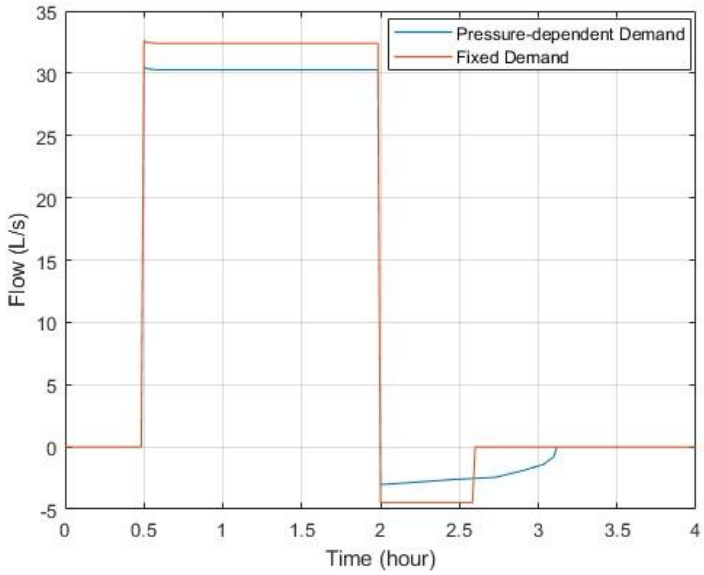

Figure 5-7. Flow in the intrusion link in the Paradise WDN model where demand is fixed and pressure dependent.

5.2.3 Potential Contaminant Intrusion in the Adelaide city WDN Model

In the Adelaide city WDN model it was also assumed that the pipe burst occurred at 00:30 and the isolation activities were finished by 03:00. It was also assumed that the water supply service was interrupted until 05:00. The burst was isolated by shutting off isolation valves (Figure 5-6) in the following sequence and times:

1) Close valve 22 at 01:00
2) Close valve 4 at 01:30
3) Close valve 8 at 02:00
4) Close valve 32 at 02:30
5) Close valve 17 at 03:00

Similar to the outcome achieved in the Paradise WDN model, the results (Figure 5-8) suggest that the burst flows in the two Adelaide city models (fixed and pressure dependent demands) dramatically reached approximately 25.5 L/s at 00:30. These values gradually decreased for several minutes and continued at a stable rate until 02:30. This flow pattern illustrates how contaminated water continued flowing out from the burst pipe to fill the cone-shape sinkhole and overflowing. The intrusion flow abruptly dropped below zero at 02:30 for fixed and pressure dependent demand models. This indicates the shutdown operation of valve 32 caused contaminant intrusion in both models regardless of the demand modelling method. We obtained intrusion flows after 03:00 for both models because demand nodes within the isolated blocks were demanding water during this time period.

Together, the simulation results in the Paradise and Adelaide city WDN models imply that contaminant intrusion is a concern for real-world WDNs. Thus, analyzing factors that may lead to a higher risk of contaminant intrusion can provide insights into the effective actions to reduce intrusion volumes.

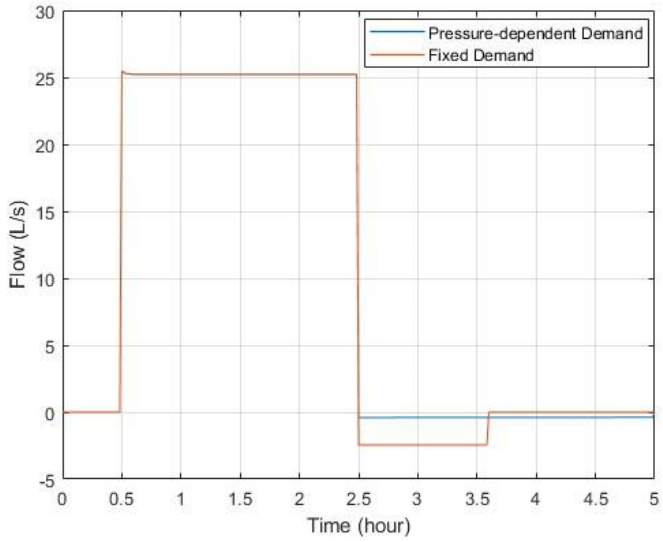

Figure 5-8. Flow in the intrusion link in the Adelaide city WDN model where demand is fixed and pressure dependent.

5.3 Effect of Isolation Block Size on Intrusion Volumes in Adelaide city WDN Model

5.3.1 Introduction to the Formulation of Two Different Sizes of the Isolation Block

The findings presented in Chapter 4 demonstrated that contaminant intrusion in WDNs can be eliminated or minimized by adopting the most effective valve shutdown sequence(s) to isolate a pipe burst. A cause-and-effect flowchart is illustrated in Figure 5-9, which shows that changing the valve shutdown sequence results in different intrusion volumes. The set of isolating valves being shut off to isolate a pipe burst determines the size of the isolation block created. For example, if operators shut off valves that are farther away from the burst to complete the isolation activities before repairing the pipeline, the isolation block will expand. Water utility operators isolate a burst pipe by operating the most effective isolation valves. These valves are located at the closest distance to the ruptured pipe. However, one or more of the most effective isolation valves may be inoperable during isolation activities. Operators need to reach other operable isolation valves to complete isolation activities, leading to a larger isolation block size.

An isolation block includes numerous pipelines and demand nodes. As such, when the isolation block expands, more demand nodes are included in the isolated block; this leads to higher water demand. When there is a constant draw of water from an isolation block without water replenishment, a vacuum condition is created which leads to negative pressure. This negative pressure forces the water to flow from the exterior environment back into the network, contaminating the treated water in the network. Accordingly, a higher continuous demand within an isolation block results in a larger magnitude of negative pressure, leading to a stronger suction effect. Consequently, the expansion of the isolation block results in larger intrusion volumes.

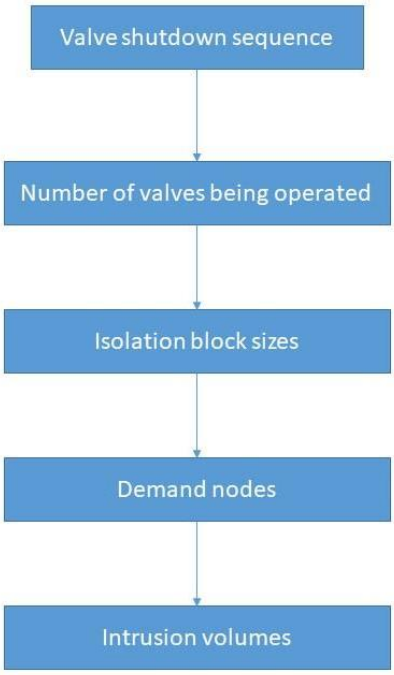

Figure 5-9. Effect of the valve shutdown sequence on the intrusion volume.

The Adelaide city WDN models with fixed and pressure dependent demands utilized in Section 5.2 were adopted again to analyze how the size of the isolation block affects intrusion volumes. The formulation of a burst and a sinkhole in the model was identical to that in Section 5.2 and two isolation blocks of different sizes were investigated. The burst and isolating valves are shown in Figure 5-6. Scenario 1 (Figure 5-10) demonstrates the isolation block (area within the red boundary) created using the same valve shutdown sequence listed in Section 5.2.3. This isolation block was treated as the original isolation block.

To evaluate the effects of a wider isolation block on intrusion volumes, Scenario 2 (Figure 5-11) was developed by creating a larger isolation block. The valve shutdown sequence and timing in Scenario 2 were identical to those in Scenario 1 except that valve 39 (Figure 5-46) was operated instead of valve 32. As a result, the isolation block in Scenario 2 included four additional demand nodes than in Scenario 1.

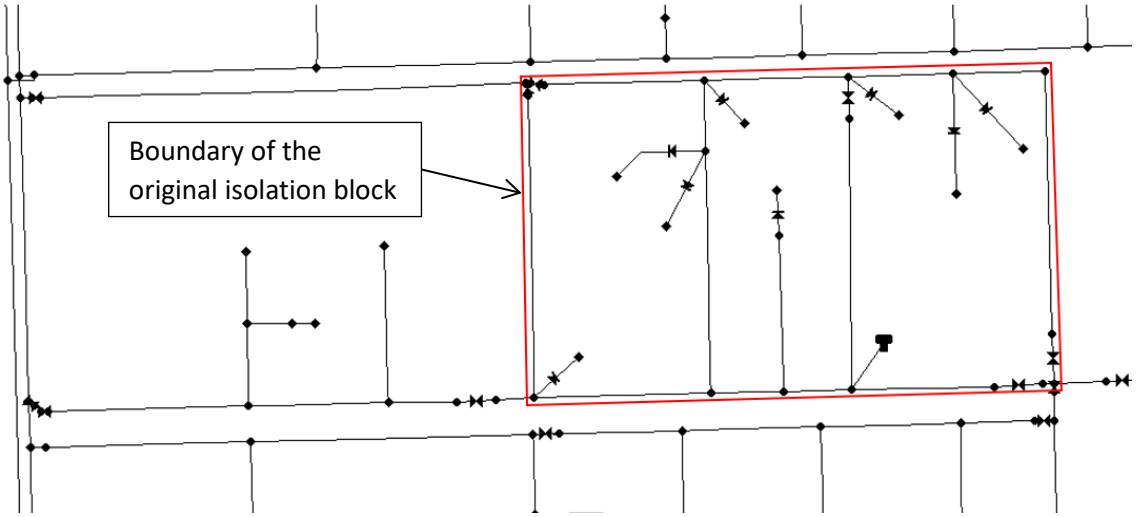

Figure 5-10. Scenario 1: Original isolation block in the Adelaide city WDN model.

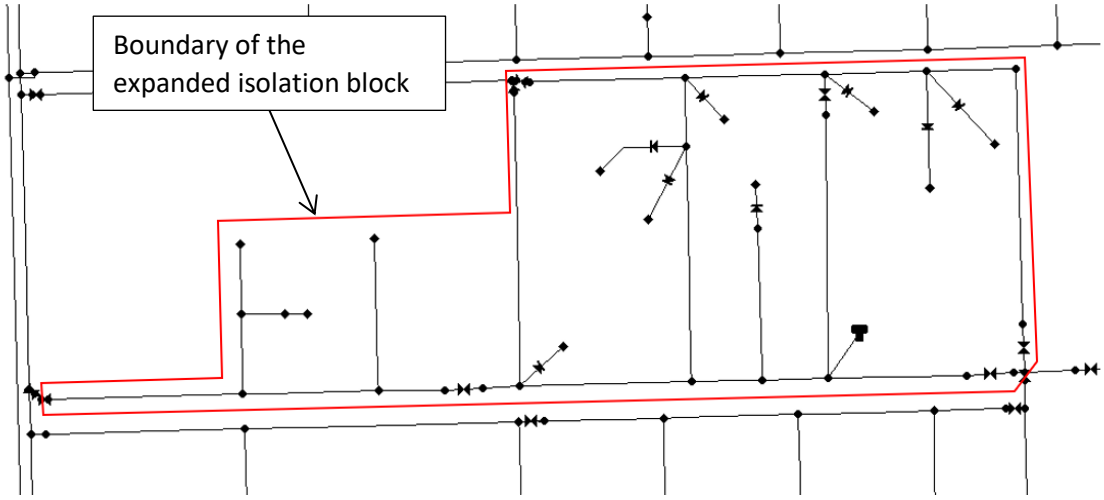

Figure 5-11. Scenario 2: Expanded isolation block in the Adelaide city WDN model.

5.3.2 Analysis of Isolation Block Sizes in the Fixed Demand Adelaide City WDN model

In Scenario 1 in the Adelaide city WDN model where demand was fixed the intrusion volume was determined as 9.56 m^3. This result suggests the maximum intrusion volume (9.63 m^3) was almost achieved during the isolation period. Scenario 2 achieved an intrusion volume of 9.58 m^3 during the same isolation period. These findings indicate that the expansion of the isolation block did not lead to a significant increase in intrusion volume. This was due to the intrusion volume nearly reaching the maximum volume of the contaminant tank (9.63 m^3) during the isolation activities; However, the impact of isolation block size on intrusion volumes should not be neglected. If the intrusion volume in Scenario 1 did not reach the

maximum volume of the contaminant tank, an expansion of the isolation block could lead to a significant increase in the intrusion volume. This is discussed in the next section.

5.3.3 Analysis of Isolation Block Sizes in the Pressure Dependent Demand Adelaide City WDN model

In contrast to the fixed demand model, an expansion of the isolation block led to a significant increase in the intrusion volume in the model where demand was driven by pressure. The intrusion volume for Scenario 1 was 0.71 m^3, where the intrusion flow rate was 0.1 L/s. The intrusion flow rate for Scenario 2 increased dramatically to 2.4 L/s with an intrusion volume of 4.83 m^3. These results confirm that a larger isolation block can indeed pose a higher risk of contaminant intrusion.

The overall outcome of the two scenarios demonstrates that contaminant intrusion can be more severe if the isolation block size increases. This is because the additional demand within the larger isolation block can increase the magnitude of the negative pressure, leading to a stronger suction effect at the burst.

5.4 Effect of Shutdown Duration Time of Valves on Intrusion Volumes in Paradise WDN Model

The shutdown duration time of isolation valves was identified as a crucial factor affecting the intrusion volume in the single water distribution pipe and loop WDN models (see Chapters 3 and 5). These models showed contaminant intrusion during the isolation process of a pipe burst. To assess if the same outcome would be obtained in more complex WDN models an analysis of the shutdown duration time of isolation valves was conducted in the Paradise WDN model using the fixed and pressure dependent demand modelling approaches.

5.4.1 Analysis of Shutdown Time of Valves in the Fixed Demand Paradise WDN Model

In the Paradise WDN model where demand is fixed, different time intervals between the operation of every two valves was analyzed at 10 mins, 15 mins, 20 mins, and 30 mins. The isolation activities were completed at 05:00, resulting in four different shutdown duration times of the isolation valves, as shown in the second column in Table 5-1. The results imply

that a longer shutdown duration time of isolation valves may lead to a larger intrusion volume in the fixed demand model.

Table 5-1. Intrusion volumes resulting from different repair completion time in the Paradise WDN model (with original node elevation).

Time Between the Operation of Every Two Valves (mins)	Shutdown Duration Time of Isolation Valves (mins)	Intrusion Volume (m^3)
10	20	2.68
15	30	4.01
20	40	5.35
30	60	8.03

Moreover, a linear relationship between the total valve shutdown duration timing (t) in mins and intrusion volume (V_{In}) in m^3, as shown in Eq. 7 below, were discovered by performing linear regression analysis (Figure 5-12) of the outcomes presented in columns 2 and 3 of Table 5-1:

$$V_{In} = 0.2676\, t \tag{7}$$

The results indicate that an additional 2.68 m^3 of contaminants could intrude into the pipe if the completion of isolation activities took an additional 10 minutes. These results further indicate it is feasible to reduce intrusion volumes during isolation activities by ensuring optimal efficiency in operating isolation valves.

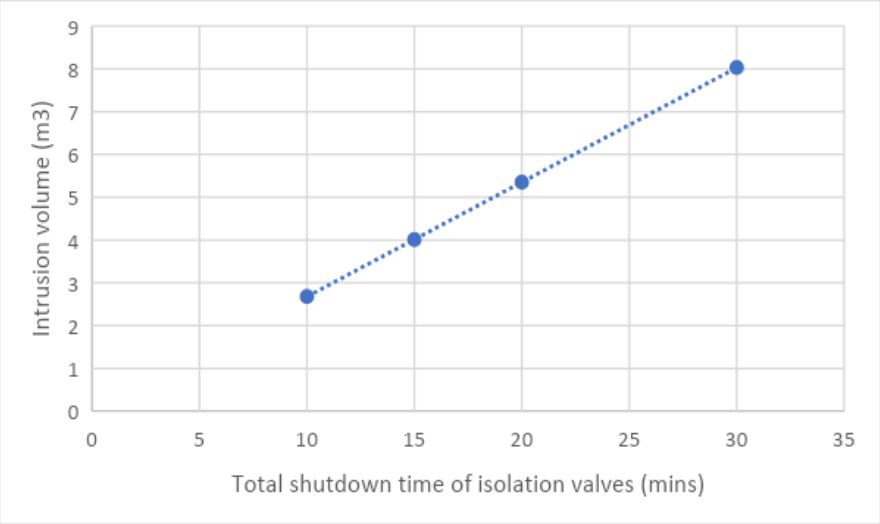

Figure 5-12. Correlation between total shutdown time of isolation valves and intrusion volumes in the Paradise WDN model where demand is fixed.

5.4.2 Analysis of Shutdown Time of Valves in the Pressure-dependent Demand Paradise WDN Model

The effects of shutdown duration time of isolation valves on intrusion volume were also explored using the pressure-dependent demand modelling approach in the Paradise WDN model. The shutdown duration times of isolation valves shown in Table 5-1 were adopted in the model. Similar to the results in Section 5.4.1, the intrusion volume increased from 0.89 m^3 to 2.53 m^3 as the shutdown duration time of isolation valves increased from 20 mins to 60 mins.

Table 5-2. Intrusion volumes resulting from different valve shutdown timing in the Paradise WDN model (with original node elevation).

Time Between the Operation of Every Two Valves (mins)	Shutdown Time of Isolation Valves (mins)	Intrusion Volume (m^3)
10	20	0.89
15	30	1.40
20	40	1.73
30	60	2.53

The relationship between the intrusion volume and the shutdown duration time of valves was further studied by performing a polynomial regression analysis, presented in Figure 5-13, which indicates a second order polynomial relationship between the total shutdown duration time of isolation valves (t) in mins and the intrusion volume (V_{In}) in m^3 as shown in Eq. 8 below:

$$V_{In} = -0.0004\,t^2 + 0.0956\,t \tag{8}$$

The result implies that an additional 0.916 m^3 of contaminants would be drawn into the pipeline if an additional 10 mins was added to the shutdown time of isolation valves. Although the additional intrusion volume due to the addition of 10 mins seems low, the result indicates the potential to reduce intrusion volumes by shutting off isolation valves more efficiently. Together, the results obtained in both Sections 5.4.1 and 5.4.2 indicate the potential to minimize the intrusion volume during isolation activities by operating isolation valves at full efficiency.

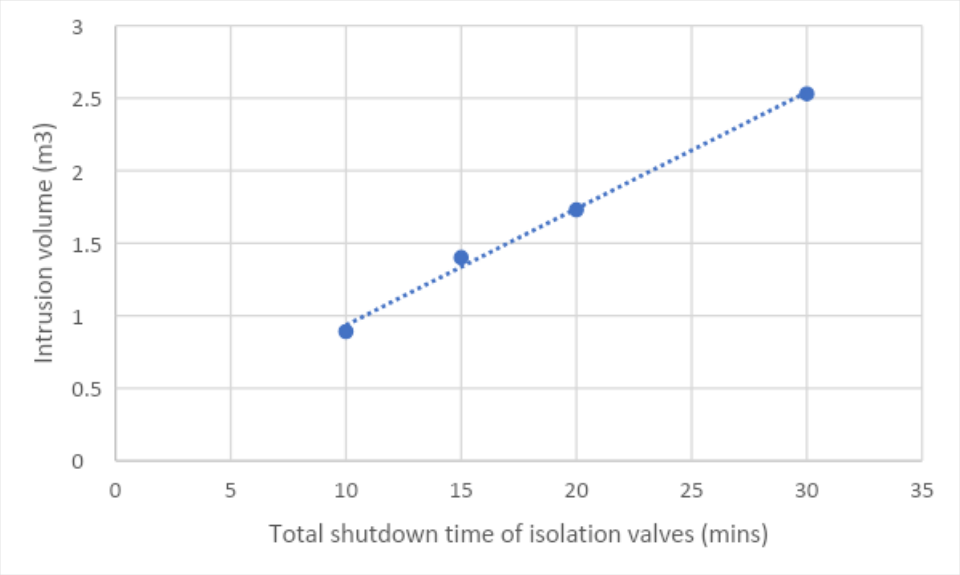

Figure 5-13. Correlation between total shutdown time of isolation valves and intrusion volumes in the Paradise WDN model where demand is pressure dependent.

5.5 Effect of Node Elevations on Intrusion Volume in the Paradise and Adelaide city WDN Models

5.5.1 Introduction of the Paradise WDN Model Modifications

The significant impacts of node elevation on intrusion volumes, particularly in WDN models where demand is dependent on pressure, was examined in the single water distribution pipe and single loop WDN models (see Chapter 3). To confirm the same findings could be obtained in more complex WDNs, the effect of node elevation to intrusion volumes was studied using the Paradise WDN model with fixed and pressure dependent demands.

As shown in Figure 5-14, the original elevations of the nodes demanding water within the isolation block (red boundary) were between 70.23 m and 70.62 m. The original elevations of the contaminant tank and junction that links to the tank (i.e., node representing the burst) were both 70.23 m. Four of the nodes demanding water (green boundary) were located at a lower elevation (i.e., 70.19 m) than the burst. The reservoir in the model was situated at an elevation of 170 m. Thus, the elevation difference between the burst and the reservoir was approximately 100 m.

To examine the influence of node elevation alterations on intrusion volumes in the model, the elevations of the contaminant tank and junction that links to the tank were increased from 70.23 m to 80.23 m (Figure 5-15) to create a steeper topography between the burst and other

nodes in the model. The node elevation modification led to approximately 10 m difference in the elevation between the burst and other nodes in the model. The repair was assumed to be completed at 07:00. The valve shutdown sequence (see Figure 5-3 for valve locations in the Paradise WDN model) employed to isolate the burst in the Paradise WDN model in Section 5.2.2 were applied again to simulate the isolation activities:

1) Close valve 7 at 01:00
2) Close valve 4 at 01:15
3) Close valve 34 at 01:30
4) Close valve 22 at 01:45
5) Close valve 9 at 02:00
6) Close valve 1 at 02:15

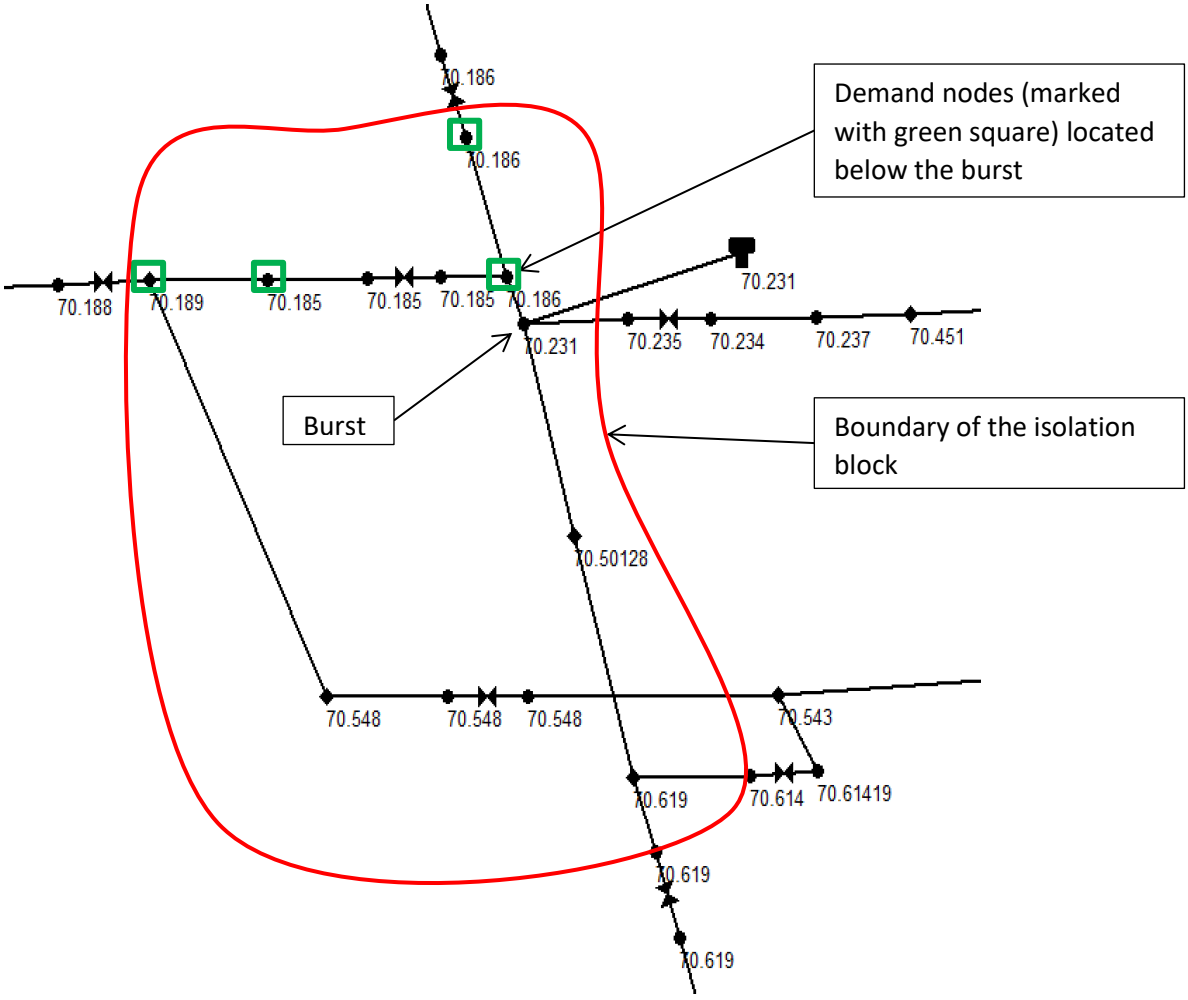

Figure 5-14. Original node elevations within the isolated block in the Paradise WDN model.

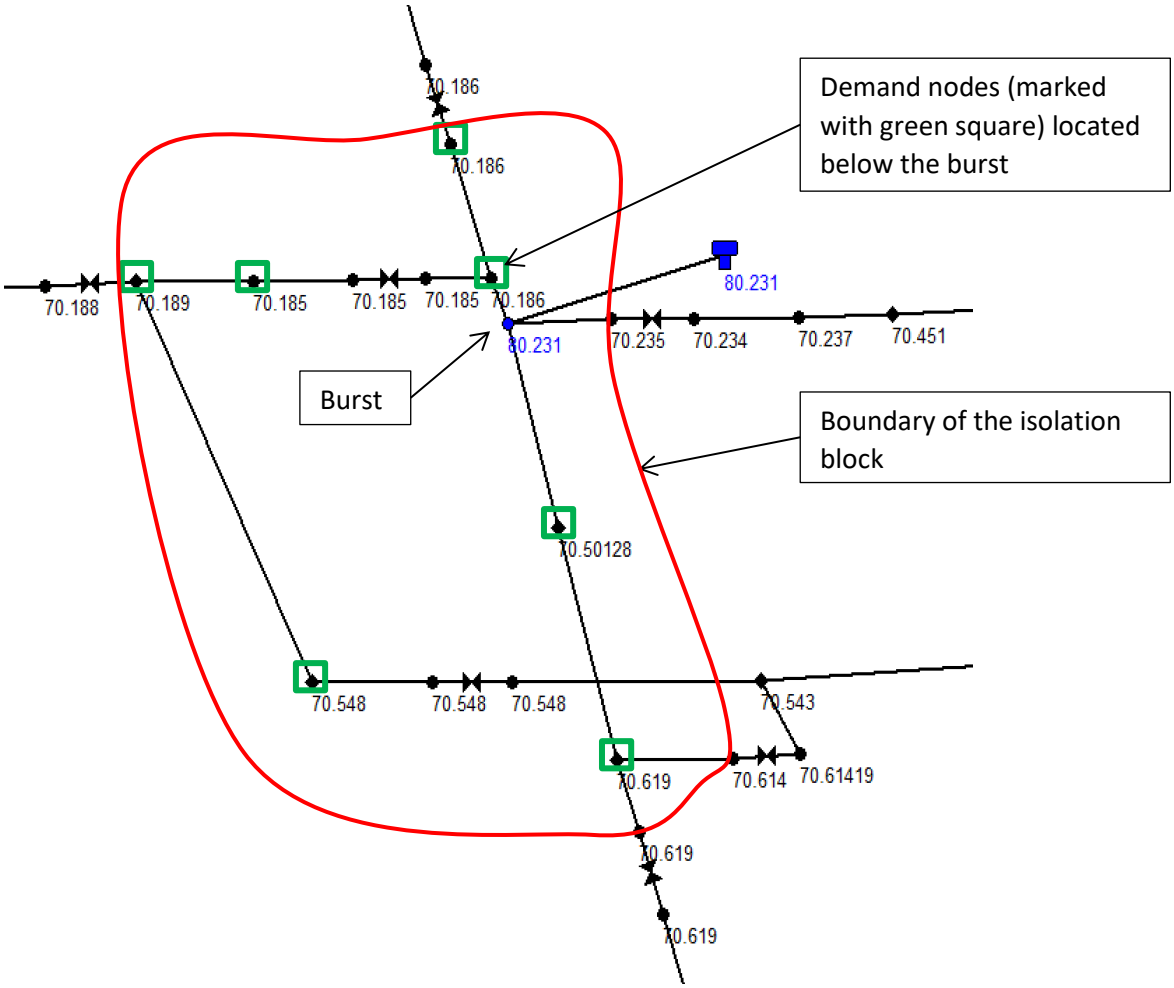

Figure 5-15. Adjusted elevation of the contaminant tank and the junction that links to the tank in the Paradise WDN model.

5.5.2 Analysis of Node Elevations in the Fixed Demand Paradise WDN Model

Using a fixed demand modelling approach to simulate the isolation activities in the Paradise WDN model with the original node elevation resulted in an intrusion volume of 9.63 m^3. The volume remained constant after changing the node elevation of the contaminant tank and the junction that links to the tank. These results illustrate that changes in node elevations do not affect the intrusion volume in WDN models where demand is fixed. However, node elevation may have an important impact on the intrusion volume in WDN models when demand is driven by pressure.

5.5.3 Analysis of Node Elevations in the Pressure-dependent Demand Paradise WDN Model

Applying a pressure dependent demand modelling method to simulate the same isolation activities in the Paradise WDN model with the original node elevations resulted in an intrusion volume of 5.02 m^3. The intrusion volume increased to 9.59 m^3 when the nodes were

elevated; this was 4.57 m^3 more than the result obtained without raising the elevation at the burst node. Furthermore, the burst flow rate before changing the node elevation of the contaminant tank and the junction that links to the tank was 32.4 L/s. However, it decreased to 30.7 L/s after the elevation of these two nodes was increased by 10 m.

The findings signify that node elevation is correlated with the severity of contaminant intrusion as well as burst flow rate. A pipe burst occurring at a higher elevation may result in a larger intrusion volume compared to a burst at a lower elevation. This is because more demand nodes are located below the burst, thus, increasing the total demand contributing to negative pressure once isolation activities are complete. Intrusion volume depends on the total demand within an isolation block.

In Figure 5-14, there were only four nodes demanding water within the isolation block and located at lower elevations (70.19 m) than the location of burst (70.23 m). When the number of the nodes demanding water and located at lower elevations than the burst increased from four to seven (shown in the green rectangles in Figure 5-15), the total demand within the isolation block increased, thus resulting in higher intrusion volume. In contrast, by increasing the burst elevation by 10 m and maintaining the reservoir at the original elevation, the elevation difference between the burst and the reservoir decreased by 10 m. Thus, the total head available in the water distribution pipe decreased by 10 m, resulting in a lower burst flow rate.

5.5.4 Introduction to the Adelaide city WDN Model Modifications

The investigations into the effects of node elevations upon intrusion volumes in three different hydraulic models, including the single water distribution pipe, single loop WDN, and the Paradise WDN models, confirmed that changes of node elevation impact the intrusion volume when the WDN demand is driven by pressure. The Paradise WDN, characterized by its steep topology, can be delineated as a representative WDN which shows the potential for contaminant intrusion. Nonetheless, the precise correlation between node elevation alteration and its impact on intrusion volumes remains ambiguous for WDNs exhibiting less steep topology. Therefore, this section details the results from simulating isolation activities in the Adelaide city WDN model which has a much flatter topography and discusses the impacts of node elevation modifications on intrusion volumes.

As shown in Figure 5-16, the original elevations of the burst and demand nodes within the isolation block in the Adelaide city WDN were at an elevation between approximately 40.90 m and 41.82 m, whereas the reservoirs (not displayed in this figure but in Figure 5-4 as representations of tanks or other larger diameter trunk mains feeding the Adelaide city WDN) were located at an elevation of 100 m. Therefore, the elevation difference between the burst and the reservoir was approximately 59 m, which is much smaller than the difference observed in the Paradise WDN model.

To study the influence of node elevation on intrusion volumes in the Adelaide city WDN model, alterations were made to the node elevation of the contaminant tank and the junction that links to the tank to create a steeper topography between the burst and other nodes demanding water within the isolation block, as shown in Figure 5-17. The elevation of the contaminant tank and the junction that links to the tank was assumed to increase from 41.63 m to 51.63 m. The repair was assumed to be completed at 05:00. The following valve shutdown sequence was employed to isolate the burst in the Adelaide city WDN model to simulate the isolation activities:

1) Close valve 22 at 01:00
2) Close valve 4 at 01:30
3) Close valve 8 at 02:00
4) Close valve 32 at 02:30
5) Close valve 17 at 03:00

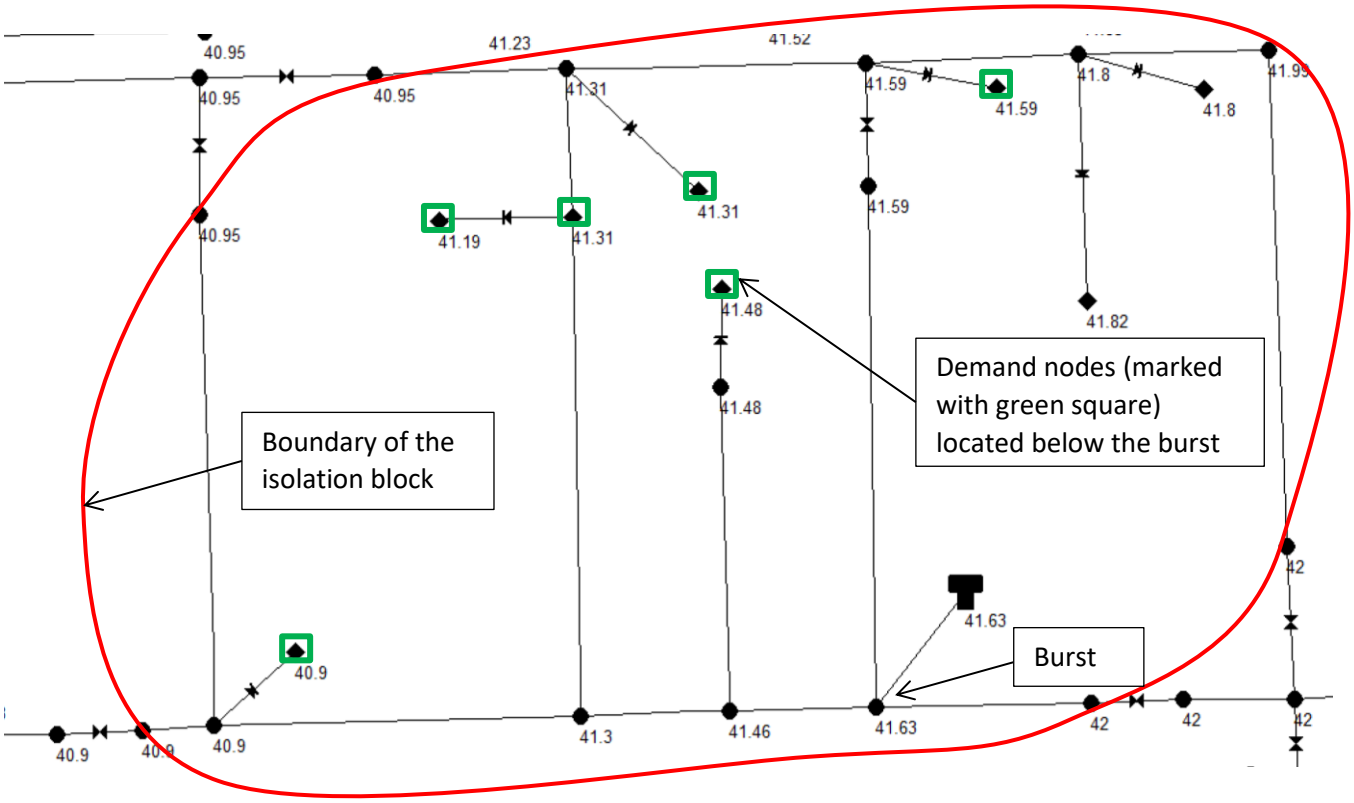

Figure 5-16. Original node elevations within the isolation block in the Adelaide city WDN model.

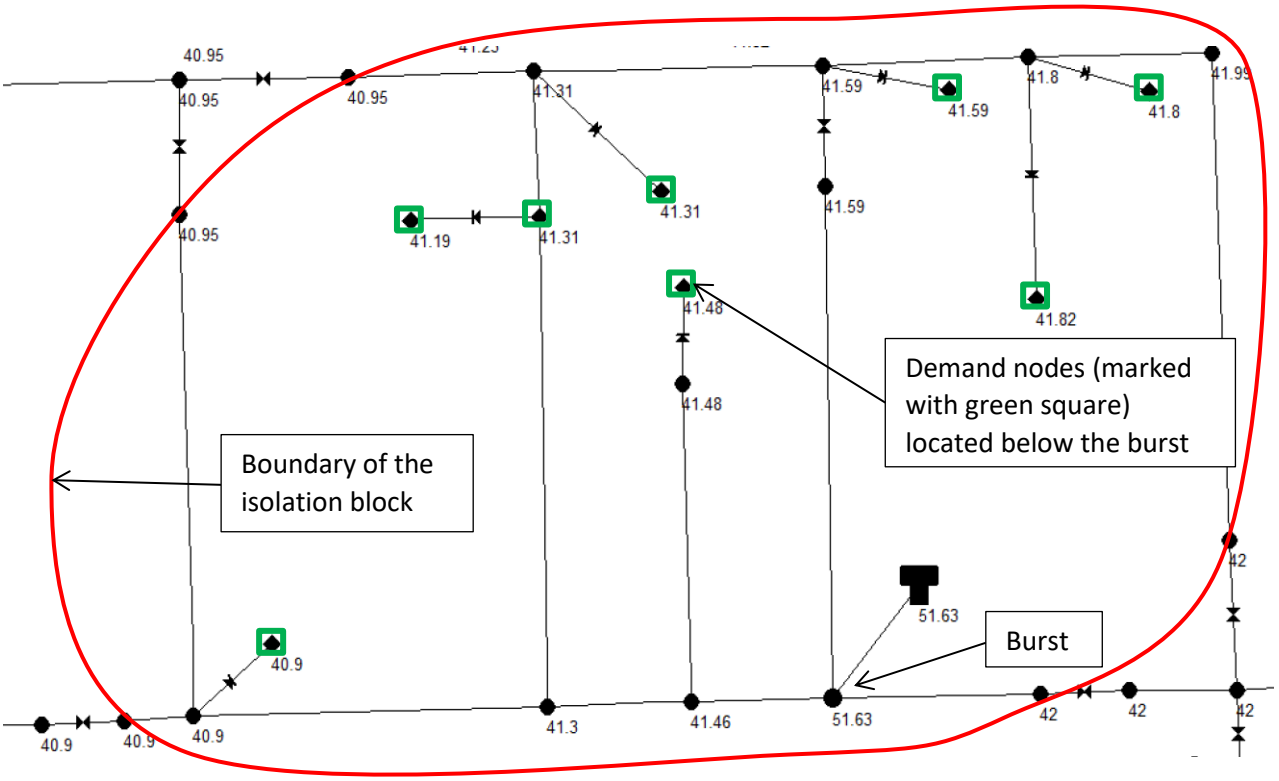

Figure 5-17. Adjusted elevations of the contaminant tank and the junction that links to the tank in the Adelaide city WDN model.

5.5.5 Analysis of Node Elevations in the Fixed Demand Adelaide City WDN Model

Using a fixed demand modelling approach to simulate isolation activities in the Adelaide city WDN model with original node elevations resulted in an intrusion volume of 9.56 m^3. The result remained constant when the elevation of the contaminant tank and the junction that links to the tank increased to 51.63 m. Thus, the finding suggests that node elevation will not affect intrusion volume when the demand in a WDN model is fixed.

5.5.6 Analysis of Node Elevations in the Pressure-dependent Demand Adelaide City WDN Model

By adopting a pressure-dependent demand modelling approach to simulate the same valve shutdown activities in the Adelaide city WDN model with the original elevations, the intrusion volume was determined as 0.71 m^3. However, after increasing the elevations of the contaminant tank and the junction that links to the tank from 41.63 m to 51.63 m, the intrusion volume increased to 1.98 m^3, which is 1.27 m^3 more than the value determined for the original elevations. Moreover, the burst flow rate before changing the node elevation of the contaminant tank and the junction that links to the tank was 20.9 L/s. This decreased to 19.1 L/s after increasing the elevation of the two nodes by 10 m.

The findings from the Adelaide city WDN model agree with the results from the Paradise WDN model, thus, emphasizing that node elevation affects the intrusion volume and burst flow rate when adopting a pressure-dependent demand modelling approach to simulate isolation activities in WDN models. Before changing the node elevation of the contaminant tank and the junction that links to the tank, six nodes located at lower elevations (40.90 – 41.59 m) than the burst (41.63 m) were demanding water (green rectangles in Figure 5-16). After increasing the node elevation of the burst and the contaminant tank that links to the burst, the number of demand nodes located at lower elevations than the burst increased to eight, as indicated by the green rectangles in Figure 5-17. Thus, the total demand within the isolation block increased and this resulted in a greater intrusion volume. Similar to the results obtained by applying a pressure-dependent demand modelling method in the Paradise WDN model, the total head available in the Adelaide city WDN reduced by 10 m after making the node elevation modifications, thus, resulting in a slower burst flow rate.

5.5.7 Further Exploration: Effects of the Elevation of a Pipe Burst and Network Topology to Contaminant Intrusion in WDNs

From examining the node elevation alterations and intrusion volumes across various hydraulic models, as detailed in Chapters 3 and here in Chapter 5, it became apparent that changes in node elevations significantly impact intrusion volumes in WDN models that operate under pressure-driven demand. The impact of node elevation modifications on intrusion volumes was observed to be more significant in a WDN characterized by a steep topology. However, there is a potential for the maximum intrusion volume to exceed the maximum volume of a sinkhole.

The actual volume of a sinkhole resulting from a pipe burst depends on variables such as the burst flow rate and the type of surrounding soil. Thus, as discussed in Chapter 3, the actual volume of a sinkhole can be small or large. In this study, the sinkhole volume was determined based on certain assumptions. In hydraulic modelling, the maximum intrusion volume was equal to the maximum volume of the sinkhole. Nevertheless, under certain circumstances within real-world WDNs, it is possible for the intrusion volume to surpass the maximum volume of the sinkhole, which can lead to serious flooding.

For example, in 2018, large parts of Lea Bridge in Hackney (London) were submerged for days after a water pipe burst (Cooper, 2019; Gelder and Alwakeel, 2018). Many vehicles were submerged (Figures 5-18 and 5-19) and the flooding lifted a road segment of approximately 2.43 m by 1.83 m plan dimensions up about 0.2 m. Although no sinkhole due to the pipe burst was reported, we can assume a large “sinkhole” (or storage volume ready for suction back into the pipe through the pipe rupture) that has a similar size to the submerged car parks and neighborhoods. The maximum volume of contaminated water was equal to the flooded area multiplied by the depth of the water. According to the news, we could confirm that the entire area of Lea Bridge was not underwater. Therefore, the volume of the sinkhole should not as large as the entire Lea Bridge area. However, if contaminant intrusion did occur, there would be a high potential for the actual intrusion volume to exceed the maximum volume of any localized sinkhole.

Figure 5-18. A large car park was flooded due to the pipe burst.

Figure 5-19. A vehicle was underwater because of the flooding caused by a pipe burst.

Moreover, there is a higher potential for the actual intrusion volume to surpass the maximum volume of a sinkhole if a water pipe burst occurs at a low point. For instance, in 2022, a sinkhole resulted from a water pipe burst in Subiaco (area pointed by red arrow in Figure 5-60), a suburb in Perth, Western Australia (Dugan, 2022). According to the topology of Perth and surrounding suburbs (Figure 5-20), Subiaco sits at approximately 20 m elevation (World topographic map, 2023). There are many surrounding areas below this elevation, as shown in blue in Figure 5-20. The sinkhole swallowed part of Subiaco and a vehicle parked on the street (Figure 5-21). A large number of roads were flooded with contaminated water. This

indicates that if the burst caused a contaminant intrusion, the intrusion volume would have surpassed the maximum volume of the sinkhole.

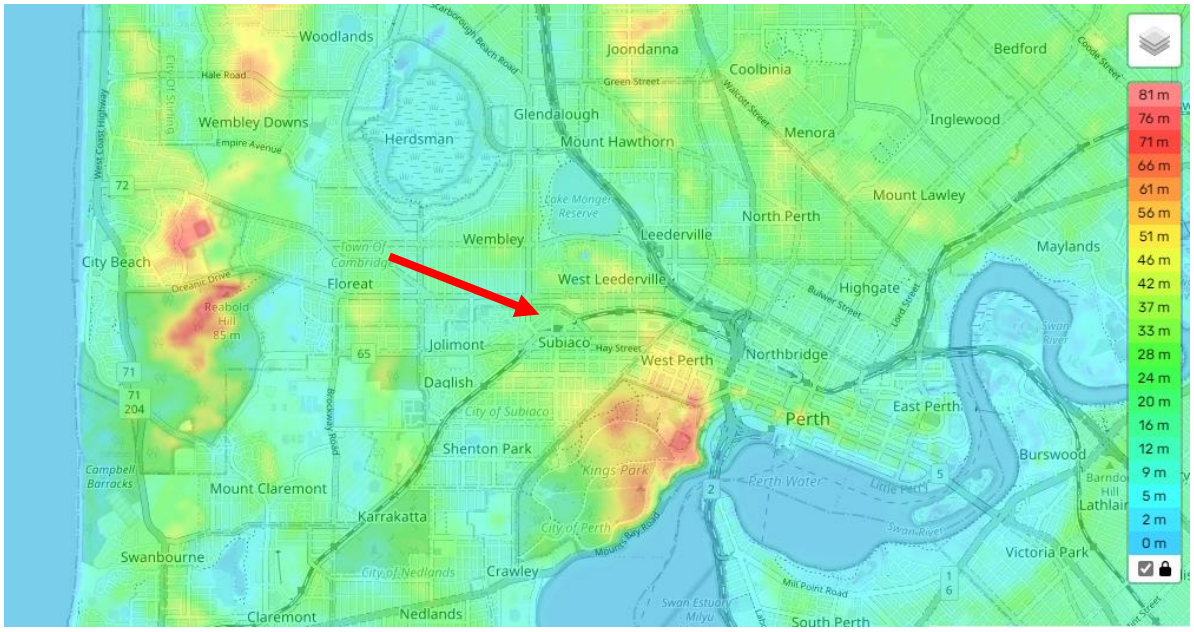

Figure 5-20. The topology of Perth and surrounding suburbs in WA.

Figure 5-21. A vehicle was swallowed by a sinkhole resulted from a pipe burst in Subiaco.

To extend on the examples above, and to ascertain if the maximum contaminant intrusion volume could exceed the maximum volume of a sinkhole, the single water distribution pipe model used in Chapter 3 was adopted again. All settings in the model were kept the same with the exception of the following:

- The elevation of the reservoir in the model (Figure 5-22) was increased from 30 m to 50 m to create a significant difference (35 m) between the burst and the reservoir. The demand node was kept below the burst to enable contaminant intrusion.

- In the hydraulic model, the contaminant tank (sinkhole) could overflow. The natural surface could hold additional contaminated water once the sinkhole was full. The isolation valves (V1 and V2) were kept open so the intrusion of contaminated water would continue if the demand node continued to demand water. The simulation was extended for 8 hours so water would keep filling the sinkhole and flooding the natural surface and roads.

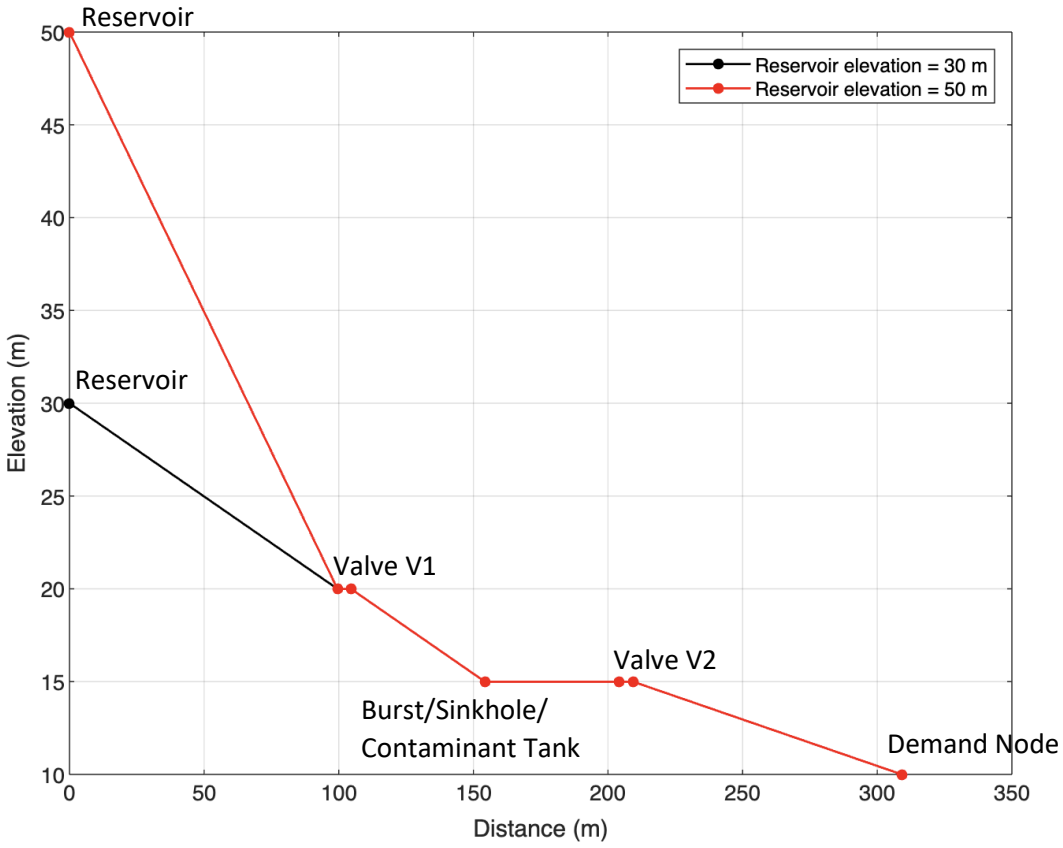

Figure 5-22. Two different elevations of the reservoir in the longitudinal view for the single water distribution pipe model.

The total volume of contaminated water due to the burst was determined as 279.53 m^3, a value obviously greater than the total volume of the contaminant tank (9.63 m^3). Therefore, there was a potential for 269.67 m^3 of contaminated water to intrude into the water distribution pipe. This analysis shows that the actual intrusion volume can be greater than the size of a sinkhole caused by a water pipe burst.

Moreover, given the overflow of the contaminated tank, there was a potential for 174.54 m^3 of contaminated water to intrude into the water distribution pipe when the elevation of the reservoir was kept at 30 m. The outcome would lead to an additional 104.99 m^3 of contaminated water (hatched area in Figure 5-23) being available to re-enter the pipe if the

elevation of the reservoir was increased from 30 m to 50 m (i.e., having a burst at a lower relative point in the WDN). This exploration illustrates that it is possible to have an actual intrusion volume that surpasses the maximum volume of a sinkhole if the water pipe burst occurs at a low point.

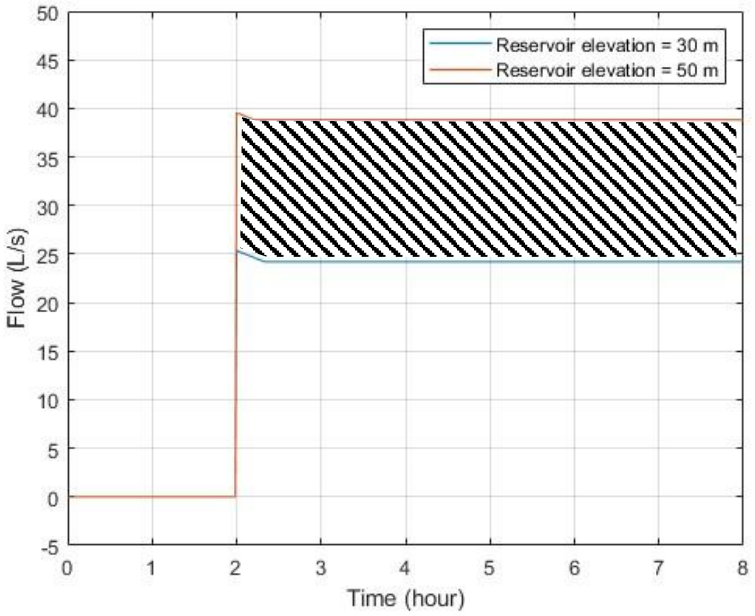

Figure 5-23. Flow in the intrusion link in the single water distribution pipe model with new reservoir elevation.

We found the occurrence of a burst in WDNs can substantially affect the flow in distribution pipes. This can change the shear stress of the biofilm in the internal pipe wall and affect turbidity in a pipe. Turbidity is a key concern in WDNs and it is the focus of the following chapter.

Chapter 6 Turbidity Changes in WDNs due to the Occurrence of Pipe Bursts

6.1 Introduction

Variations in the velocity of water within a pipe from events such as pipe bursts can result in fluctuations in the turbidity measurements in WDNs. Turbidity is extensively utilized as a crucial parameter for evaluating water quality in WDNs. This chapter investigates the impacts of pipe bursts and isolation activities in WDNs on turbidity by analyzing the changes of turbidity measurements in pipes. The chapter addresses two primary objectives to assess the adverse impacts of pipe bursts on water quality.

- To develop refined hydraulic model to demonstrate turbidity in WDNs without the occurrence of a pipe burst.
- To evaluate turbidity changes in WDNs following the implementation of a pipe burst in the conditioned model.

The PODDS EPANET model, a unique variant of EPANET incorporating the PODDS model functionality introduced in Chapter 2 (Boxall and Husband, 2005), was employed to condition the Adelaide City WDN model, to simulate pipe bursts in the model, and reveal any potential shifts in turbidity across the pipes. The PODDS EPANET model has five turbidity-related parameters (i.e., C_{max}, k, b, P, and n) that must be determined and input into the EPANET pipe settings. These parameters can be selected based on the material and size of each pipe (Boxall and Husband, 2005). These factors determined the PODDS EPANET as a reliable model to assess turbidity in WSNs after a pipe burst and during isolation activities.

6.2 Impacts of Having a Pipe Burst on Turbidity

6.2.1 Turbidity in the Adelaide City WDN model Without a Pipe Burst

To assess turbidity changes in the Adelaide city WDN model it was essential to condition the undisturbed model without incorporating any pipe bursts. One condition was that the turbidity measurements remained below an initial threshold. The recommended desirable threshold for Australian drinking water is 1 NTU. This threshold is 4 NTU for Adelaide city and may be different for other places. During a simulation it is crucial to be able to confirm

that turbidity levels remain above the initial threshold for an extended duration. This ensures the pipe burst incident or isolation activities affect turbidity in the WDN.

Figure 6-1 presents the turbidity measurements in the Adelaide city WDN model prior to successful conditioning. Following a 24-hour simulation of the peak network flow in this model, the pipes within the model were depicted in various colors, exhibiting turbidity levels ranging from below 0.5 NTU to above 2 NTU. In Figure 6-1, red rectangles labeled as numbers 1 to 4 represent four zones where turbidity in pipes surpasses 1 NTU. Pipelines depicted in red indicate turbidity measurements exceeding 2 NTU, suggesting potential concerns with water quality in those pipes. However, it is important to note that these turbidity measurements are based on a single time step.

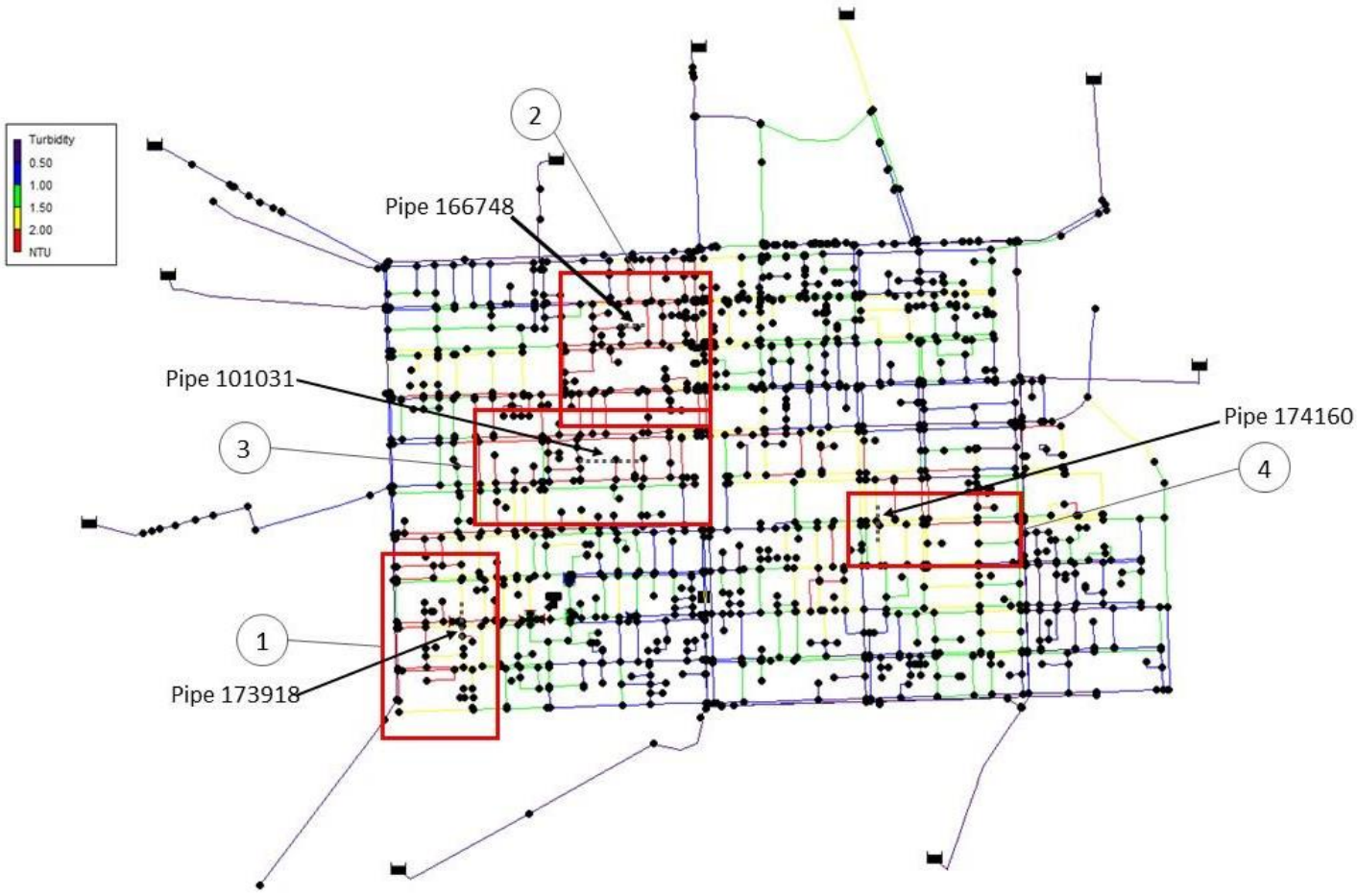

Figure 6-1. PODDS EPANET model results of turbidity in the Adelaide city WDN model before conditioning.

Consequently, sample pipelines, as listed in Table 6-1, were chosen from each zone to display the turbidity measurements over a 24-hour extended simulation period.

Table 6-1. Sample pipelines selected for four different regions in the Adelaide city WDN model.

Zone	Pipe
1	173918
2	166748
3	101031
4	174160

As illustrated in Figure 6-2, without the disruption of a pipe burst in the model, turbidity in all the sample pipes exceeded 1 NTU during the simulation period. The turbidity in pipe 101031 rose above 1 NTU and remained stable at approximately 1.6 NTU after 10 h. Similarly, the turbidity in pipes 173918 and 174160 increased rapidly after 3 h. The former reached a maximum turbidity of just above 3 NTU shortly after 16 h and stabilized thereafter. The latter displayed a tendency to stabilize at 2.5 NTU after 24 h. Turbidity in pipe 166748 rose above 2 NTU after 24 h without showing any indication of stabilization. This might become a concern of turbidity in the Adelaide city WDN model.

These chaotic outcomes show a lack of PODDS EPANET model conditioning at this stage. It is crucial to successfully condition the PODDS EPANET model before introducing a pipe burst to disrupt it. This approach ensures that the turbidity measurements in this model remain below the desired initial threshold and produces reliable results to depict the changes in turbidity in a disrupted PODDS EPANET model.

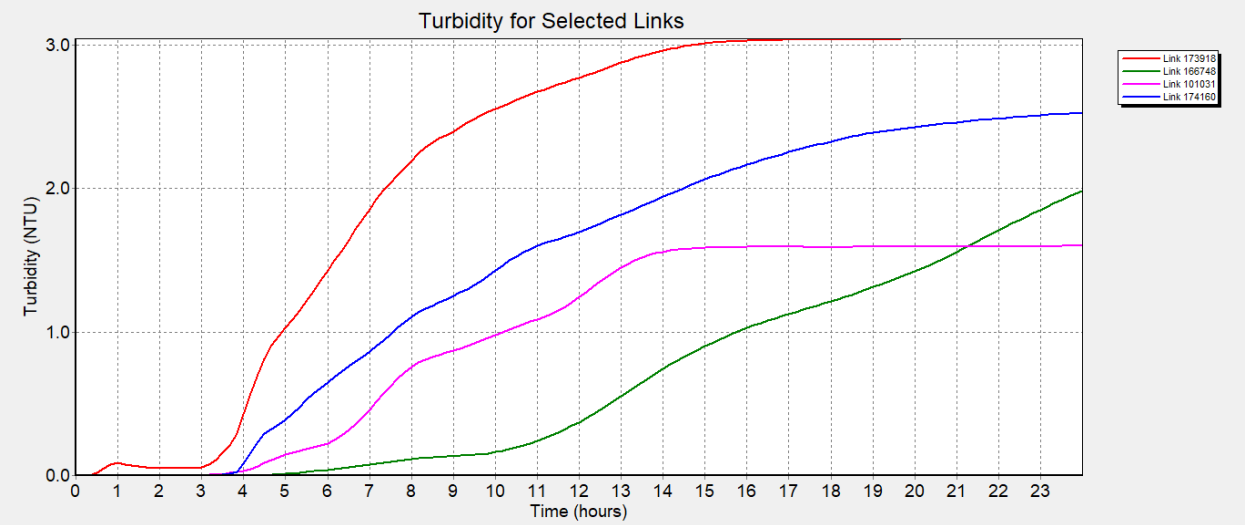

Figure 6-2. Turbidity readings for pipes 173918 (red), 166748 (green), 101031 (pink), and 174160 (blue) over a 24-hour extended simulation period in the Adelaide city WDN model before conditioning.

To condition the model, the initial yield strength, equivalent to peak shear stress, must be computed for every pipe based on its peak daily headloss (equivalent to peak daily hydraulic gradient) in EPANET during the extended 24-hour simulation period.

Peak shear stress was determined using Eq. 9 and input as the initial yield strength in the pipe settings.

$$\tau_s = \rho g \frac{D}{4} S_0 \tag{9}$$

where τ_s is the boundary shear stress, ρ is the density of water at 25 $°C$, g is the gravitational constant, D is the internal diameter of a pipe, and S_0 is the peak daily headloss.

The pipe roughness coefficient was set to 1 mm for each pipe in the model. The Adelaide city WDN model comprises pipes made of cast iron with various internal diameters and lengths. The pipe internal diameters range from 80 mm to 250 mm. The pipe lengths range from 10 m to 988 m. Adopting the PODDS EPANET model parameters (Boxall and Husband, 2005), the values presented in Table 6-2 were applied to the pipe settings in this model.

Table 6-2. PODDS EPANET model parameter values.

Notation	Values	Units
C_{max}	100	NTUm
k	-0.5	$NTUm^3N^{-1}$
b	1	N/A
P	0.00022	$NTUm^3N^{-1}\ s^{-1}$
n	3	N/A

- k is the gradient term representing the relationship between yield strength and the ability of the cohesive layer to increase turbidity.
- b is the power term allowing for non-linear forms that illustrate the correlation between yield strength and the capability of the cohesive layer to increase turbidity.
- P is the rate of supply coefficient.
- n is the power term to connect the release of material to the excess shear stress.

Turbidity readings in the pipes remained below 0.5 NTU after successfully conditioning of the model. This result is evident in turbidity in pipe 173918 rose rapidly from zero to 0.3 NTU within 9 h and then stabilized at approximately 0.34 NTU. Turbidity in pipe 101031 reached 0.34 NTU within 16 h and remained at this level for the rest of the simulation period. The maximum turbidity in pipe 174160 was around 0.22 NTU, which was observed after 19 hours of simulation; this turbidity reading was maintained until 24:00. Turbidity in pipe 166748 increased from zero to 0.28 NTU during the extended 24-hour simulation period. It should be noted that although turbidity in pipe 166748 exhibited several mild increases between 18:00 and 24:00, it remained below 0.4 NTU after simulating the model for 24 h. Collectively, these results confirm the successful conditioning of the PODDS EPANET Adelaide city WDN model, which displays a stable purple color for all pipes in the model at 24:00 (Figure 6-3). To reinforce this finding, turbidity measurements in the sample pipelines were adopted again as examples to demonstrate that turbidity readings in these pipes remained below 1 NTU during the extended 24-hour simulation period, thereby confirming the successful conditioning of the model. As depicted in Figure 6-4 below, turbidity readings in all the pipes remained below 0.4 NTU throughout the extended 24-hour simulation of the peak network flow.

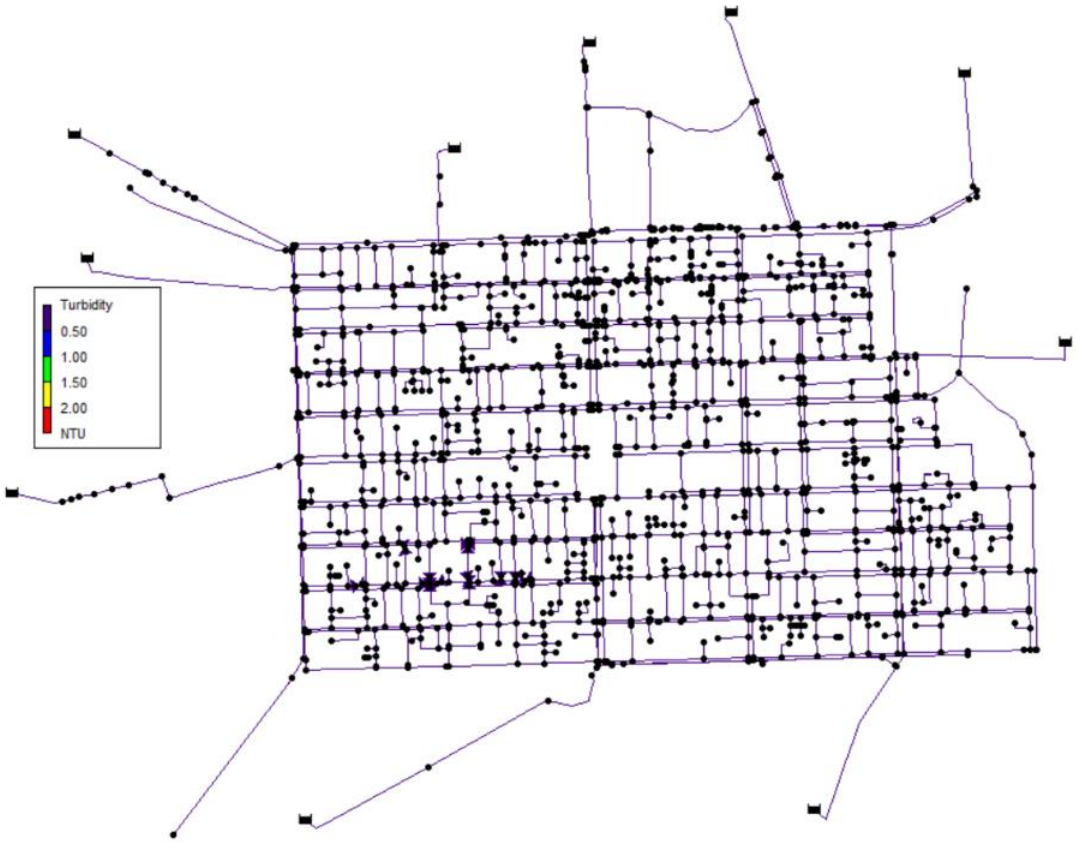

Figure 6-3. Turbidity readings in the Adelaide City WDN model after successful conditioning.

Turbidity in pipe 173918 rose rapidly from zero to 0.3 NTU within 9 h and then stabilized at approximately 0.34 NTU. Turbidity in pipe 101031 reached 0.34 NTU within 16 h and remained at this level for the rest of the simulation period. The maximum turbidity in pipe 174160 was around 0.22 NTU, which was observed after 19 hours of simulation; this turbidity reading was maintained until 24:00. Turbidity in pipe 166748 increased from zero to 0.28 NTU during the extended 24-hour simulation period. It should be noted that although turbidity in pipe 166748 exhibited several mild increases between 18:00 and 24:00, it remained below 0.4 NTU after simulating the model for 24 h. Collectively, these results confirm the successful conditioning of the PODDS EPANET Adelaide city WDN model.

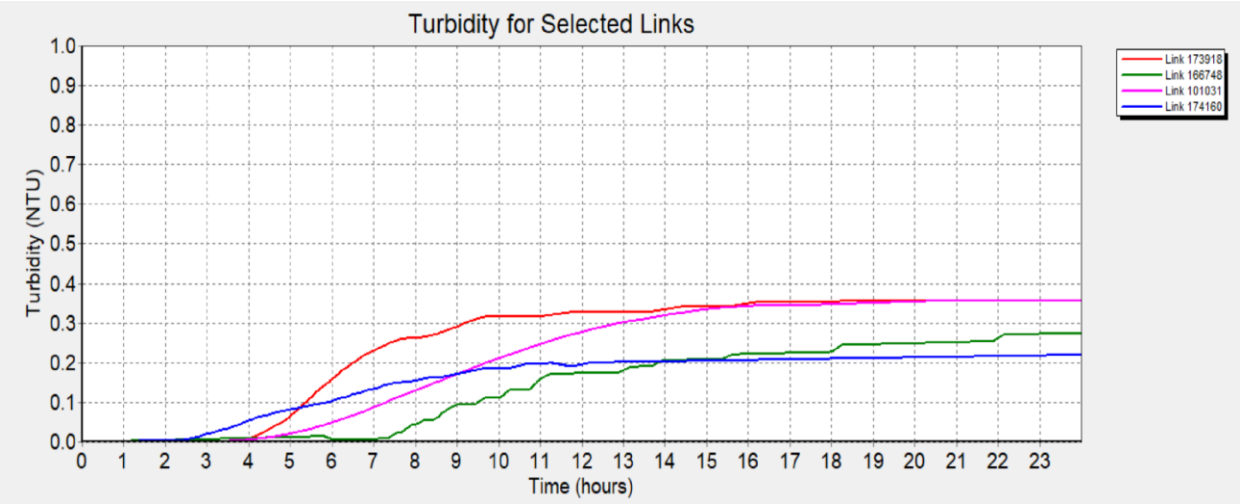

Figure 6-4. Turbidity readings for pipes 173918 (red), 166748 (green), 101031 (pink), and 174160 (blue) over a 24-hour extended simulation period in the conditioned Adelaide City WDN model.

6.2.2 Turbidity Fluctuations in the Adelaide City WDN Model after a Pipe Burst

A pipe burst in the Adelaide city WDN model can induce high pressure at the burst location, significantly increasing flow velocity in the ruptured pipe and affecting flow velocity in adjacent pipes. Ultimately, a pipe burst can lead to fluctuations in turbidity in pipes and a deterioration in water quality.

A pipe burst was assumed and incorporated into the conditioned Adelaide City WDN model to examine potential effects on turbidity in water distribution pipes. The simulation of a pipe burst in PODDS EPANET differs from that in EPANET because PODDS EPANET lacks the same setting functions. The following essential steps were undertaken to complete the simulation:

1) Assumed a burst occurrence at 08:00 at the location depicted in Figure 6-68
2) Proposed a burst node, as illustrated in Figure 6-5, and applied an emitter coefficient of 0.842 to this node to generate a 21.73 L/s burst flow rate in the intrusion link - the short (1m long) and smooth (0.01 mm roughness) pipe employed in Chapter 3.
3) Implemented a control rule to open the intrusion link at 08:00 to simulate the occurrence of the burst.

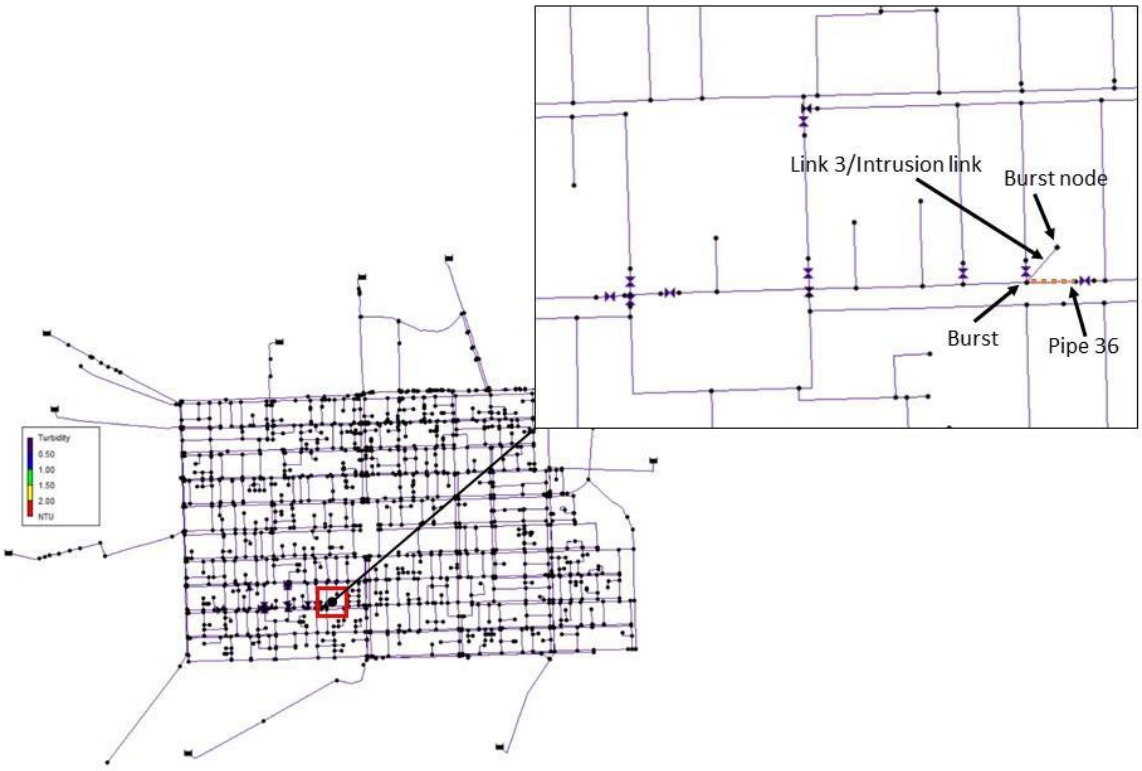

Figure 6-5. Location of the assumed pipe burst in the Adelaide city WDN model.

Through the simulation of the burst, notable increases in turbidity were observed. The varying colors of the pipes depicted in Figure 6-6 reveal the immediate impact of a burst on turbidity in pipes near the burst in a WDN. The highest turbidity in pipes can reach above 2 NTU, as indicated in red in this figure. The pipes which are marked as orange have turbidity above 1.5 NTU. In contrast, the pipes which are shown in green or blue have turbidity below 1.5 NTU.

In some pipes located near the burst, turbidity rose slightly but did not exceed 1 NTU. The inconsistent results from these pipes may be attributed to their flow. Pipes with low flow exhibited minor turbidity fluctuations because there was only minimal mobilization of biofilms from the internal pipe wall. In contrast, pipes with high flow can generate excessive

wall shear stress which exceeds conditioned cohesive strength. Thus, biofilms can detach from the internal pipe wall and become mobilized in the pipe. The initial yield strength for the biofilm layers in pipes also contributes to the potential for pipes to exhibit a sensitive turbidity response to a pipe burst. For example, pipes that are dead ends will be more sensitive to changes in hydraulic force. Consequently, they have a high potential to experience significant turbidity fluctuations when the flow in pipes becomes abnormal (i.e., due to a burst or emergency operational activity).

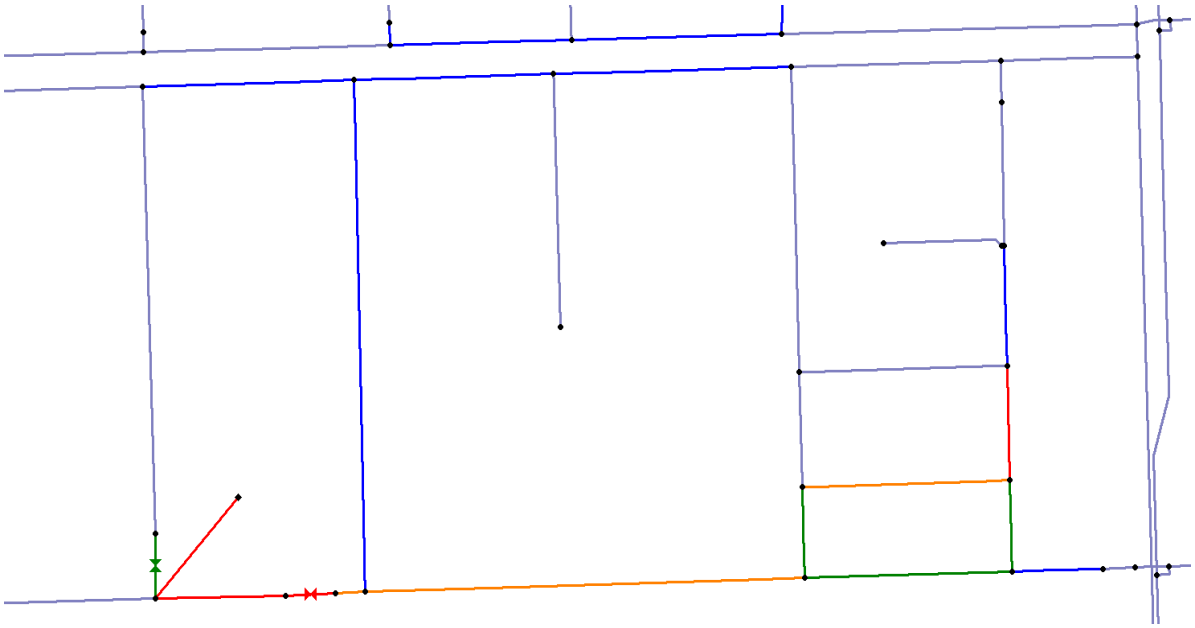

Figure 6-6. Turbidity changes in surrounding pipes triggered by a pipe burst in the Adelaide City WDN model.

Turbidity in pipe 36, one of the closest pipes to the burst, exhibited a substantial increase in turbidity, as illustrated in Figure 6-7. The turbidity in this pipe rose from zero to a peak of 2.8 NTU in approximately 10 mins before declining. It decreased from the peak to around 0.4 NTU and ultimately stabilized at about 0.4 NTU at 15:00. A similar pattern was observed in other pipes near the burst.

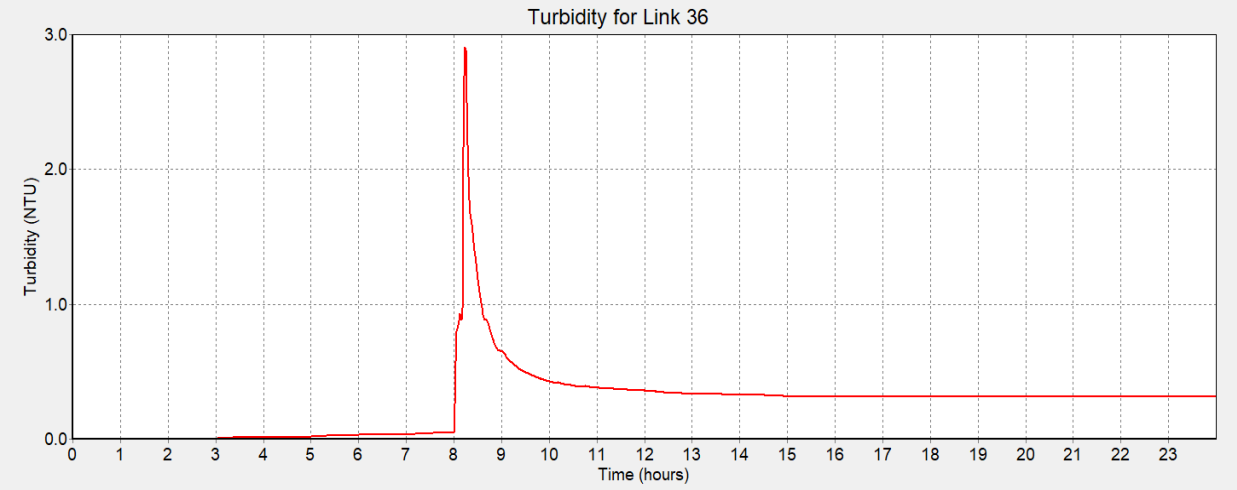

Figure 6-7. Turbidity changes in pipe 36 after having a pipe burst in the Adelaide City WDN model.

As depicted in Figure 6-8, the turbidity responses of the selected four pipes near pipe 36 to the pipe burst were similar to the results displayed in Figure 6-7. The turbidity in pipe 92831 (indicated by the blue line) was nearly identical to that in pipe 36 (indicated by the red line), as they reached the same peak value in less than 10 mins. This then declined and gradually stabilized at approximately 0.3 NTU. Although the turbidity fluctuations in pipe 101875 (indicated by the grey line) were almost identical to those in pipes 36 and 92831, the peak turbidity in this pipe reached approximately 3.5 NTU and ultimately stabilized at around 0.25 NTU. In contrast to the other selected pipes, peak turbidity in pipes 104312 (indicated by the green line) and 16 (indicated by the pink line) were approximately 1.1 NTU and 0.8 NTU, respectively. Even though turbidity measurements in these two pipes eventually stabilized at approximately 0.5 NTU, both peak turbidity readings were considerably lower than those in the other selected pipes.

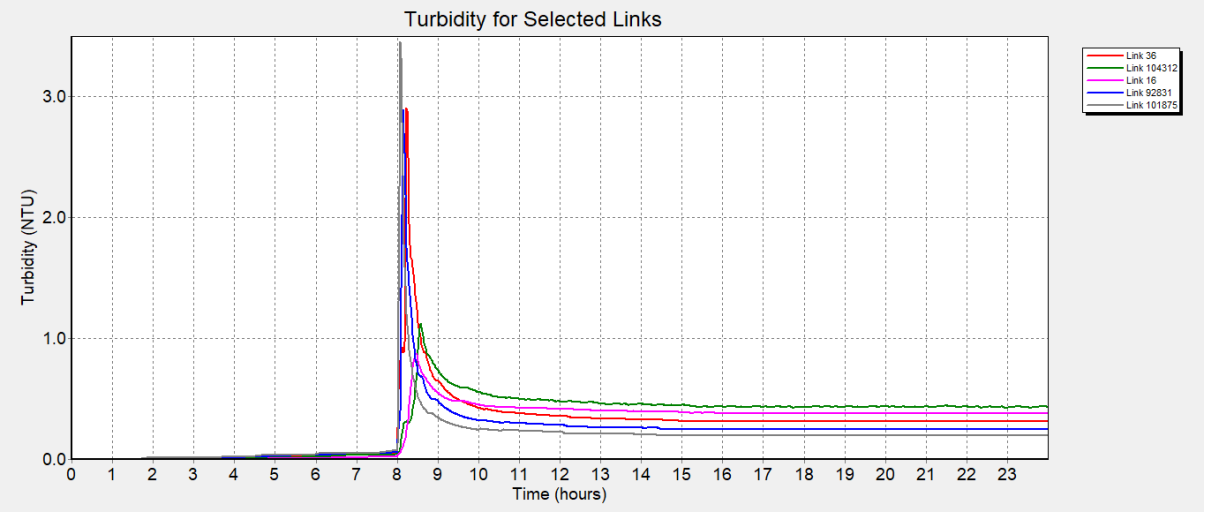

Figure 6-8. Turbidity changes in selected pipes after incurring a pipe burst in the Adelaide City WDN model.

Collectively, the outcomes derived from simulating a pipe burst in this model demonstrate that the occurrence of a pipe burst in WDNs can induce a significant rise in turbidity, consequently impacting water quality in water distribution pipes. To minimize the impacts on turbidity from a pipe burst, optimal valve shutdown operations are essential for isolating the burst effectively and efficiently. The flow in pipes will be disrupted once more by these subsequent operational shutdown procedures, since the flow will be suspended in some pipe segments. It is, therefore, crucial to further explore the effects of valve shutdown operations on turbidity in water distribution pipes. This is the focus of the following chapter.

Chapter 7 Turbidity Changes When Implementing Valve Shutdown Operations in WDNs

7.1 Introduction

Chapter 6 presents the research findings regarding the impact of pipe bursts on the turbidity of WDNs. Repairing a ruptured pipe involves operating isolation valves to manage the burst and create an isolation block where the flow of contaminants is restricted. However, the operation of these valves can influence the turbidity within the isolation block. Furthermore, shutting off isolation valves may also affect the flow of pipes outside the isolation block. Considering these factors, this chapter investigates changes in turbidity in WDNs resulting from valve shutdown operations after a pipe burst., The following three objectives are explored and underpin this chapter:

- To examine the potential changes in turbidity that may occur within an isolation block as a consequence of valve shutdown operations.
- To analyze the potential turbidity changes outside the isolation block resulting from valve shutdown operations.
- To investigate the possible impact of valve shutdown sequences on turbidity in a WDN.

7.2 Turbidity Changes in Pipes Within and Outside of an Isolation Block

In Chapter 6, the Adelaide city model was utilized to simulate a pipe burst scenario on pipe P1, as depicted in Figure 7-1. This particular pipe was chosen because it is one of the primary supply mains in the network and it carries a significant volume of flow. Isolating this pipe from the network may result in the redirection of a large amount of water through alternate pipe routes to fulfill the required demand at nodes. Such a substantial increase in flow through certain pipes can cause excessive shear stress, resulting in the erosion of biofilm layers on the inner walls of pipes. This, in turn, can lead to an increase in turbidity within the pipes.

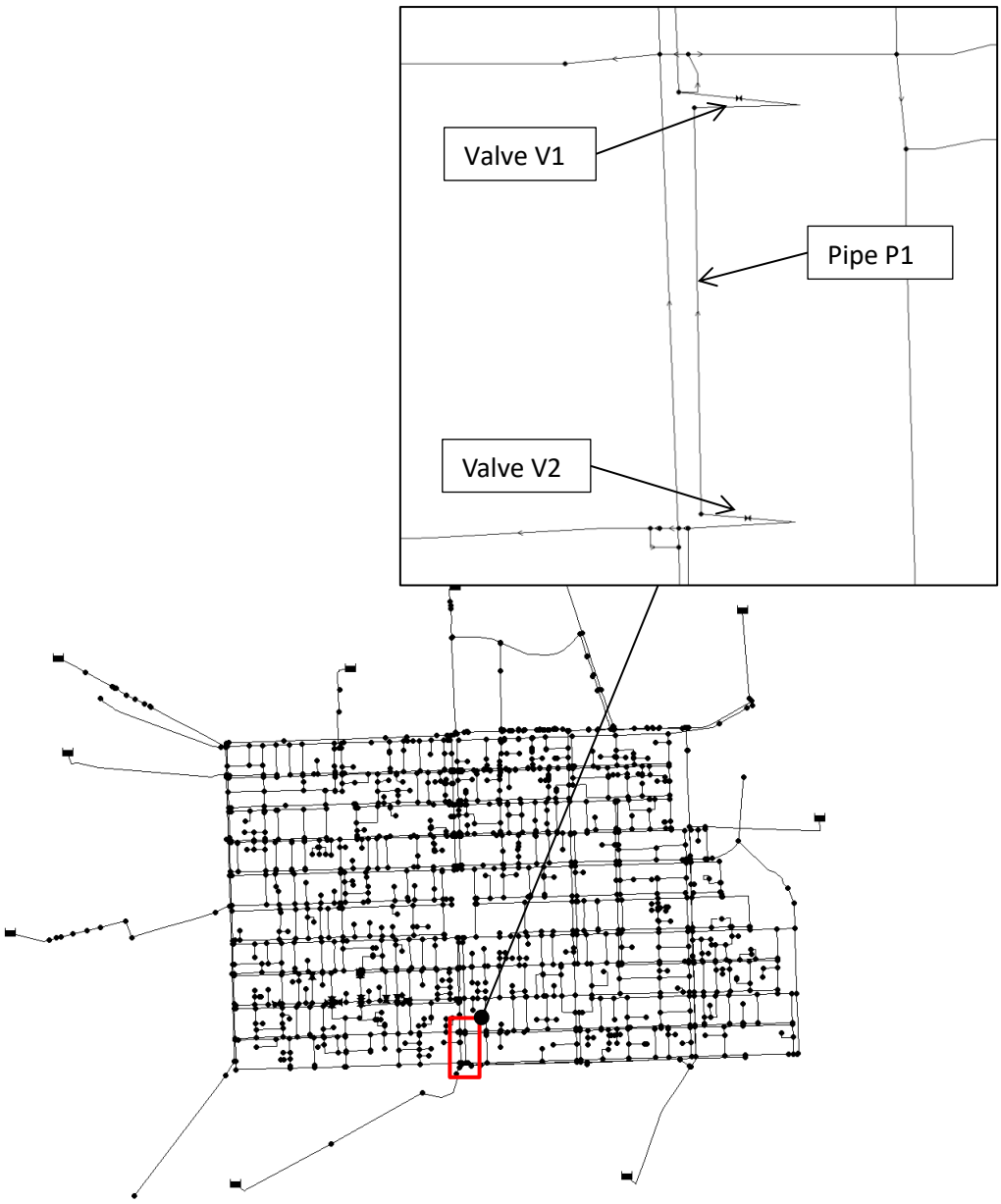

Figure 7-1. Location of pipe P1 and operated isolation valves.

To assess the impact of valve shutdown operations, the model was configured with the following assumptions:

- The model assumed a pipe burst on pipe P1 at 01:45, which led to a significant increase in turbidity. The turbidity levels continued to rise until they stabilized at 02:15.
- The study confirmed that the stabilized turbidity measurements in pipes were practically greater than zero. However, these measurements were treated as a new uniform baseline (benchmark) equal to zero for the purposes of analysis.
- The following control rules were implemented to isolate pipe P1 from the network:

1) isolation valve V1 closed at 02:15
2) isolation valve V2 closed at 02:30

The findings indicate no significant increase in turbidity in the isolated pipe P1 resulting from the isolation activities. This is due to the fact that pipe P1 is one of the primary supply mains in the WDN with high routine hydraulic forces. Such pipes are less likely to have high turbidity levels because the constant high flow will continuously remove biofilms and other solids from the inner walls of the pipe, resulting in a low turbidity baseline. If the isolation block contained additional smaller pipes (i.e., pipes with low hydraulic forces than P1) but we obtained no substantial increase in turbidity in all isolated pipes, it could be the fact that the smaller pipes were located inside the isolation block and the water velocity reduced in these smaller pipes once the isolation activities were completed (i.e., isolation block was formed).

The turbidity in the pipes outside the isolation block may be of concern however due to the redirection of a large amount of flow from pipe P1 to other pipes that typically carry a lower load of flow. The study revealed a significant increase in turbidity measurements in the pipes outside the isolation block following the isolation activities. To demonstrate the changes in turbidity measurements, several pipes located outside the isolation block (i.e., pipe P1), specifically pipes P2, P3, P4, P5, and P6, as shown in Figure 7-2, were selected from the model and the turbidity in the pipes was analyzed after simulating the proposed valve shutdown sequence.

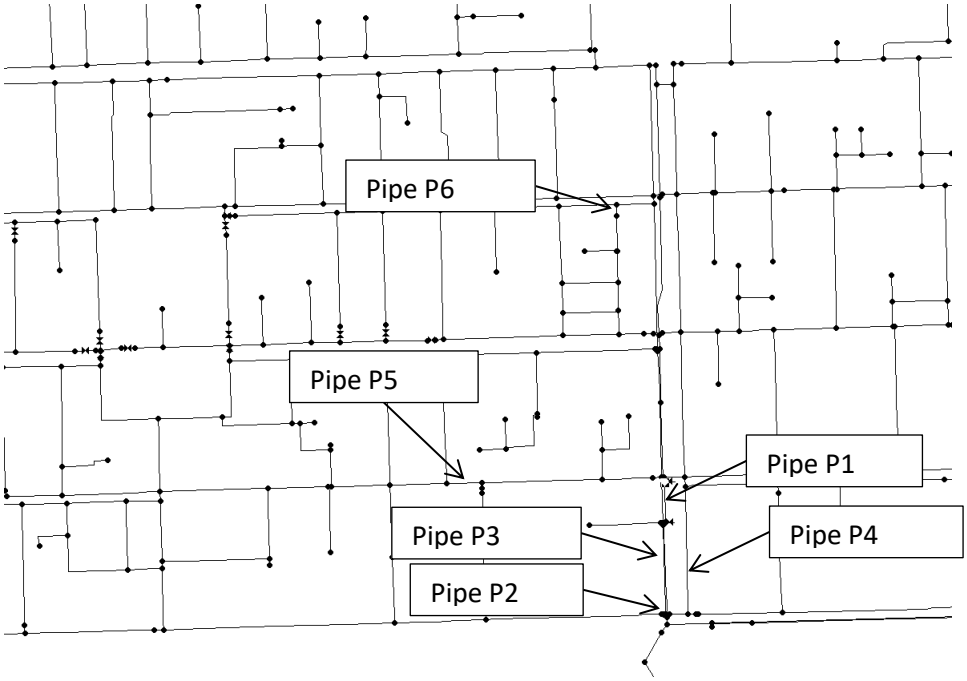

Figure 7-2. Location of selected pipes in the model.

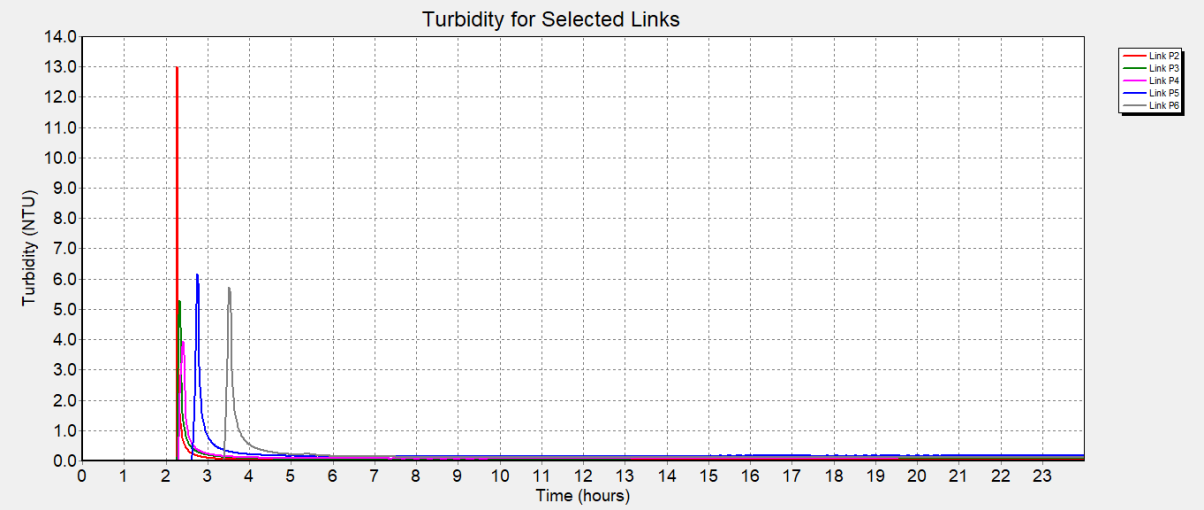

Figure 7-3. Turbidity changes in selected pipes after pipe P1 was isolated from the network.

Figure 7-3 illustrates the changes in turbidity measurements in the selected pipes. Turbidity in pipe P2 (indicated by the red line) exhibited a significant increase from 0 to 13 NTU at 02:16. This is due to the pipe's proximity to isolated pipe P1, which necessitated the same amount of flow to be redirected through this pipe to distribute the same volume of flow to the network. As a result, excessive hydraulic shear stress was induced in the pipe, resulting in a relatively high turbidity peak. Similarly, the turbidity measurement in pipe P3 (indicated by the green line) responded to the isolation activities at the same time, but the peak was only 5.4 NTU, much lower than that of pipe P2. The turbidity spike appeared almost simultaneously due to the pipe's proximity to pipe P2. The turbidity peak in pipe P3 was much lower than that in

pipe P2 because the changes in flow rate in pipe P3 were smaller than those in pipe P2. This is supported by monitoring the flow rate, which changed from 1.6 L/s to 10.25 L/s in pipe P3 and from 1.96 L/s to 16.07 L/s in pipe P2.

The turbidity profiles in pipes P4, P5, and P6 followed a similar trend, albeit with different peak magnitudes and appearance times compared to pipes P2 and P3. Turbidity in pipe P4 (indicated by the pink line) increased from 0 to 3.9 NTU at approximately 02:17. This is because the additional flow that was redirected to this pipe was lower than that in pipes P2 and P3, as evidenced by the monitoring data showing that the flow in this pipe increased from 1.15 L/s to 5.34 L/s. Turbidity in pipe P5 (indicated by the blue line) increased from 0 to 6.2 NTU at around 02:30, whereas turbidity in pipe P6 (indicated by the grey line) increased from 0 to 5.8 NTU at approximately 03:30. Based on their location in Figure 7-2, pipe P5 is closer to the isolated pipe P1, resulting in an earlier turbidity response to the valve shutdown operations. However, the turbidity peak in pipe P5 is higher than that in pipe P6 because the former experienced a larger flow change than the latter.

To further support the discussion above, a pipe that did not carry a significant load of water (i.e., P7) was also considered. It was assumed that a burst occurs at the same location as in Section 6.2.2. The same model was used, and it was necessary to isolate pipe P7, as shown in Figure 7-4. To simplify the modelling process, valve V3 was assumed and added to the model. Thus, shutting off isolation valves V3 and V4 was necessary to fully isolate the burst. The following assumptions were made for the model settings:

- It was assumed a burst occurred on pipe P7 at 01:45, the turbidity was impacted and dramatically increased until stabilizing at 02:15.
- The stabilized turbidity readings in pipes may be practically greater than zero, but for the sake of analysis, they were treated as a new uniform baseline equal to zero.
- The following control rules were implemented to isolate pipe P7 from the network:
  1) isolation valve V4 closed at 02:15
  2) isolation valve V3 closed at 02:30

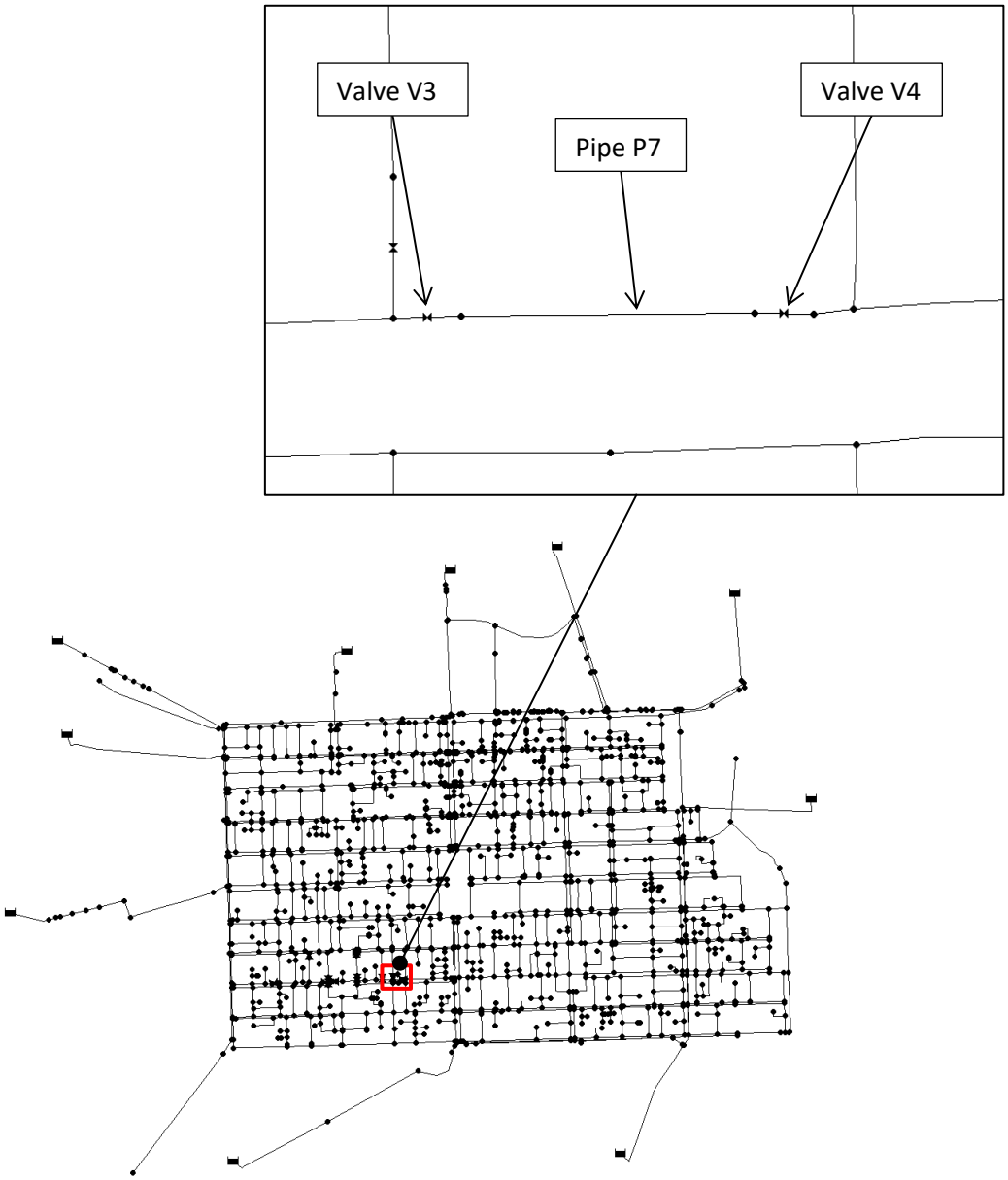

Figure 7-4. Location of pipe P7 and operated isolation valves.

Figure 7-5 shows that the turbidity levels in the same pipes, as shown in Figure 7-2, increased only slightly from 0 to 0.2 NTU. These fluctuations are considered negligible according to the desired level of turbidity (i.e., 1 NTU) in the Australian drinking water standard, as the values are very low. When compared to the scenario in which a main supply pipe (i.e., P1) was isolated, disturbing a pipe that carries a small amount of flow did not trigger a significant increase in turbidity in other pipes outside of the isolated pipe or isolation block. This was because the majority of the flow was still distributed by many other adjacent pipes. Since there was no dramatic increase in the routine flow in these pipes, the hydraulic force in these pipes remained relatively constant, resulting in little to no erosion of biofilm layers and only minor increases in turbidity.

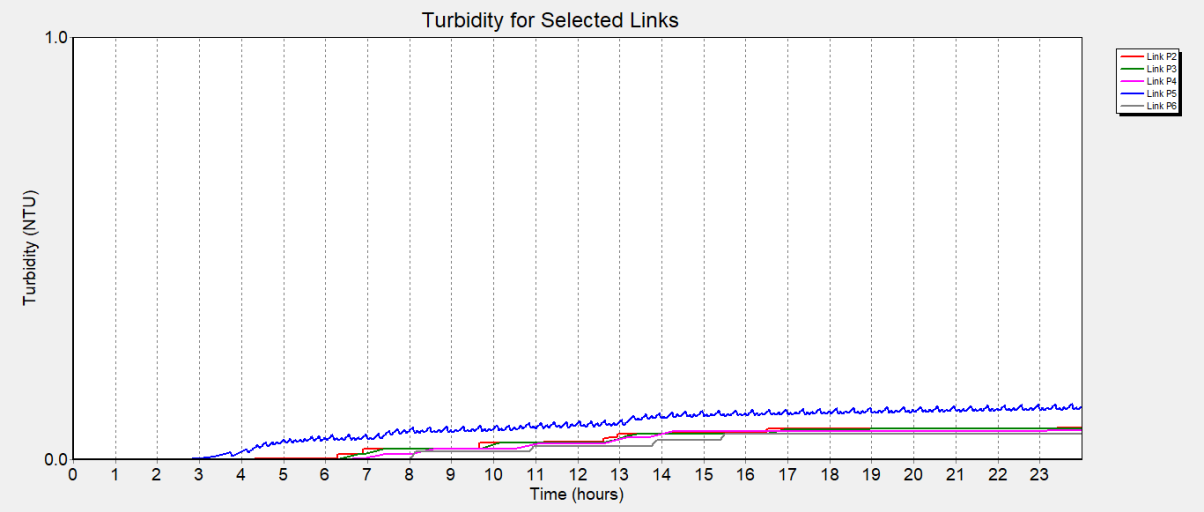

Figure 7-5. Turbidity changes in selected pipes when pipe P7 was isolated from the network.

The results above indicate that valve shutdown operations may not significantly affect turbidity in a pipe that does not carry a significant load of water but it can have an impact on turbidity in other water supply mains. The extent of turbidity change depends on the amount of additional flow being rerouted. Generally, when there is a significant change in flow in a pipe, it is likely that more significant turbidity changes (increases) will be observed, leading to concerns about water quality. When one of the primary water supply mains is disturbed or isolated by operational activities, for example, more severe turbidity changes can be expected in a WDN. The impact of valve shutdown operations on turbidity in pipes is particularly significant if the pipes are responsible for distributing a large amount of flow.

7.3 Turbidity Changes due to Different Valve Shutdown Sequences

Section 7.2 investigated the impact of valve shutdown operations on turbidity in the event of a pipe burst. It is important to note that shutting off isolation valves can also affect the hydraulic behavior of the WDN, as the flow in pipes is disrupted.

As established in earlier chapters, when a pipe burst occurs, operators must close a series of isolation valves to isolate the ruptured pipe(s). The valve shutdown sequence may vary depending on the specific operational procedures, such as:

- Scenario 1: Operators may opt to close the same set of isolation valves, while prioritizing the closure of specific valve(s) due to their ease of access.

- Scenario 2: In instances where operators encounter a malfunctioning isolation valve, they may be required to close an alternate set of isolation valves in order to isolate the same pipe burst. These isolation valves could be situated on various streets, consequently leading to variations in the size of the isolated block.

To provide a comprehensive understanding of the impact valve closure sequences can have on turbidity in water supply pipes this section examines both situations to determine the effects of valve shutdown sequence on turbidity in WDNs.

7.3.1 Scenario 1: Operate the Same Set of Isolation Valves in Different Sequences (Adelaide City WDN Model)

The first scenario investigates the changes in turbidity due to the changes of shutdown order of a fixed set of isolation valves. The Adelaide city WDN model was employed once more to simulate the operations. The identical pipe burst, including its location and flow rate, as depicted in Figure 6-5, was incorporated into the model. Six isolation valves, as illustrated in Figure 7-6, were chosen to isolate this particular burst. In order to model potential changes in turbidity within pipes due to differing valve shutdown sequences, the subsequent four options were proposed:

(1) 2–6–26–11–13–37
(2) 2–37–6–26–11–13
(3) 6–26–11–13–2–37
(4) 6–11–13–2–26–37

Pipe P8, as outlined in Figure 7-6, was chosen to illustrate potential turbidity changes arising from the proposed valve shutdown sequence options. Figure 7-7 displays the distinct turbidity responses in this pipe when implementing the four varied valve shutdown sequences to isolate the pipe burst in the Adelaide city WDN model. As depicted in this figure, all four sequences exhibited identical responses to the pipe burst, as evidenced by the spike at 08:00, which reached approximately 1.1 NTU.

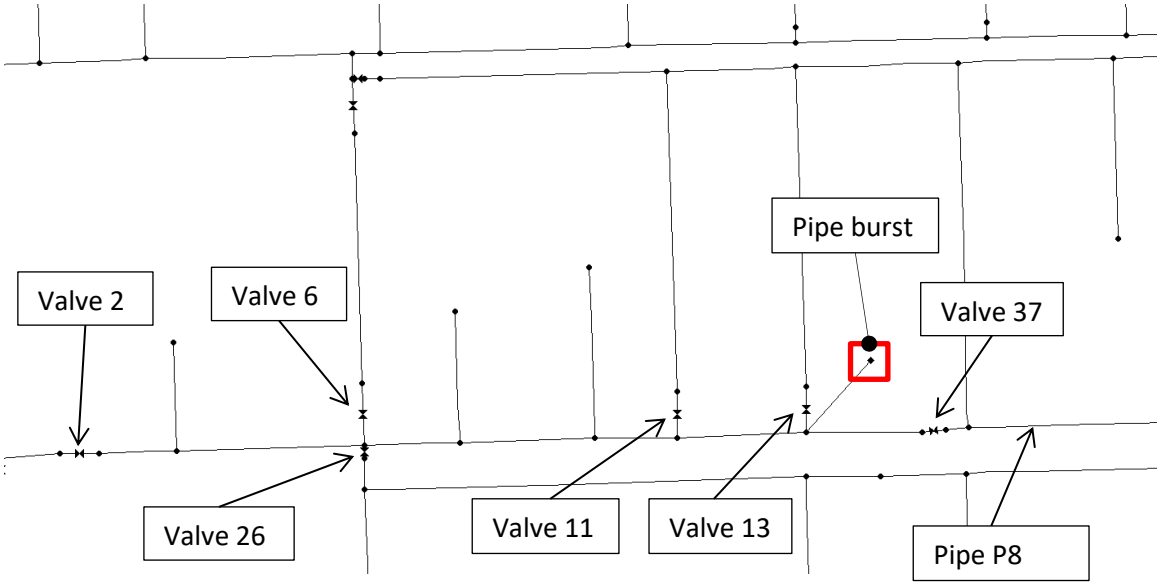

Figure 7-6. Location of selected isolation valves and pipe P8.

Although the turbidity responses to the pipe burst at 08:00 are identical, sequences 1, 3, and 4 exhibited similar turbidity fluctuations between 08:42 and 11:00, while sequence 2 displayed a distinct turbidity profile. Turbidity in pipe P8 increased significantly when valve shutdown operations commenced at 08:30, as evidenced by the second spike shown in the purple, yellow, and blue turbidity plots in Figure 7-7. The peaks of these second spikes ranged from approximately 0.38 NTU to 0.44 NTU. Sequence 1 resulted in the lowest peak (0.38 NTU), while sequences 3 and 4 had the second highest (0.4 NTU) and highest peaks (0.44 NTU), respectively. Upon reaching the peak, turbidity in pipe P8 began to decrease considerably and stabilized at around 0.19 NTU when employing either valve shutdown sequence 1, 3, or 4. Analysis of the valve shutdown sequence associated with isolation valve V4 revealed its importance, indicating it should be closed at the end of an operational shutdown sequence.

Turbidity changes resulting from the adoption of valve shutdown sequence 2 were entirely different. As shown in Figure 7-7, the orange plot represents the turbidity fluctuations in pipe P8, demonstrating a rapid decline in turbidity from 08:00 to 09:00. Subsequently, minor fluctuations were consistently observed from 09:00 to 12:00. The turbidity measurements corresponding to this valve shutdown sequence in the plot did not exhibit significant peaks, suggesting that valve shutdown sequence 2 may have limited effects on turbidity in pipe P8.

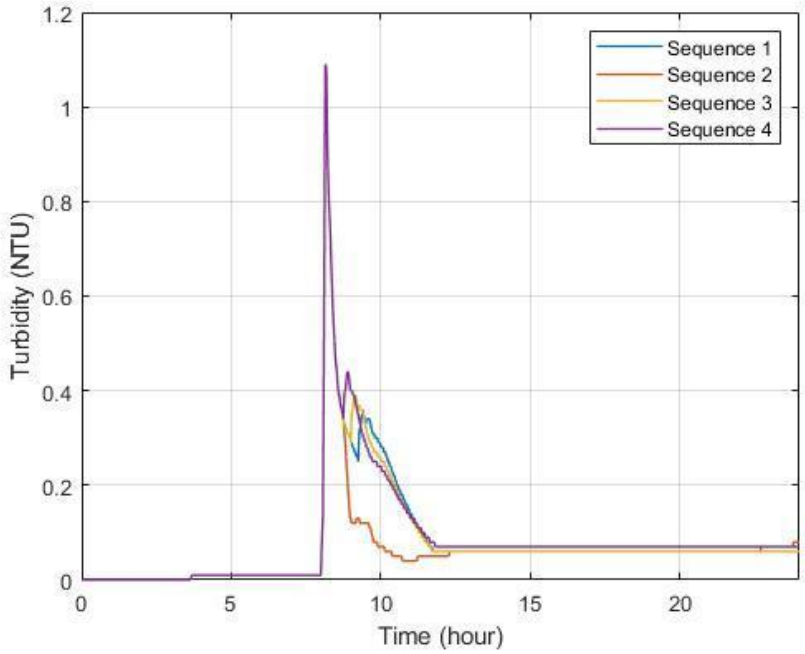

Figure 7-7. The effects of implementing four different valve shutdown sequences on turbidity readings in pipe P8.

The turbidity measurements in a WDN can be affected by the valve shutdown sequence used to isolate a pipe burst. The use of the same set of isolation valves but in different sequences to isolate a pipe burst can result in varying degrees of turbidity responses in the same size of isolation block. Therefore, choosing the most effective operational shutdown sequence is crucial to isolate the burst and minimize fluctuations in turbidity.

Although the valve shutdown sequence can have an impact on the turbidity in water supply mains, the changes in turbidity observed in pipe P8 did not trigger a water quality alarm. The peak turbidity fluctuations in this pipe caused by valve shutdown operations were recorded at around 0.44 NTU, which is below the desired Australian drinking water turbidity level of 1 NTU. This may be attributed to the fact that isolated pipes are responsible for distributing a relatively small flow of water, and shutting down certain isolation valves will not result in significant flow changes in nearby pipes, such as pipe P8. This point is elaborated in the following section.

7.3.2 Scenario 2: Operate Different Sets of Isolation Valves (Paradise WDN Model)

This second scenario focuses on analyzing the turbidity responses in pipes resulting from the isolation of the same burst but with different sets of isolation valves being closed. Variations in valve shutdown sequences occur due to the selection of isolation valves.

Using different sets of isolation valves and varying valve shutdown sequences in WDNs can expand or contract the isolation block, leading to a change in its boundary and causing some pipes to be included within or excluded from it. When more pipes are isolated from the network, a larger volume of source water must flow through other pipes to meet water demand. As the volume of water that a pipe can hold remains constant, the flow rate in that pipe will increase due to the larger load of source water flowing through it. Consequently, turbidity in some pipes located outside the isolation block may be affected (i.e., increased and usually appeared spikes) by the increased flow rate in those pipes.

As the simulation of a pipe burst in a WDN model progresses, the impact of the burst gradually decreases, resulting in the removal of most solids in the network. Therefore, the turbidity in the network pipes would decrease to a level below the desired threshold of 1 NTU and stabilize. This stabilized turbidity level would serve as the new baseline for the network model. This baseline was shown as 0 NTU in the turbidity profile plots in Scenario 2. However, valve shutdown procedures implemented after the occurrence of the burst may cause spikes in the turbidity responses, potentially altering the new turbidity baseline.

To simulate the shutdown operations of selected isolation valves, the Paradise WDN model was used. This scenario utilized the same pipe burst, including its location and flow rate, as in Section 5.2, to allow for the simulation of shutdown activities.

To demonstrate how different valve shutdown sequences (resulting in various isolation block sizes) affect turbidity in water distribution pipes, the following valve shutdown sequences were formulated:

(1) 10–15–7–34–1–22–9
(2) 10–18–19–7–34–1–22–9
(3) 10–18–20–21–24–25–27–7–34–1–22–9

To illustrate the impact of each valve shutdown sequence on turbidity in water supply mains, two pipes (P9 and P10) were chosen from the model and analyzed, as shown in Figure 7-8. Pipe P9 has a length of 113 m, an internal diameter of 375 mm, a roughness of 0.07, and an initial yield of 1.02 N/m^2. Pipe P10, has a length of 200 m, an internal diameter of 89 mm, a roughness of 0.05, and an initial yield of 0.0042 N/m^2. Figure 7-9 displays three distinct

isolation blocks created by implementing the proposed valve shutdown sequences. The red pipes were isolated from the rest of the network. The location of selected isolation valves, as well as how the valve shutdown operations are carried out to create the isolation blocks, are depicted in Figure 7-10.

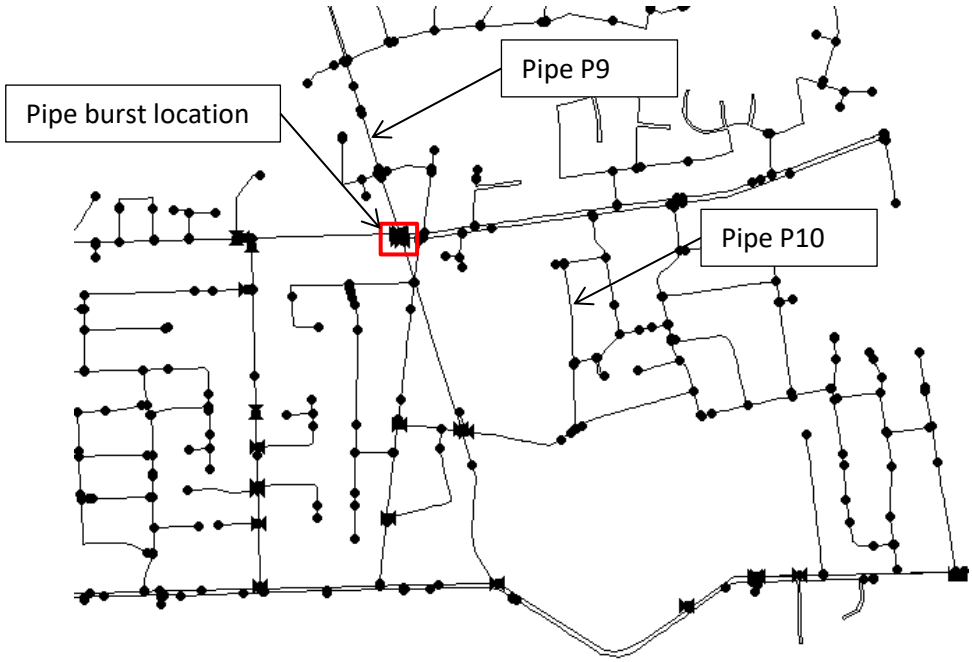

Figure 7-8. Location of pipes P9 and P10, respectively.

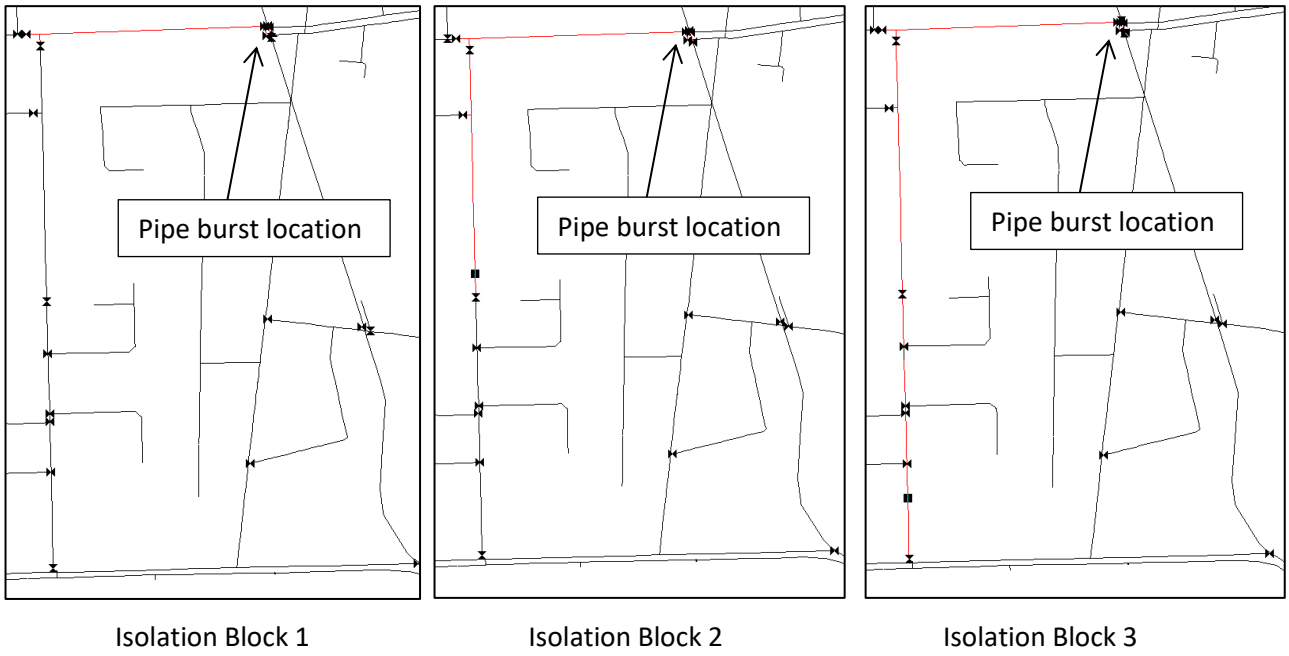

Figure 7-9. Isolation blocks (see Figure 7-10 for detail locations of isolation valves) formed by adopting three different valve shutdown sequences in the Paradise WDN model.

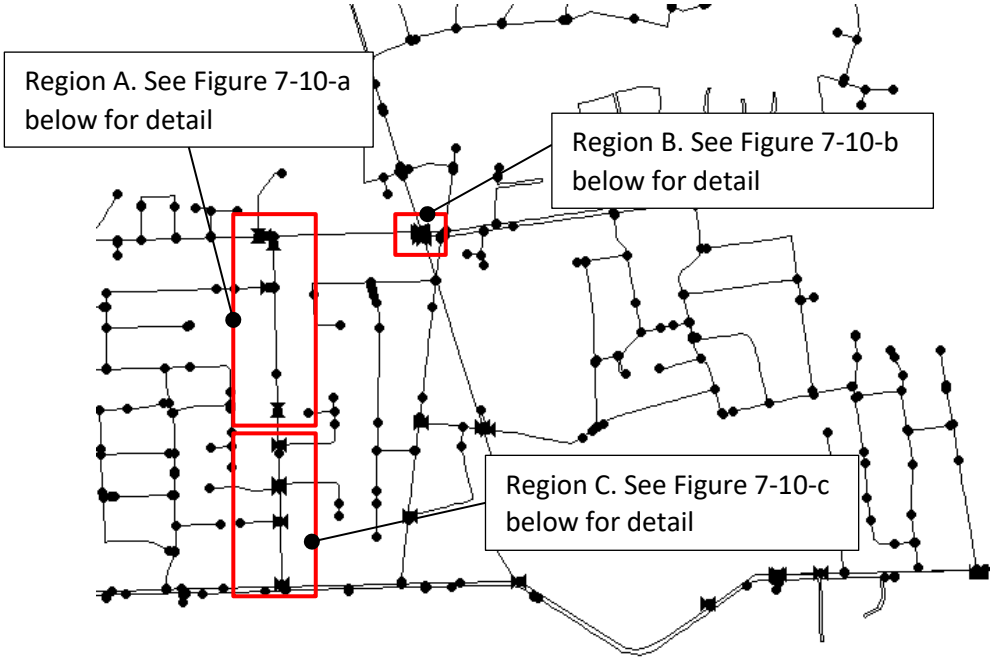

Figure 7-10. Location of selected isolation valves.

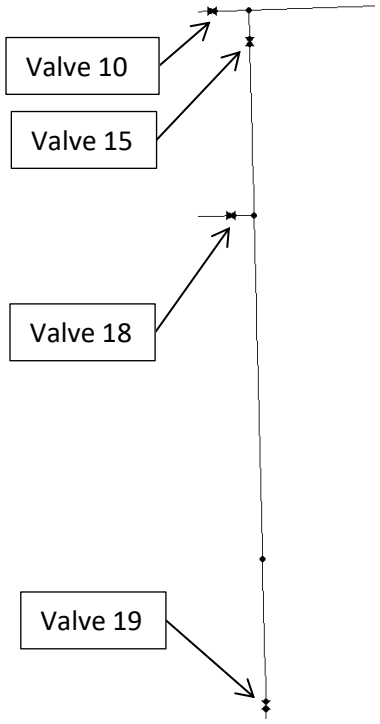

Figure 7-10-a. Location of selected isolating valves in region A.

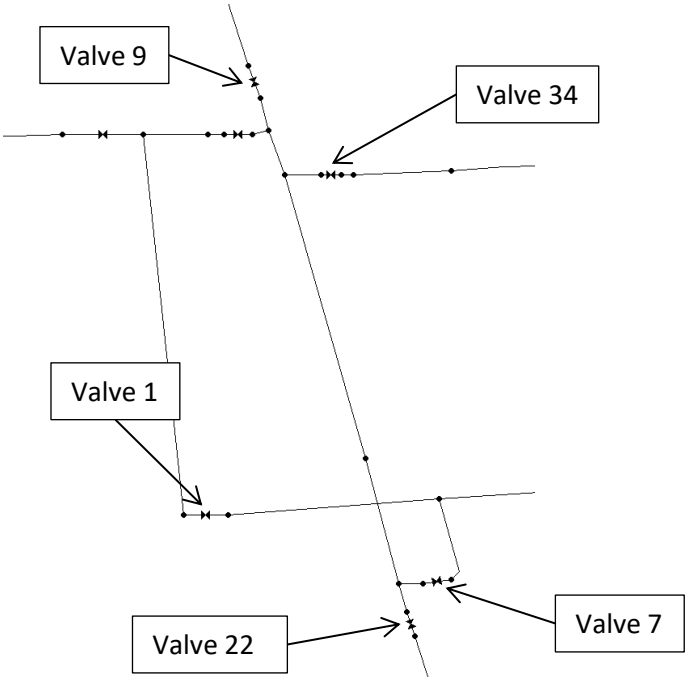

Figure 7-10-b. Location of selected isolating valves in region B.

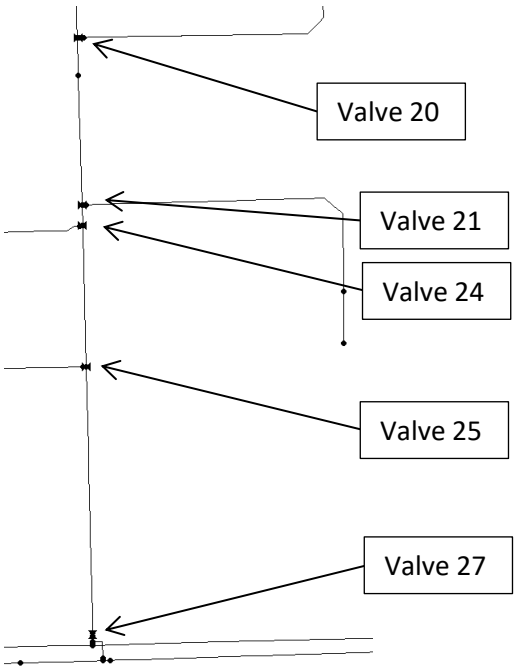

Figure 7-10-c. Location of selected isolating valves in region C.

As shown in Figure 7-11, the implementation of different valve shutdown sequences caused changes in turbidity measurements in pipe P9. The peak turbidity readings in this pipe increased when the valve shutdown sequence was changed from 1 to 3, resulting in the expansion of the isolation block. The highest peak, approximately 11 NTU, occurred at around 11:46. In contrast, the peak turbidity was about 8.5 NTU when valve shutdown sequence 1 or 2 was used in the model. It is worth noting that all turbidity peaks exceeded 1 NTU, which could potentially indicate water quality issues.

The turbidity in pipe P10, as shown in Figure 7-12, displayed different patterns based on the valve shutdown sequence used. The peaks of turbidity spikes resulting from the application of valve shutdown sequences 1 or 2 were lower than those resulting from valve shutdown sequence 3. The peak turbidity recorded when adopting valve shutdown sequence 3 was around 1.48 NTU, while the peak turbidity for the other two sequences did not exceed 1 NTU. These findings suggest that changes made to the valve shutdown sequence by closing different sets of isolation valves can affect the turbidity in pipes, as observed in pipes P9 and P10.

On the other hand, a noticeable contrast between the turbidity peaks in pipe P9 can be observed by comparing Figure 7-11 to Figure 7-12. The difference between the peak values

of the blue and yellow lines in Figure 7-11 is approximately 3.0 NTU, whereas it is only 0.5 NTU in Figure 7-12. This suggests that changing valve shutdown sequences have a greater impact on pipe P9 than on pipe P10. It could be the fact that the initial yield of pipe P9 is higher than that of pipe P10, which increases its turbidity potential and may eventually lead to water quality issues. Additionally, pipe P9 is directly connected to one of the primary water supply mains affected by the shutdown activities and is located in close proximity to the burst or isolation block. Unlike pipe P10, there are no available pipe routes for water circulation in this pipe. Therefore, besides the initial yield of a pipe, the location of the pipe may also influence the sensitivity of potential turbidity changes after changing the valve shutdown sequence.

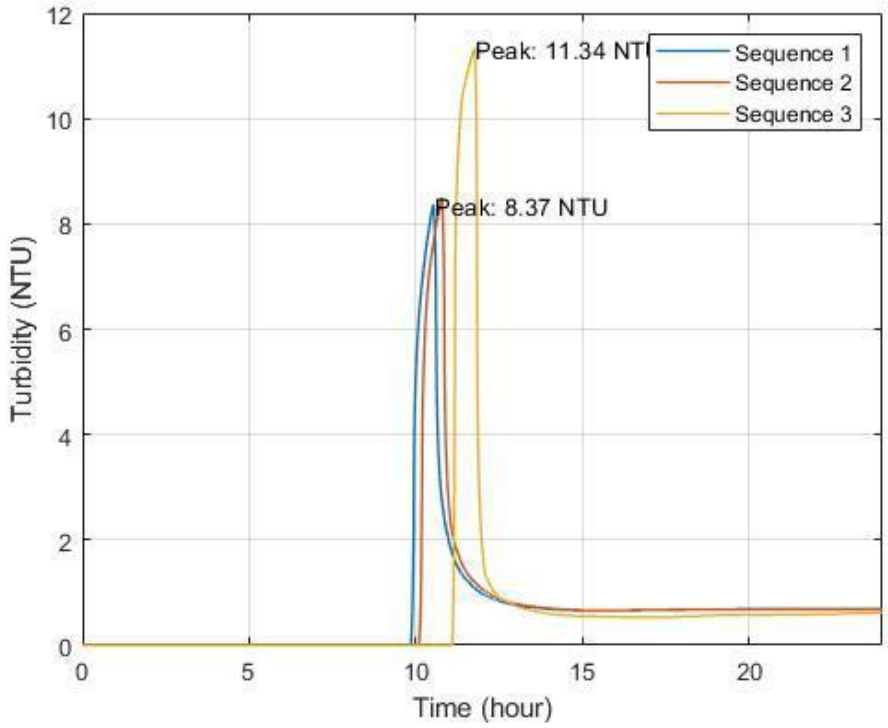

Figure 7-11. Turbidity changes in pipe P9 when adopting three different valve shutdown sequences to isolate the same pipe burst.

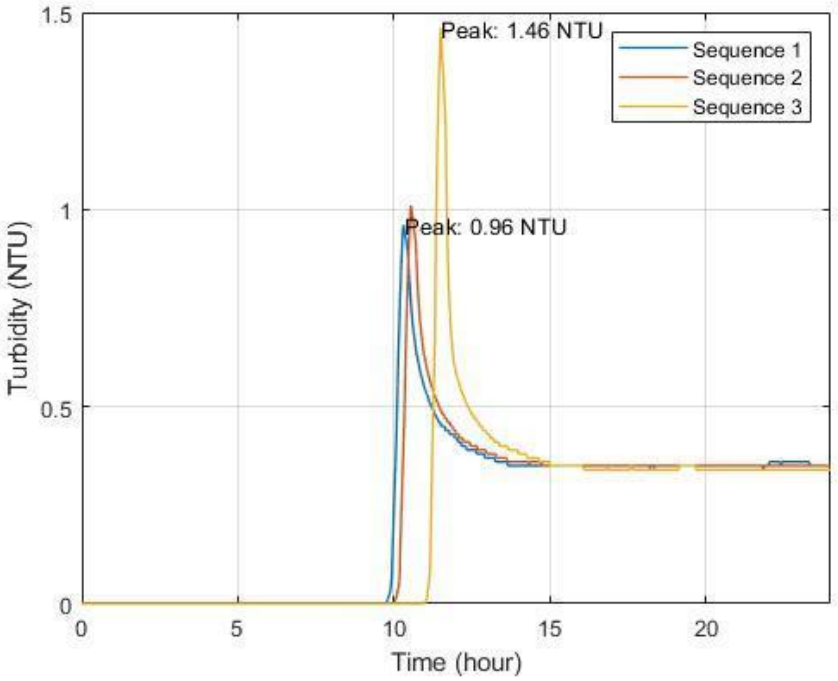

Figure 7-12. Turbidity changes in pipe P10 when adopting three different valve shutdown sequences to isolate the same pipe burst.

In both Figures 7-11 and 7-12 turbidity spikes occurred at different times across different valve shutdown sequences, with sequence 1 showing the earliest turbidity response and sequence 3 revealing the latest turbidity spike. Consequently, the impact of valve shutdown operations on turbidity in both pipes P9 and P10 was delayed due to the longer shutdown process and larger isolation block (when using valve shutdown 3). The effects of valve shutdown operations on turbidity are not triggered until the isolation activities are completed. This finding further confirms that valve shutdown sequences can affect the magnitude and timing of turbidity changes in water distribution pipes. A valve shutdown sequence that results in more pipes being isolated from the network may increase the peak turbidity in some pipes.

Furthermore, as shown in Figure 7-11, the turbidity readings in pipe P9 remained stable at approximately 13:20 for the adoption of valve shutdown sequences 1 and 2, while adopting sequence 3 resulted in turbidity stabilizing at approximately 14:10. The appearance of the turbidity spike following the implementation of sequence 1 was only slightly earlier than that of sequence 2, the minor difference being negligible. The appearance of the turbidity reading following the implementation of sequence 3 was delayed by 50 mins compared to sequences 1 and 2. Therefore, we obtained the same values by measuring the time between the

appearance and stabilization of the turbidity spike for each valve shutdown sequence. This outcome illustrates that the duration of the impact of operational shutdown activities on turbidity in pipe P9 was consistent across all three valve shutdown sequences.

In contrast, the duration of the impact of operational shutdown activities on turbidity in pipe P10 varied significantly across different valve shutdown sequences. The turbidity spikes resulting from three different valve shutdown sequences appeared at different times in pipe P10 (Figure 7-12). They stabilized at approximately the same time. Therefore, the shutdown activities had a more enduring effect on turbidity in pipe P10. This finding could potentially be attributed to the pipe being 87 m longer than pipe P9. A longer travel time is required to remove all solids, such as detached biofilm, from the pipe, resulting in a delay in reaching stable turbidity.

To support the previous findings, a further exploration of the correlation between valve shutdown sequences and turbidity changes in more water distribution pipes (located nearer or farther from the isolation block in the model) was determined to be necessary due to the complexity of WDNs. Figure 7-13 shows the pipes whose turbidity measurements were affected by applying valve shutdown sequence (3) to isolate the pipe burst in the Paradise WDN model. The turbidity measurements are classified by five different colours based on the peak:

- Navy blue: turbidity peak less than 1 NTU
- Light blue: turbidity peak greater than or equal to 1 NTU but less than 5 NTU
- Green: turbidity peak greater than or equal to 5 NTU but less than 20 NTU
- Yellow: turbidity peak greater than or equal to 20 NTU but less than 50 NTU
- Red: turbidity peak greater than or equal to 50 NTU

It should be noted that where pipes have two different colours, it does not necessarily indicate a significant difference in turbidity. For instance, the peak turbidity in one pipe may be 0.99 NTU, which is nearly equal to 1 NTU, and will be shown in navy blue. Another pipe adjacent to this pipe may have a peak turbidity of 1.1 NTU, thereby being light blue in colour. The

impacts of valve shutdown sequence on the turbidity in these two pipes are approximately the same but incrementally different, even though the colours of the pipes are different.

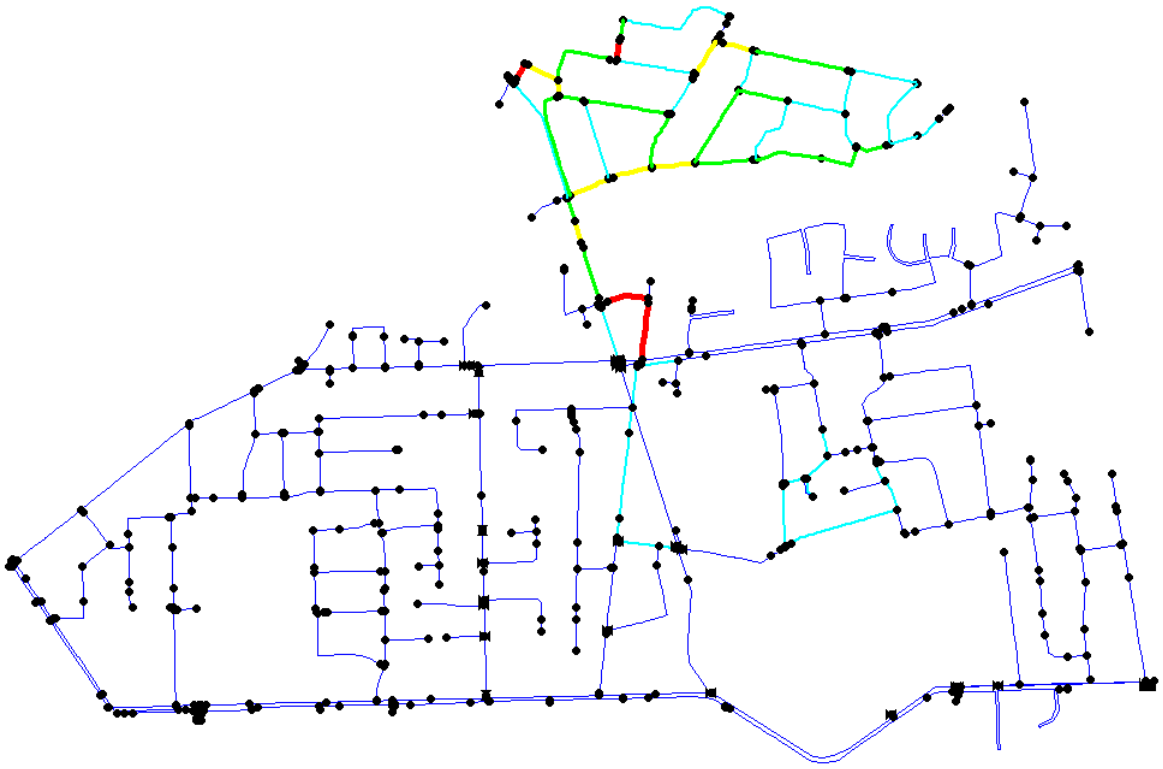

Figure 7-13. Distribution of pipes affected by implementing valve shutdown sequence (3) in the Paradise WDN model.

Figure 7-14 displays a selection of pipes chosen to show how changes in valve shutdown sequences have an impact on turbidity in more pipes, with some pipes located in high-elevation regions and others at similar elevations in the Paradise WDN model. Pipes (a) and (b) are connected to one of the main supply pipes, carrying a larger load of flow in the network. Pipe (c) is a dead end and can only distribute water in one direction. Pipes (d), (e), and (g) are at higher elevations than the burst but may have water circulating through them since they are not dead ends. Pipe (h) is situated closest to the reservoir and should receive a constant large load of water. Finally, pipe (f) is closer to the reservoir, but water may circulate in this pipe because it is not a dead end.

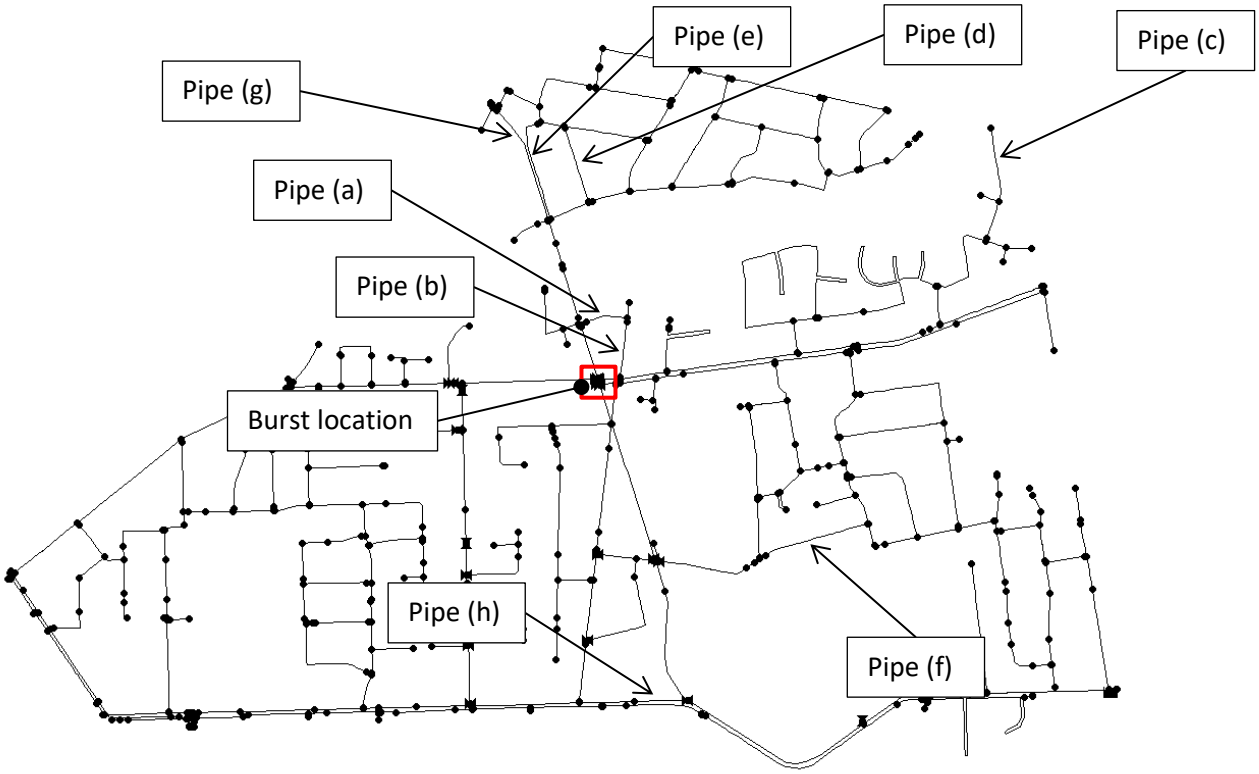

Figure 7-14. Locations for selected pipes in the Paradise WDN model.

The results shown in Figure 7-15 provide strong evidence that changes in valve shutdown sequences impact turbidity in pipes. The extent of turbidity changes may vary depending on pipe characteristics, such as their proximity to the burst or isolation block.

Figure 7-15 depicts the significant impacts of proposed valve shutdown sequences on pipes (a) and (b) by triggering a considerable increase in turbidity levels above 30 NTU. Additionally, changing from valve shutdown sequence 1 to 3 results in a turbidity increase of 56 NTU in pipe (a) and 48 NTU in pipe (b). This finding highlights that variations in valve shutdown sequences can cause a substantial rise in turbidity in pipes that are in close proximity to the main water distribution pipes, which experience significant flows.

Pipe (c) in this figure demonstrates that the corresponding pipe's turbidity can be impacted by valve shutdown sequences, even though the effect is minor, as evidenced by three spikes, each indicating a 0.6 NTU increase in turbidity. This could be attributed to the fact that pipe (c) is located at a dead end and at the farthest distance from the burst or isolation block. Once a valve shutdown sequence is completed, an isolation block is created, which forces a large amount of water to re-route. The effect of increased flow in another primary water

distribution pipe may gradually dissipate when travelling through other pipes before reaching pipe (c). As a result, the flow in this pipe may not be as significantly impacted, and turbidity will not dramatically change due to completing or changing a valve shutdown sequence.

Pipes (d), (e), (f), and (g) exhibit similar turbidity responses when transitioning from valve shutdown sequence (1) to (3). The differences in peak turbidity for pipes (d), (e), (f), and (g) are 0.8 NTU, 2.7 NTU, 0.38 NTU, and 0.6 NTU, respectively. This difference in peak turbidity is the difference between the peak value of the blue curve (turbidity measurement for sequence 1 in Figure 7-15) and the yellow curve (turbidity measurement for sequence 3 in Figure 7-86) for each pipe. Due to their direct connection to the main water distribution pipe, pipes (d) and (e) demonstrate more sensitive turbidity responses to flow disruptions caused by the implementation of different valve shutdown sequences. Additionally, pipes (a), (b), and (f) exhibit earlier turbidity spikes since they are located in close proximity to the main water distribution pipe, resulting in a larger volume of flow being diverted to adjacent pipes. These observations support the previous discussion regarding how pipe location in the network can impact its turbidity response to changes in the valve shutdown sequence.

The turbidity response of pipe (h) to the valve shutdown sequence was significantly different. Although there was a slight increase in turbidity, the spikes were below 0.05 NTU, which is considered to have no impact on water quality. The reason for this difference is that pipe (h) has a low turbidity potential. It is directly connected to the primary water supply main and located before the burst. Therefore, biofilms or solids have been regularly washed off the pipe, resulting in a consistently low turbidity potential before the network was disturbed. As a result, pipe (h) is not expected to experience dramatic flow changes even if a pipe burst occurs and operational shutdown activities are performed in the model.

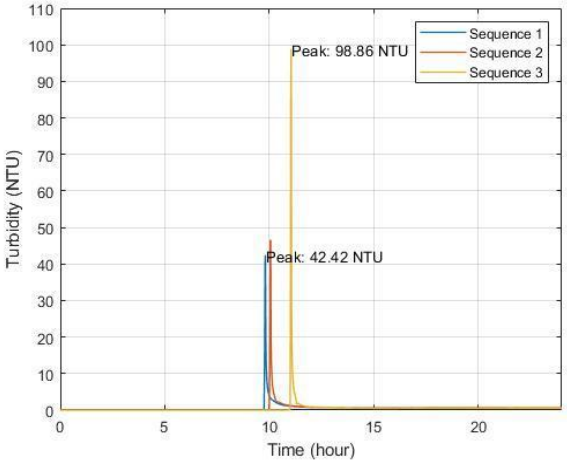

Pipe (a)

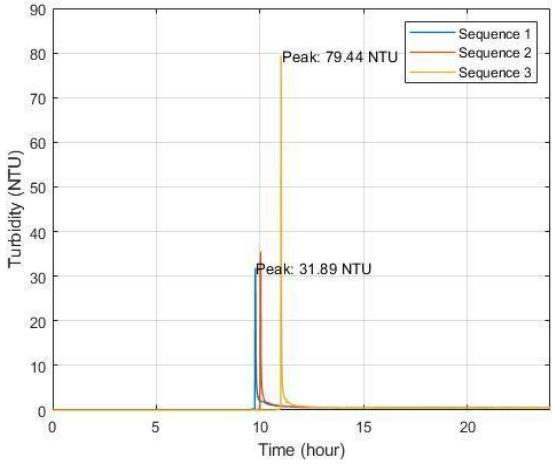

Pipe (b)

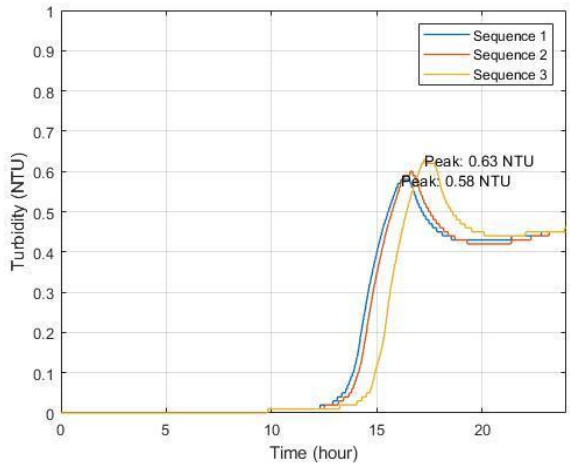

Pipe (c)

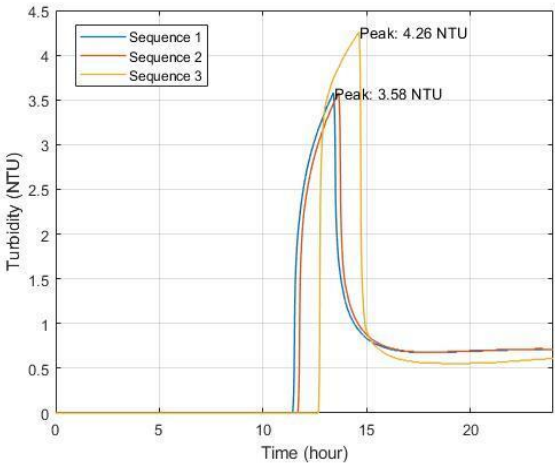

Pipe (d)

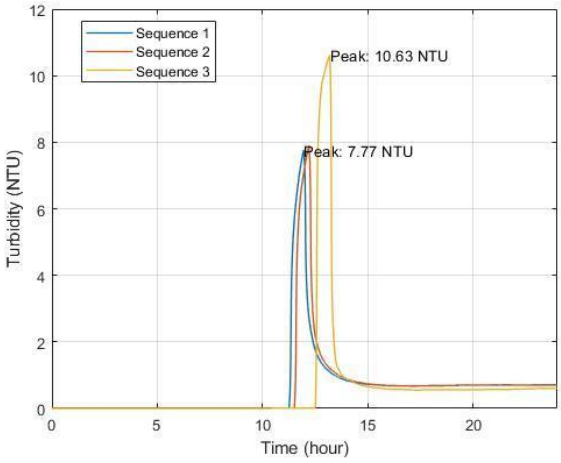

Pipe (e)

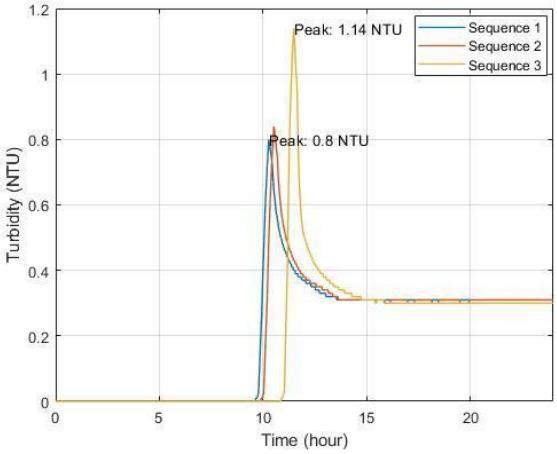

Pipe (f)

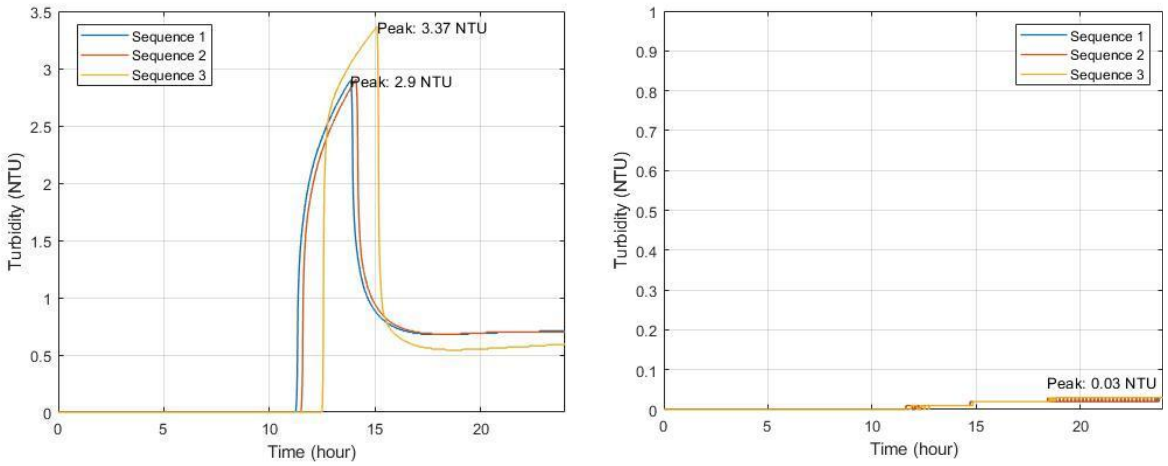

Pipe (g) Pipe (h)

Figure 7-15. Turbidity changes in selected pipes in the Paradise WDN model.

Chapter 8 Conclusion

This research investigated the effects of isolation activities following a pipe burst in a water distribution network and potential mitigation by utilising computer simulation programs. The predominant findings of this study reveal that valve shutdown operations following a pipe burst in WDNs can lead to contaminant intrusion. The contamination can be mitigated in simple WDN models by selecting the most effective valve shutdown sequences. In more complex WDN models, intrusion volumes can be minimised by adopting the most effective valve shutdown sequences, even when the elimination of contaminant intrusion is not feasible (see Chapters 4 and 5). This is a significant finding that has the potential to improve valve shutdown operations following a pipe burst in WNDs and minimise the impacts of isolation activities on customers.

Furthermore, in exploring other aspects of contaminant intrusion this thesis shows:

- Implementing different demand modelling approaches influences intrusion volume estimates. A pressure demand modelling approach was determined to promote more accurate intrusion volumes (i.e., 69% less intrusion volumes) because network demand is sensitive to pressure deficiencies during isolation activities (Chapter 3).
- Node elevations may affect burst flow rate and intrusion volumes with a pressure dependent demand modelling approach adopted. A smaller difference in elevation between the reservoir and the pipe burst can reduce the burst flow but increase intrusion volumes due to more demand nodes being located downstream of the burst (Chapters 3 and 5). For example, if the elevation difference between the reservoir and the demand node in a pressure driven demand water distribution network model reduces by 10 m, the burst flow decreases by 1.8 L/s whereas the intrusion volume increases by 0.71 m^3. The size of an isolation block and the shutdown duration time of isolation valves are associated with the severity of contaminant intrusion (Chapters 3 and 5). For instance, it is feasible to reduce the intrusion volume by 1 m^3 by accelerating the valve shutdown operation for 12 mins in a pressure-dependent demand single pipe model which consists of two isolation valves.

Therefore, in addition to the adoption of best valve shutdown sequences, the following recommendations should be considered to reduce the potential intrusion volume:

- A smaller isolation block may lead to lower demand within the isolation block. The negative pressure that many occur within the isolation block will decrease, resulting in a reduction of the suction effect at the burst location (i.e., pipe rupture). Therefore, the intrusion volume will decrease (Chapter 5).
- Reducing the shutdown duration time of isolation valves (e.g., reducing the time between every two consecutive shutdown operations) may reduce intrusion volumes (Chapters 3 and 5).

Nevertheless, the models implemented in this research only represented simplified WDNs. The maximum intrusion volume presented in this research was in relation to the volume of the contaminant tank. The intrusion volume may vary due to (1) the depth of the sinkhole (2) the type of soil surrounding a ruptured pipeline (which results in different angle of repose values) and (3) the depth of a pipe burst. Therefore, further investigation on valve shutdown operations following a pipe burst in real WDNs and the potential contaminant intrusion volumes is necessary to enable water utility operators to have a comprehensive understanding of how operational shutdown operations affect water quality and customers.

A further important outcome of this study is the finding that a pipe burst and subsequent valve shutdown operations in WDNs may lead to higher turbidity, as detailed in Chapters 6 and 7. The magnitude of the turbidity spike depends on the volume of flow that is re-routed from the disturbed pipes to alternative pipes. The worst scenario arises when a pipe carrying a large amount of flow is disturbed by isolation activities, leading to increased turbidity in the surrounding pipes. The turbidity spikes can reach approximately 100 NTU from an initial state of less than 0.4 NTU.

Furthermore, valve shutdown sequences can also impact the turbidity response in WDNs. The shutdown sequences for a fixed set of isolation valves can be switched, thus, affecting the turbidity response in the pipes, including the peak turbidity and the time at which the turbidity spikes are observed. The shutdown sequences for isolation valves can also be changed by selecting a different set of isolation valves, which leads to variations in the size of the isolation block and the number of demand nodes that are affected. Accordingly, both the timing and magnitude of the turbidity spikes will appear differently. Pipes that are closely connecting to the pipe responsible for a large volume of flow may reveal more sensitive

turbidity responses. In contrast, the pipes located further away from the disturbed pipe may exhibit lower turbidity spikes because the effects of increased flow will dissipate with increasing distance from the isolated pipes. Pipes that routinely experience high flow rates may not exhibit sensitive turbidity responses to changes in valve shutdown sequences as they have low turbidity potentials, as elaborated in Chapter 7.

REFERENCES

Alfonso, L., Jonoski, A., & Solomatine, D. (2010). Multiobjective optimization of operational responses for contaminant flushing in water distribution networks. *Journal of Water Resources Planning and Management*, *136*(1), 48–58. https://doi.org/10.1061/(asce)0733-9496(2010)136:1(48)

Ali, H., & Choi, J. (2019). A review of underground pipeline leakage and sinkhole monitoring methods based on wireless sensor networking. *Sustainability*, *11*(15), 4007. https://doi.org/10.3390/su11154007

Australian Bureau of Statistics. (2020-2021). *Water Account, Australia*. ABS. Retrieved from: https://www.abs.gov.au/statistics/environment/environmental management/water-account-australia/latest-release.

Besner, M. C., Ebacher, G., Jung, B. S., Karney, B., Lavoie, J., Payment, P., & Prevost, M. (2010). Negative pressures in full-scale distribution system: Field investigation, modelling, estimation of intrusion volumes and risk for public health. *Drink. Water Eng. Sci.*, *3*, 101–106. https://doi:10.5194/dwes-3-101-2010

Bouchart, F., & Goulter, I. (1991). Reliability improvements in design of water distribution networks recognizing valve location. *Water Resources Research*, *27*(12), 3029-3040. https://doi.org/10.1029/91WR00590

Boulos, P. F., Karney, B. W., Wood, D. J., & Lingireddy, S. (2005). Hydraulic transient guidelines for protecting water distribution systems. Journal of American Water Works Association, 97(5), 111-124. https://doi.org/10.1002/j.1551 8833.2005.tb10892.x

Boxall, J. B., & Husband, S. (2005). An introduction and guide to the PODDS model. Prediction and control of discolouration events in distribution systems, University of Sheffield. https://sites.google.com/sheffield.ac.uk/podds/podds

Boxall, J. B., & Saul, A.J. (2005). Modeling discoloration in potable water distribution systems. *Journal of Environmental Engineering*, *131*(5), 716-725. https://doi.org/10.1061/(ASCE)0733-9372(2005)131:5(716)

Burlingame, G. A., Pickel, M. J., & Roman, J. T. (1998). Practical applications of turbidity monitoring: To take the use of turbidity measurements to a level at which accuracy is critical without the support of quality assurance-quality control would be inappropriate. Journal of American Water Works Association, 90(8), 57–69. https://doi.org/10.1002/j.1551-8833.1998.tb08485.x

Cattafi, M., Gavanelli, M., Nonato, M., Alvisi, S., & Franchini, M. (2011). Optimal placement of valves in a water distribution network with CLP (FD). *Theory and Practice of Logic Programming, 11*(4-5), 731-747. https://doi.org/10.1017/S1471068411000275

Chu, F. H., Pilkey, W. D., & Pilkey, O. H. (1979). An analytical study of turbidity current steady flow. *Marine Geology*, *33*, 205-220. https://doi.org/10.1016/0025-3227(79)90081-1

City of Subiaco topographic map. (2023). *World topographic map*. Retrieved from: http://en-au.topographic-map.com/map-txlhdn/City-of-Subiaco/?center=-31.95478%2C115.8168

Collins, R., Boxall, J., Besner, M. C., Beck, S., & Karney, B. (2010, September). Intrusion Modelling and the Effect of Ground Water Conditions. 12th Annual International Conference on Water Distribution Systems Analysis, Tucson, AZ, United States. http://doi.org/10.1061/41203(425)55

Collins, R., & Boxall, J. (2013). Influence of ground conditions on intrusion flows through apertures in distribution pipes. *Journal of Hydraulic Engineering*, *139*(10), 1052-1061. https://doi.org/10.1061/(ASCE)HY.1943-7900.0000719

Collins, R. P., Boxall, J. B., Karney, B. W., Brunone, B., & Meniconi, S. (2012). How severe can transients be after a sudden depressurization. *Journal of American Water Works Association*, *104*(4), 67–68. https://doi.org/10.5942/jawwa.2012.104.0055

Cooper, L. (2019). Running out or flooded out? London's water crisis. London Assembly Labour. Greater London Authority. Retrieved from: http://www.london.gov.uk/sites/default/files/running_out_or_flooded_out_-_londons_water_crisis_by_leonie_cooper_am.pdf.

de Roos, A. J., Gurian, P. L., Robinson, L. F., Rai, A., Zakeri, I., & Kondo, M. C. (2017). Review of epidemiological studies of drinking-water turbidity in relation to acute gastrointestinal illness. *Environmental Health Perspectives*, *125*(8), 086003. https://doi.org/10.1289/EHP1090

Department for Infrastructure and Transport, Government of South Australia (2020). Roads, Master specification, RD-DK-D1 Road drainage design. https://www.dit.sa.gov.au/__data/assets/pdf_file/0003/553224/MASTER_SPECIFICATION_-_PART_RD-DK-D1_-_ROAD_DRAINAGE_DESIGN.pdf

Di Nardo, A., Di Natale, M., Giudicianni, C., Musmarra, D., Rodriguez, J. M., Santonastaso, G. F., Simone, A., & Tzatchkov, V. (2017). Redundancy features of water distribution systems. *Procedia Engineering*, 186, 412-419. https://doi.org/10.1016/j.proeng.2017.03.244

Do, C. N., Simpson, A. R., Deuerlein, J. W., & Piller, O. (2018). Locating inadvertently partially closed valves in water distribution systems. *Journal of Water Resources Planning and Management, 144*(8), 04018039. https://doi.org/10.1061/(ASCE)WR.1943-5452.0000958

Douterelo, I., Husband, S., Loza, V., & Boxall, J. (2016). Dynamics of biofilm regrowth in drinking water distribution systems. *Applied Environmental Microbiology*, *82*, 4155–4168. https://doi:10.1128/AEM.00109-16

Dugan, B. (2022). Subiaco sinkhole bursts water main and causes flooding as luxury Mercedes swallowed and power cut. PerthNow. Retrieved from: http://www.perthnow.com.au/news/perth/subiaco-sinkhole-bursts-water-main-and-causes-flooding-as-luxury-mercedes-swallowed-and-power-cut-c-8283886

Engineering ToolBox. (2003). NPS - 'Nominal Pipe Size' and DN - 'Diametre Nominal'. Retrieved from: https://www.engineeringtoolbox.com/nps-nominal-pipe-sizes-d_45.html

Environmental Policy and Planning Division, Department of Environment and Science, State of Queensland (2022). Guideline environmental protection (water and wetland biodiversity) policy 2019, Deciding aquatic ecosystem indicators and local water quality guideline values. https://environment.des.qld.gov.au/__data/assets/pdf_file/0029/88148/deriving-local-water-quality-guidelines.pdf

Fontanazza, C. M., Notaro, V., Puleo, V., Nicolosi, P., & Freni, G. (2015). Contaminant intrusion through leaks in water distribution system: Experimental analysis. *Procedia Engineering*, *119*(1), 426–433. https://doi.org/10.1016/j.proeng.2015.08.904

Francisque, A., Shahriar, A., Islam, N., Betrie, G., Siddiqui, R. B., Tesfamariam, S., & Sadiq, R. (2014). A decision support tool for water mains renewal for small to medium sized utilities: a risk index approach. *Journal of Water Supply: Research and Technology-AQUA*. 63(4), 281-302. http://doi: 10.2166/aqua.2013.305

Gelder, S., & Alwakeel, R. (2018). *Clapton flooding: Waterworks Lane off Lea Bridge Road underwater after pipe bursts.* Ham & High. Retrieved from: http://www.hamhigh.co.uk/news/21155557.clapton-flooding-waterworks-lane-off-lea-bridge-road-underwater-pipe-bursts/

Georgoulas, A. N., Angelidis, P. B., Panagiotidis, T. G., & Kotsovinos, N. E. (2010). 3D numerical modelling of turbidity currents. *Environmental Fluid Mechanics*, *10*, 603-635. https://doi.org/10.1007/s10652-010-9182-z

Ginige, M. P., Wylie, J., & Plumb, J. (2011). Influence of biofilms on iron and manganese deposition in drinking water distribution systems. *Biofouling*, *27*(2), 151-63. https://doi:10.1080/08927014.2010.547576

Gullick, R. W., Lechevallier, M. W., Svindland, R. C., & Friedman, R. J. (2004). Occurrence of transient low and negative pressures in distribution systems. *Journal of American Water Works Association*, *96*(11), 52-66. https://doi.org/10.1002/j.1551-8833.2004.tb10741.x

Husband, S., & Boxall, J. (2010). Field studies of discoloration in water distribution systems: Model verification and practical implications. *Journal of Environmental Engineering*, *136*(1), 86-94. https://doi.org/10.1061/(ASCE)EE.1943-7870.0000115

Husband, S., & Boxall, J. (2016). Understanding and managing discolouration risk in trunk mains. *Water Research*, *107*, 127-140. https:// doi.org/10.1016/j.watres.2016.10.049

GWM Water. (2023). How much water do you use? Water audit kit. [Brochure]. Retrieved from: https://www.gwmwater.org.au/component/edocman/708-water-audit-kit/download

Islam, N., Farahat, A., Al-Zahrani, M. A. M., Rodriguez, M. J., & Sadiq, R. (2015). Contaminant intrusion in water distribution networks: Review and proposal of an integrated model for decision making. *Environmental Reviews*, *23*(3), 337–352. https://doi.org/10.1139/er-2014-0069

JCM Industries (2019). General pipe repair information & repair fitting selection guidelines. Retrieved from: https://www.jcmindustries.com/wp-content/uploads/JCM-Resources-Product-Application-Repair-General-Pipe-Repair-Information-and-Guidelines-2019.pdf

Jones, S., Shepherd, W., Collins, R., & Boxall, J. (2019). Experimental quantification of intrusion volumes due to transients in drinking water distribution systems. *Journal of Pipeline Systems Engineering and Practice*, *10*(1), 04018026. https://doi.org/10.1061/(asce)ps.1949-1204.0000348

Khadr, W., Hamed, M., & Nashwan, M. (2022). Pressure driven analysis of water distribution systems for preventing siphonic flow. Journal of Hydro-environment Research, *44*, 102-109. https://doi.org/10.1016/j.jher.2022.09.001

Kingdom, B., Liemberger, R., & Marin, P. (2006). The challenge of reducing non-revenue water (NRW) in developing countries how the private sector can help: A look at performance-based service contracting. *World Bank Group Water Supply and Sanitation Board discussion paper series*, 8. http://hdl.handle.net/10986/17238

LeChevallier, M. W., Gullick, R. W., Karim, M. R., Friedman, M., & Funk, J. E. (2003). The potential for health risks from intrusion of contaminants into the distribution system from pressure transients. *Journal of Water and Health*, *1*(1), 3–14. https://doi.org/10.2166/wh.2003.0002

Liu, H., Walski, T., Fu, G., & Zhang, C. (2017). Failure impact analysis of isolation valves in a water distribution network. *Journal of Water Resources Planning and Management*, *143*(7), 04017019. https://doi.org/10.1061/(asce)wr.1943-5452.0000766

Mahmoud, H. A., Kapelan, Z., & Savić, D. (2018). Real-time operational response methodology for reducing failure impacts in water distribution systems. *Journal of Water Resources Planning and Management*, *144*(7), 04018029. https://doi.org/10.1061/(asce)wr.1943-5452.0000956

Mansour-Rezaei, S., Naser, G., & Sadiq, R. (2014). Predicting the potential of contaminant intrusion in water distribution systems. *Journal of American Water Works Association*, *106*(2), 47–48. https://doi.org/10.5942/jawwa.2014.106.0019

Melbourne Water (2016). Water outlook for Melbourne. Retrieved from: https://www.melbournewater.com.au/sites/default/files/Water-outlook-Melbourne2016.pdf

Mounce, S. R., Gaffney, J. W., Boult, S., & Boxall, J. B. (2015). Automated data-driven approaches to evaluating and interpreting water quality time series data from water distribution systems. *Journal of Water Resources Planning and Management*, *141*(11), 04015026. https://doi.org/10.1061/(ASCE)WR.1943-5452.0000533

Muranho, J., Ferreira, A., Sousa, J., Gomes, A., & Marques, A. S. (2020). Pressure-driven simulation of water distribution networks: Searching for numerical stability. *Environmental Sciences Proceedings, 2*, 48. https://doi.org/10.3390/environsciproc2020002048

NHMRC, NRMMC (2011). Australian drinking water guidelines 6 National water quality management strategy. National Health and Medical Research Council, National Resource Management Ministerial Council, Commonwealth of Australia, Canberra.

Office of the Auditor General Western Australia (2014). WA Water Corporation: Management of water pipes. Retrieved from: https://audit.wa.gov.au/wp-content/uploads/2014/02/report2014_01-Water-Corporation-Management-of-Water-Pipes.pdf

Rossman, L. A. (2000). EPANET 2 users manual. U.S. Environmental Protection Agency, Washington, D.C., EPA/600/R-00/057.

SA Water. (2011, December). Water supply code of Australia agency requirements.. Retrieved from: https://www.sawater.com.au/__data/assets/pdf_file/0015/6162/TG105.pdf

SA Water. (2012, September). Allowable pipe size, class and materials for water mains. Retrieved from: https://www.sawater.com.au/__data/assets/pdf_file/0010/6220/Construction.pdf

SA Water. (2023, March). Techinical standard 0136 - pipework access and protection. Retrieved from: http://www.sawater.com.au/__data/assets/pdf_file/0017/612242/SAWS-ENG-0136.pdf

Shamir, U. (1974). Optimal design and operation of water distribution systems. *Water Resources Research*, *10*(1), 27–36. https://doi.org/10.1029/WR010i001p00027

Shirzad, A. (2020). A model for pressure driven analysis-design of water distribution networks. *Journal of Applied Water Engineering and Research, 8*(2), 79-87. https://doi.org/10.1080/23249676.2020.1761895

Starczewska, D., Gaffney, J., Boult, S., Mounce, S., & Boxall, J. (2017). Water network characterisation based on mass balance with regards to discolouration risk using high frequency turbidity monitoring. *CCWI2017:F149 Computing and Control for the Water Industry, University of Sheffield. Journal contribution.* https://doi.org/10.15131/shef.data.5364502.v1

State of Victoria (2009). Guidelines for private drinking water supplies at commercial and community facilities. Food Safety and Regulatory Activities, Victorian Government Department of Health, Melbourne, Victoria. Retrieved from: https://content.health.vic.gov.au/sites/default/files/migrated/files/collections/policies-and-guidelines/1/1_guidelines_report---pdf.pdf

Stephens, M., Simpson, A., Lambert, M., Vítkovský, J., & Nixon, J. (2002, July). *The detection of pipeline blockages using transients in the field* [Conference paper]. Australia Water Association SA Branch Regional Conference, Adelaide, SA, Australia.

Sterling, M. J. H., & Bargiela, A. (1984). Leakage reduction by optimised control of valves in water networks. *Trans. Inst. Meas. & Control*, *6*, 293–298. https://doi.org/10.1177/014233128400600603

StructX. (2022, April 25). Typical angle of repose values for various soil types. Retrieved from: https://structx.com/Soil_Properties_005.html

Tanyimboh, T., Tahar, B., & Templeman, A. (2003). Pressure-driven modelling of water distribution systems. *Water Science and Technology: Water Supply, 3*(1-2), 255-261. http://doi.org/10.2166/ws.2003.0112

Thompson, S., Shanafield, M., Manero, A., Claydon, G. (2021). When urban stormwater meets high groundwater - part 1. Water e-Journal, *6*(1). http://doi.org/10.21139/wej.2021.006

Tihansky, A. B. (1999). Sinkholes, west-central Florida. In Galloway, D., Jones, D. R., & Ingebritsen, S.E., (Eds.), *Land subsidence in the United States: U.S. Geological Survey Circular* (1182, pp. 121-140).

U.S. Centers for Disease Control and Prevention (U.S. CDC) (2016). Community assessment for public health emergency response (CASPER) After the Flint Water Crisis: May 17-19, 2016. National Center for Environmental Health, Division of Environmental Hazards and Health Effects, Health Studies Branch.

U.S. Environmental Protection Agency (U.S. EPA) (2004). Long term 1 enhanced surface water treatment rule turbidity provisions: Technical guidance manual. Office of Water (4606M) EPA 816-R-04-007.

Van, N. T. T., Shima, K., Keigo, M., & Satoshi, M. (2019). An investigation into the effect of cavities on the behavior of model pile under axial loading in weak rock. *Hokkaido Branch, Japanese Geotechnical Society*, *59*, 43-50. https://jgs-hokkaido.org/pastweb/tech-rep-pdf/59/index.html

Volk, C., Dundore, E., Schiermann, J., & LeChevallier, M. (2000). Practical evaluation of iron corrosion control in a drinking water distribution system. *Water Research*, *34*(6), 1967-1974. https://doi.org/10.1016/S0043-1354(99)00342-5

Walski, T. M. (1993). Water distribution valve topology for reliability analysis. *Reliability Engineering and System Safety*, *42*(1), 21–27. https://doi.org/10.1016/0951-8320(93)90051-Y

Watkins, R., Keil, B., Mielke, R., & Rahman , S. (2010). *Pipe Zone Bedding and Backfill: A Flexible Pipe Perspective* [Conference paper]. ASCE Pipelines Conference 2010, Keystone, Colorado, USA.

World Health Organization (WHO) (1992). Water supply and sanitation sector monitoring report 1990. Retrieved from: https://washdata.org/sites/default/files/documents/reports/2017-06/JMP-1992-Report.pdf

World Health Organization (WHO) (2017). Water quality and health - review of turbidity: Information for regulators and water suppliers. https://apps.who.int/iris/handle/10665/254631

WSAA (2019). Reducing leakage in Australia. Retrieved from: https://www.wsaa.asn.au/sites/default/files/publication/download/leakage%20report%20screen.pdf